UNIVERSITY OF OKLAHOMA

GRADUATE COLLEGE

CAMBRIAN TRILOBITES FROM THE STEPTOEAN-SUNWAPTAN BOUNDARY INTERVAL (JIANGSHANIAN), NEVADA AND UTAH

A THESIS

SUBMITTED TO THE GRADUATE FACULTY

in partial fulfillment for the requirements for the

Degree of

MASTER OF SCIENCE

By

KATIE FOSTER WELCH

Norman, Oklahoma

2020

CAMBRIAN TRILOBITES FROM THE STEPTOEAN-SUNWAPTAN BOUNDARY INTERVAL (JIANGSHANIAN), NEVADA AND UTAH

A THESIS APPROVED FOR THE SCHOOL OF GEOSCIENCES

BY THE COMMITTEE CONSISTING OF

Dr. Stephen Westrop, Chair

Dr. Richard Cifelli

Dr. Richard Lupia

Acknowledgements

I would like to thank Dr. Westrop for guiding and motivating me throughout this process. You have been so patient and kind, and I have learned so much. Even during a pandemic, I could always reach out to you for help and support. I could not have asked for a better mentor.

I would also like to thank Roger Burkhalter for his help at the museum. I knew that if I ever had a question, whether it was related to sample preparation, photography, or how to use the rock saw, he always had the answer.

Additionally, I would like to express gratitude to my committee members, Dr. Richard Lupia and Dr. Richard Cifelli, for taking the time to review my work. Your insight and guidance mean so much to me, and I appreciate how patient you have been.

Lastly, I would like to thank all of my friends and family who have been there for me. Without your support, I would not have completed this thesis. I would like to especially thank my parents, Teresa, Mark and Angie, who made sure that I understood the value of hard work and perseverance. I would like to thank my siblings, Cassidy and Chase, for making me laugh and brightening my day with every phone call. To Cameron, I want to say thank you for being the best road-trip buddy anyone could ask for. To Alicia, Steve, and Lily, thank you for letting me invade your office. Y'all are so funny and I will miss our fishing trips. I would like to thank Rafael for all the trips to Braums and Dairy Queen. And most importantly, I would like to thank Ralphie for always being there for me.

Table of Contents

List of Figures

Chapter I

Chapter II

Abstract

This thesis documents previously unknown latest Steptoean (*Elvinia* Zone) trilobite faunas from Nevada and Utah, including their geological context. Samples from Nevada are from the Barton Canyon Member of the Windfall Formation in the Cherry Creek and North Egan ranges of White Pine County. The sample from Utah was collected from the Sneakover Member of the Orr Formation in the northern House Range of Millard County. At both study sites, lithologies are dominantly bioturbated lime wackestone with cm-thick packstone layers, and record deposition under subtidal conditions on a carbonate ramp; sites in Nevada represent a deeper, more distal setting than the site in Utah. The samples yielded trilobite sclerites from 10 species and 15 genera. *Labiocephalus cassia* is the type species of a new genus, and *Anechocephalus ralphi* and *Noelaspis primitiva* are new species. The faunas are assigned to a new latest Sunwaptan *Labiocephalus cassia* Zone that can be correlated with successions in central Oklahoma and southern British Columbia. The base of the zone is marked by the lowest occurrence of *A. ralphi* and *L. cassia*. The faunas provide a glimpse of the paleoecology of an interval that immediately precedes a major trilobite extinction event at the base of the Sunwaptan Stage (base of the *Irvingella major* Zone). As such, they provide a baseline for understanding the impact of the extinction on the faunas in the region. The faunas comprise two biofacies. The *Pterocephalia-Iddingsia* Biofacies is from the more proximal ramp settings in Utah. It is dominated by the eponymous genera and has a diversity of nine species. The more distal *Labiostria-Anechocephalus* Biofacies in Nevada has slightly lower diversity (eight species). New carbon isotope data from

Nevada record a positive excursion of $\delta^{13}C$ that begins near the onset of the extinction event at the top of the Barton Canyon Member, and rises to peak of 2.17‰ in the lower part of the overlying Catlin Member. A similar positive excursion is expressed in new data from central Oklahoma, although it begins a little higher in the succession, at the top of the *I. major* Zone. The general pattern is consistent with published reports of positive excursions of $\delta^{13}C$ associated with the extinction in Utah and Wyoming, which have been interpreted as the result of increased carbon burial due to upwelling of anoxic water, possibly in response to a sea level rise. These changes may have been at least partly responsible for triggering the extinction.

Chapter I: Introduction

The Cambrian trilobite faunas of the Great Basin of Utah and Nevada have a long history of study that extends back to the late 19th Century (Hall and Whitfield, 1877; Walcott, 1884). Much of this early work was prompted by the economic importance of the Cambrian rocks in production of silver, gold and other metals that began in the 1860s and 1870s in the Eureka (Nolan, 1962) and Pioche (Merriam, 1964) mining districts in Nevada. Palmer (1955, 1960, 1962, 1965) conducted extensive field work in the region in the 1950s, and his monographs remain the standard reference on the trilobite faunas of the Upper Cambrian Steptoean Stage. Given the extent of prior studies in the region, it was surprising that a new program of field work (e.g., Westrop and Adrain, 2007, 2013) discovered previously unknown faunas from the youngest Steptoean strata at three sites in Utah and Nevada. These new faunas are the subject of this thesis, and they are of particular interest because they record the composition of trilobite assemblages immediately prior to the onset of an extinction event at the end of the Steptoean (e.g., Palmer, 1984).

The end-Steptoean extinction is one of three such events that occurred within a 15 MY interval during the Late Cambrian (Palmer, 1965a; Stitt, 1971a; Westrop and Cuggy, 1999). Each of these extinctions is associated with termination of clades, a decrease in both within-habitat diversity and in the number of biofacies present across the North American shelf (Westrop and Cuggy, 1999). Saltzman et al. (1995; Saltzman et al. 1998) investigated the carbon isotope stratigraphy through the Steptoean–Sunwaptan boundary interval, and documented a modest positive excursion in $\delta^{13}C$ that they

interpreted as possibly recording upwelling of dysoxic water during an interval of sea level rise.

The purpose of this thesis is to fully document the new trilobite faunas that occur in the Barton Canyon Member of the Windfall Formation of Nevada and the middle of the Sneakover Limestone Member of the Orr Formation of Utah. This part of my research will contribute to an ongoing, long-term project to revise the systematics of the trilobites of the Upper Cambrian succession of the Great Basin (e.g., Adrain and Westrop, 2004, 2005; Westrop and Adrain, 2007, 2016; Westrop et al., 2007, 2010). In addition to describing the paleoenvironmental context of the faunas, my study will offer a regional view of trilobite paleoecology, and also provide new information on the age and correlation the succession. I will combine the faunal data with new information on the carbon isotope stratigraphy of the Steptoean–Sunwaptan boundary interval at Barton Canyon, Nevada, and compare it to a $\delta^{13}C$ curve for the correlative interval in the Honey Creek Formation in Oklahoma that was also developed as part of this study.

The present chapter will continue with an introduction to the study area and the stratigraphy and sedimentary facies. Chapter two will deal with the trilobite biostratigraphy, biofacies and carbon isotope stratigraphy of the succession, and Chapter three will provide treatment of the systematic paleontology of the trilobites that are the basis of much of this study.

Study area

The material that forms the basis of this thesis is from stratigraphic sections at three localities in eastern Nevada and western Utah that were measured by Jonathan Adrain and logged lithologically by S.R. Westrop (Fig. 1). Two sections in Nevada are in White Pine County. At Barton Canyon in the Cherry Creek Range (Fig. 1.1), a section through the Steptoean and basal Sunwaptan strata was studied on the ridge along the south side (section CHC–2). The Barton Canyon Member of the Windfall Formation, which is a major focus of this thesis, was sampled here (Fig. 2). A thick Sunwaptan succession was measured and logged on the ridge on the north side of canyon (section CHC–1). Trilobites from the base of the section were included in this study. The carbon isotope curve is a composite of the two sections, with *Elvinia* and *Irvingella major* zone samples from CHC–2 and younger samples from section CHC–1. The other section (STR), 47 km to the south of Barton Canyon, is on the Steptoe Ranch in the North Egan Range (Fig. 1.2). It encompasses the Barton Canyon Member and the lower part of the overlying Catlin Member.

The third locality is at Orr Ridge (section ORR) in the northern House Range, Millard County, Utah (Fig. 1.3). It lies on a NE–SW trending ridge that forms the southern side of Big Horse Canyon; the type section of the Orr Formation (Hintze and Palmer, 1976) is on the ridge immediately to the north. The entire Steptoean and lower part of the Sunwaptan sucession has been studied here, but this thesis focused on a single collection made from the uppermost Steptoean in the Sneakover Member of the Orr Formation

Stratigraphic setting

The Upper Cambrian succession in western Utah and eastern Nevada was deposited on a distally steepened carbonate ramp (Osleger and Read, 1993) that lay on a passive margin formed by Neoproterozic rifting (e.g., Merdith et al., 2017). Localities CHC and STR were outboard and down ramp of ORR, and, as a result, the stratigraphic successions are different.

Stratigraphy and sedimentary facies in the North Egan and Cherry Creek ranges, White Pine County.

The same succession occurs at the study sites in White Pine County. The shales and carbonates of the Dunderberg Formation are succeeded by the Windfall Formation, which is divided into three units. In ascending order, these are the Barton Canyon, Catlin and Bullwhacker members (Adrain and Westrop, 2004, fig. 2). Figure 2 summarizes the stratigraphy and correlation of the study interval.

Barton Canyon Limestone

This member forms a conspicuous low cliff of light grey carbonates (Fig 3.1) between the more recessive slopes formed by the Dunderberg Formation and the Catlin Member (Fig 4.1, 4.2). It varies in thickness from 11.1 m at STR to 14.1 m at CHC. It consists mostly of thick, stylo-bedded, bioturbated wakestone and cm-thick horizons of bioclastic packstone (Figs 5.1–5.3), with a bioclast-rich interval at the base, and a 10–20 cm thick condensed bioclastic lag at the top that includes the *Irvingella major* Zone, which defines

the base of the Sunwaptan Stage and marks the onset of a trilobite extinction event. Brady and Rowell (1976) characterized the Barton Canyon as having formed in a widespread area of shallow carbonate deposition that blanketed the shelf. They showed that it passed landward (toward what is now west-central Utah) into high-energy shoal deposits of cross-bedded grainstone. To the west, in central Nevada, the Barton Canyon carbonates are bounded by continental slope facies (Brady and Rowell, 1976) that include debris flows and soft-sediment slumping (Taylor and Cook, 1976). The large areal extent (more than 40,000 km^2 according to Brady and Rowell, 1976) of a rather monotonous, subtidal carbonate facies between west-central Utah and east-central Nevada implies a low gradient to the carbonate ramp.

*Wackestone-Packstone Fac*ies.—Almost all of the Barton Canyon Member consists of gray bioclastic wackestones (Fig. 6) and cm-thick bioclastic packstone layers with trilobite and echinoderm debris (Fig. 5.3). Bioturbation is recorded by irregular, often dolomitic swirls (Fig. 6; Fig. 5.3). Micritized peloids are also common. Spar-filled shelter porosity occurs beneath some bioclasts (Fig. 8).

As noted, by Brady and Rowell (1976), wackestone-packstone facies represents an open shelf below fairweather wave base. Echinoderms and trilobites record normal marine conditions. Thin concentrations of bioclasts in packstone layers, however, indicate that there was at least minor winnowing of the sea floor, as does spar-filled shelter porosity. As such, the Barton Canyon Member was probably deposited close to storm wave base.

In a broader context, the appearance of clean carbonates above the mixed carbonate-fine siliciclastic succession of the Dunderberg Formation implies a sea level

rise that pushed the clastic source onshore (see also Evans et al., 2003). Miller et al. (2012) identified it as the Sauk III transgression, a major flooding event that can be recognized widely in Laurentian North America. A second, equally abrupt sea level rise terminated carbonate deposition, with the appearance of the Catlin Member above the Barton Canyon Member. The onset of each of these sea level rises is marked by a bioclastic lag.

Bioclastic Lag Facies.—Bioclastic lags occur at the bottom and top of the member. From their stratigraphic positions at the onset of sea level rise, they represent onlap shell beds (Zecchin, 2007; Catuneanu and Zecchin, 2013). Such beds form under conditions of sediment starvation and rest on ravinement surfaces (Zecchin, 2007).

The basal meter of the Barton Canyon is bioclastic pack-, grain- and rudstone with dm-thick intercalations of stylolitic lime mudstone–wackestone. Bioclastic intervals lack primary sedimentary structures like cross-bedding, but yield trilobites of the *Elvinia* Zone. The unit is interpreted as recording higher energy conditions in the initial phase of the Sauk III transgression. Above the basal meter, in the lower half of the member, cm-thick intervals of grainstone occur as minor interbeds in the wackestone-packstone facies (Fig. 11.1).

The very top of the Barton Canyon Member is a 10–20 cm thick, condensed interval of trilobite-rich, bioclastic grainstone and rudstone that includes the *Irvingella major* Zone (Westrop and Adrain, 2013; Westrop, unpublished). In detail, this lag deposit is divided internally into four (in CHC sections) or three (at STR section) bioclastic layers that are separated by planar to irregular hardgrounds (Westrop and Adrain, 2013). At both localities, the basal layer yield trilobites of the *Elvinia* Zone, with the overlying

layers containing the *Irvingella major* Zone fauna. The lag is overlain abruptly by the deeper water facies of the Catlin Member (Fig. 4.1), and its stratigraphic position indicates that is a strongly condensed onlap shell bed.

Catlin Member

The trilobite faunas of the Catlin Member were not considered in this study. However, the member is a source of carbon isotope data and it is described briefly from published sources (Westrop and Adrain, 2007, 2013) and unpublished information from S.R. Westrop. The carbon isotopic data are from the lower 15 m that consists of thin-bedded, dark colored, cherty lime mudstone and calcisiltite, both of which include laminae of terrigenous silt, and shale (Fig 11.2). Minor bioturbation is present, but undisturbed plane lamination becomes more prevalent up section. Cm-thick echinoderm-trilobite grainstone horizons 0.47 m and 1.39 m above the base of the member at section CHC-2 yield low diversity assemblages dominated by olenid trilobites related to *Parabolinoides* Frederickson, 1949, and confirm the disappearance of the faunas of the *Elvinia* and *I. major* zones (Westrop, unpublished). In thin section (Fig. 9), the grainstone exhibits early prismatic synsedimentary cements radiating off trilobite sclerites. The facies change at the base of the Catlin indicates deepening and reduced bioturbation, with primary sedimentary lamination is consistent with dysoxic conditions.

Stratigraphy and sedimentary facies in the northern House Range, Millard County

Section ORR at Big Horse Canyon, Orr Ridge, was measured and logged within a kilometer of the type section of the Orr Formation, whose five subunits are, in ascending order, the Big Horse Limestone, Candland Shale, Johns Wash Limestone, Corset Spring Shale and Sneakover Limestone members (Hintze and Palmer, 1976). Section ORR starts at the top of the cliff formed by the Johns Wash Limestone and extends through the Corset Spring Shale and Sneakover Limestone to the base of the Notch Peak Formation (Field Photo Fig 1.2). One collection from the Sneakover Member, 59.4 m above the base of the section and immediately below the *Irvingella major* Zone, is an important source of trilobites for the systematic component of this thesis. A few sclerites of *Deckera* Frederickson, 1949 from a collection in the Corset Spring Shale, 7.5 m above the base of the section, are also included in the study. The rest of the trilobite faunas, as well as the stratigraphy and facies of the Corset Spring Shale and Sneakover Limestone, are under study by S.R. Westrop, and only a brief description is present here.

The Corset Spring Shale at Orr Ridge includes a poorly exposed, basal 8 m interval of green shale with minor carbonates that records a lowstand (Evans et. al., 2003; Miller et al. 2012). Collection ORR 7.5 is a float sample from near the top of the interval. The Sneakover Limestone is a ledge-forming, thick-bedded carbonate unit (Fig. 7.1) that is a readily mapped interval (Hintze and Palmer, 1976). As a map unit, the base of the Sneakover is marked by a steepening of the slope above the Corset Spring Shale. At section ORR, the lower boundary is drawn at the bottom of a 5 m interval of bio-intraclastic grainstone and packstone that rests on an irregular hardground with cm-scale

relief, 31.7 m above the base of the section (Westrop, unpublished data). Above this coarser-grained interval, lithologies through to the base of the *Irvingella major* Zone (about 59.6 m above the base of the section) are identical to the wackestone–packstone facies of the Barton Canyon Member in the South Egan and Cherry Creek ranges of Nevada. They include bioturbated wackestone with cm-thick, trilobite-echinoderm packstone horizons. Like the similar succession in Nevada, this segment of the Sneakover was deposited in relatively deep subtidal setting (Osleger and Read, 1991) although, again, the winnowing of the substrate to produce packstone horizons indicates that depths were above maximum storm wave base.

The sharp facies change above the *I. major* Zone recorded by the Catlin Member of east-central Nevada is absent in Utah, and ledge-forming carbonates of the Sneakover continue up section for about 20 m to the base of the Notch Peak Formation. Strata above the *I. major* Zone have been interpreted as recording a deepening (Evans et al., 2003), although the evidence, including darker color and loss of packstone horizons, is far more subtle than in Nevada.

Figure 1: Sampling locations, where: 1) Cherry Creek (CHC), Barton Canyon, Cherry Creek Range, White Pine County, Nevada; 2) Steptoe Ranch (STR), North Egan Range, White Pine County, Nevada; and 3) Orr Ridge (ORR), Northern House Range, Millard County, Utah

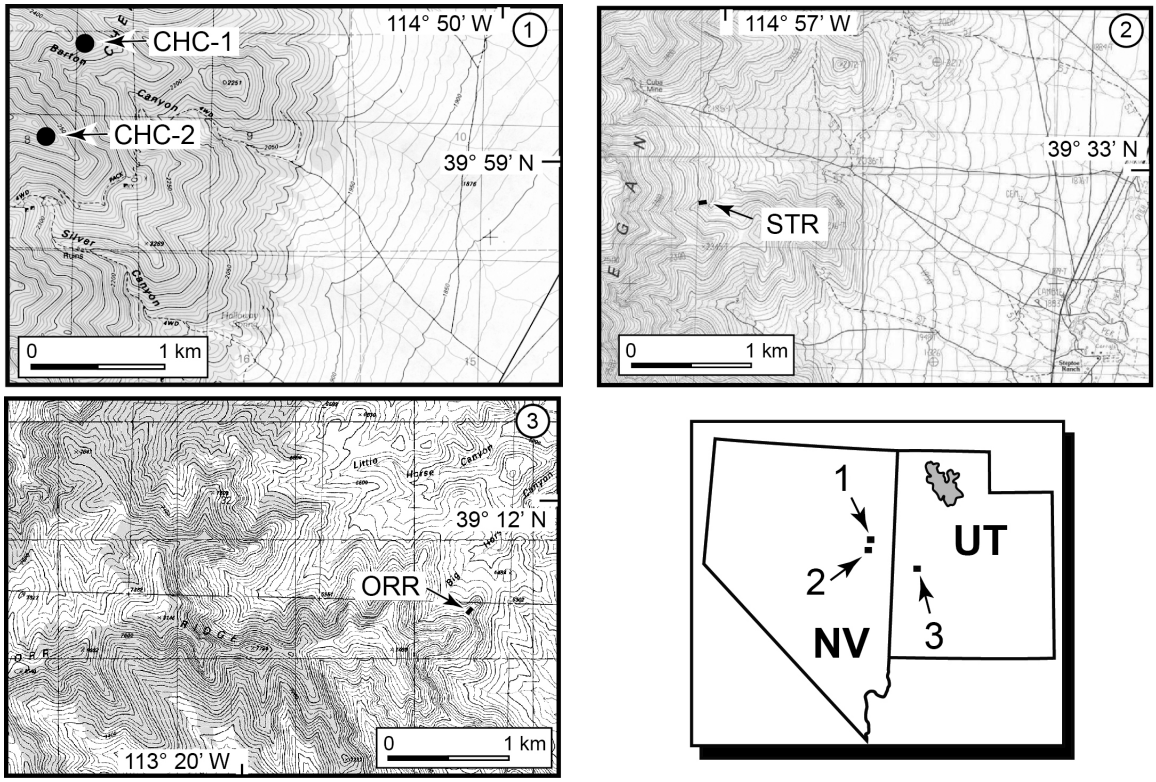
CHC-1
CHC-2
114° 50' W
39° 59' N
Silver Canyon
Barton Canyon
0 1 km
1
114° 57' W
39° 33' N
STR
0 1 km
2
39° 12' N
ORR
Little Horse Canyon
RIDGE
0 1 km
113° 20' W
3
1
2
3
NV
UT

Figure 2: Lithostratigraphy and trilobite biostratigraphy of the Steptoean-Sunwaptan boundary interval for the study locations of Nevada and Utah. The systematics portion of this thesis is based on trilobites sampled from the *Elvinia* Zone. However, carbon isotope data are derived from the *Elvinia* Zone through the *Taenicephalus* Zone.

Zones
Nevada
Utah
Sunwaptan
Steptoean
Taenicephalus
I. major
Elvinia
Windfall Formation
Catlin Member
Barton Canyon Limestone
Orr Formation
Sneakover Member

Figure 3: 1. Cliff-forming Barton Canyon Limestone Member of the Windfall Formation above talus-covered and vegetated slope of uppermost Dunderberg Formation. Backpack for scale in circle. Section CHC-1, Barton Canyon, Nevada.

2. Upper half of the ORR Formation, south side of Big Horse Canyon, northern House Range, Utah. Section ORR extends from the base of Corset Spring Shale Member to the base of the Notch Peak Formation. Line of section runs along the skyline.


1
Section CHC-1
Barton Canyon Member


2
Section ORR
Notch Peak Formation
Orr Formation
Sneakover Member
Corset Spring Shale Member
Johns Wash Limestone Member

Figure 4: 1. Cliff-forming Barton Canyon Limestone Member of the Windfall Formation above talus-covered and vegetated slope of uppermost Dunderberg Formation, and overlain by recessive slope of the Catlin Member. Section STR, Steptoe Ranch, Nevada. Figure in circle for scale.

2. Barton Canyon–Catlin boundary interval, showing location of the *I. major* Zone at the top of the Barton Canyon, and sharp contact with the mostly covered Catlin Member. Section STR, Steptoe Ranch. Backpack in rectangle for scale.

.


1
Section STR
Catlin Member
Barton Canyon Member

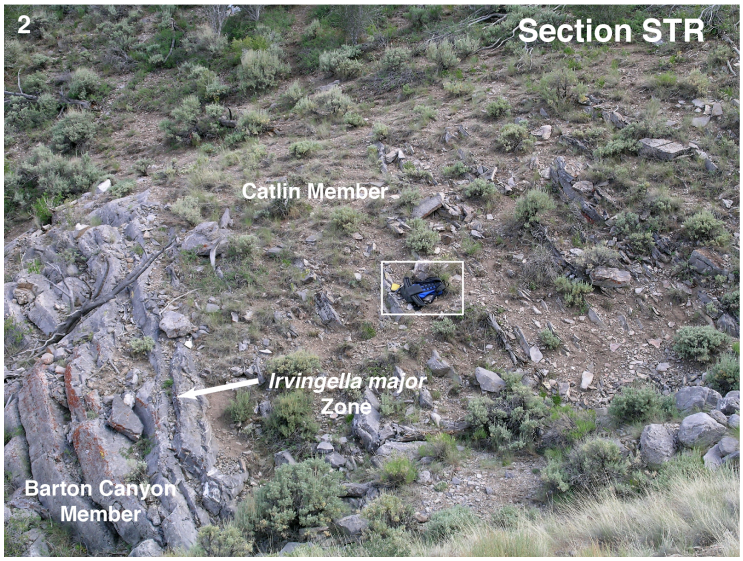
2
Section STR
Catlin Member
Irvingella major Zone
Barton Canyon Member

Figure 5: 1. Lower Barton Canyon Member, showing light grey color and typical thick-bedding. Section STR, 5.5 m above the base of the member. Notebook and hammer scale.

2. Bioturbated bioclastic wackestone to packstone, Barton Canyon Member. Section STR, 2 m above the base of the member. Pencil scale.

3. Bioturbated bioclastic wackestone with thin layers of packstone. Large trilobite sclerite near center of image. Section STR, 5.5 m above the base of the member. Fingertip scale.


1

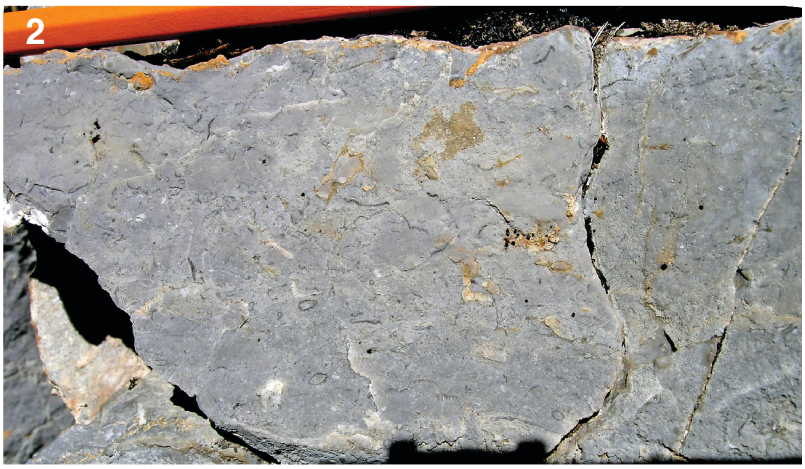
2


3

Figure 6: Polished slab of bioturbated wackestone with dolomitic burrow mottles. Section CHC-2, 7 meters above the base of the Barton Canyon Member.

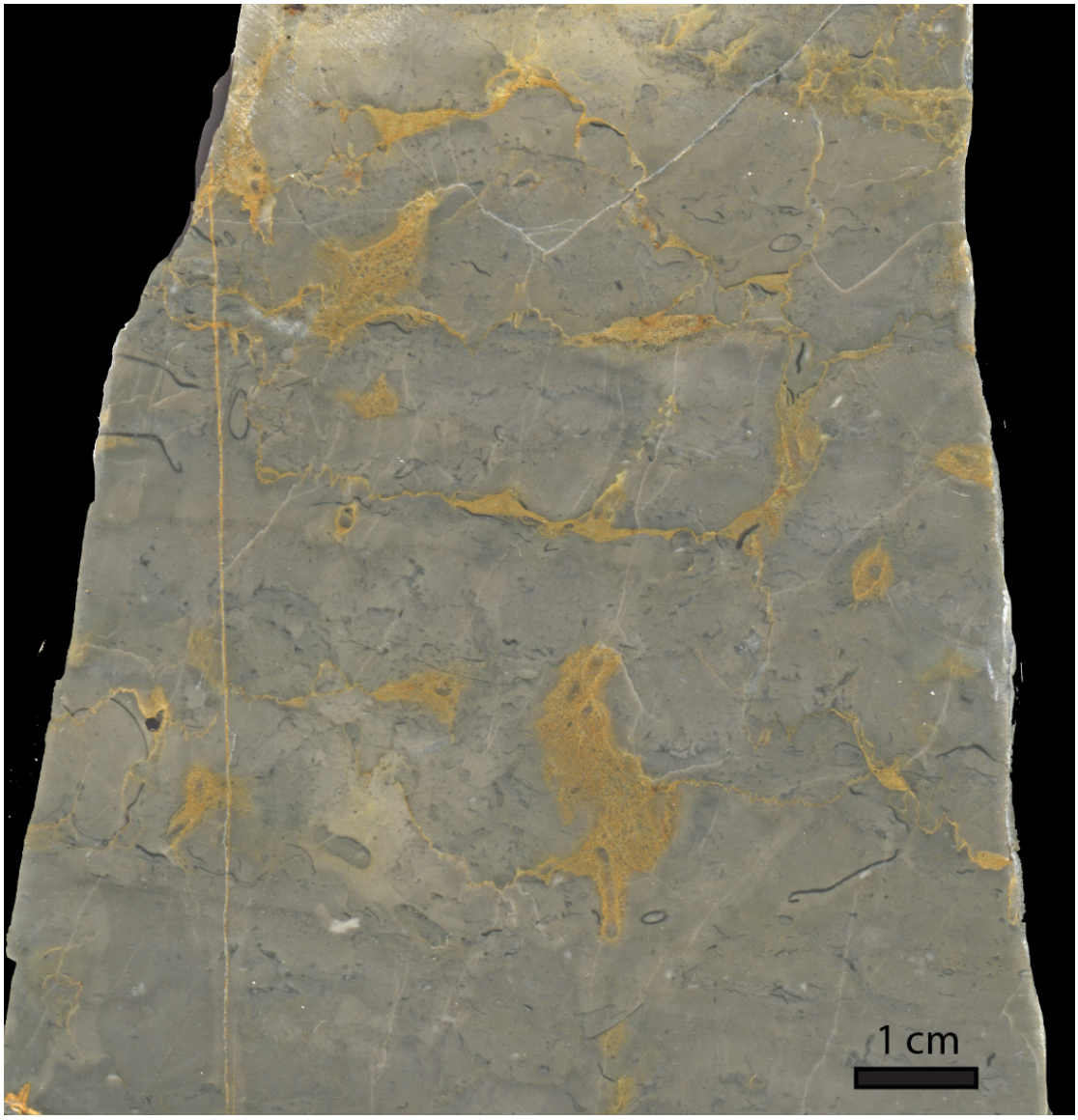
1 cm

Figure 7: 1. Typical exposure of Sneakover Limestone Member of the Orr Formation, showing typical thick-bedded, ledge-forming character. Backpack for scale. Steamboat Pass, southern House Range, Utah, about 45 km south of section ORR.

2. Bioturbated packestone with thin bioclastic packstone layers similar to the lithology of the Barton Canyon Member in Nevada. Pen scale. Section ORR, 37 m above the base of the section.

3. Cm-thick trilobite-echinoderm packstone layer with brown dolomitic burrow-mottles interlayered with lime mudstone–wackestone. Section ORR, about 42 m above the base of the section.


1

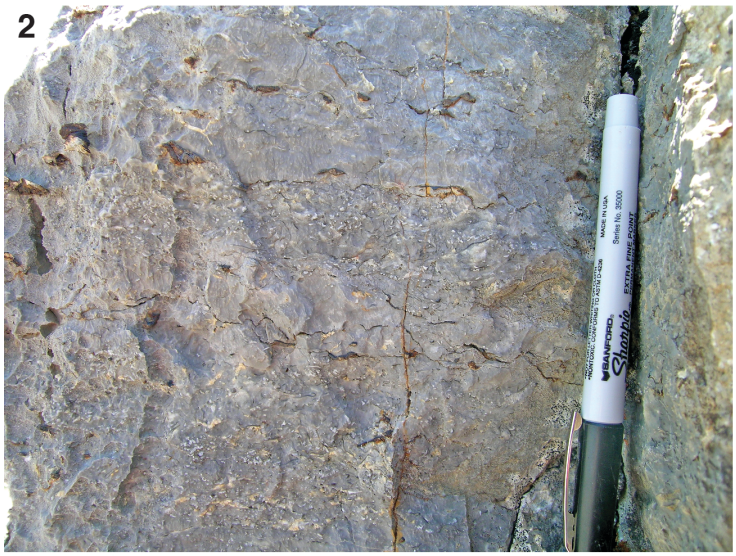
2
SANFORD
Sharpie
EXTRA FINE POINT


3

Figure 8: Spar-filled shelter porosity beneath a trilobite sclerite from CHC.

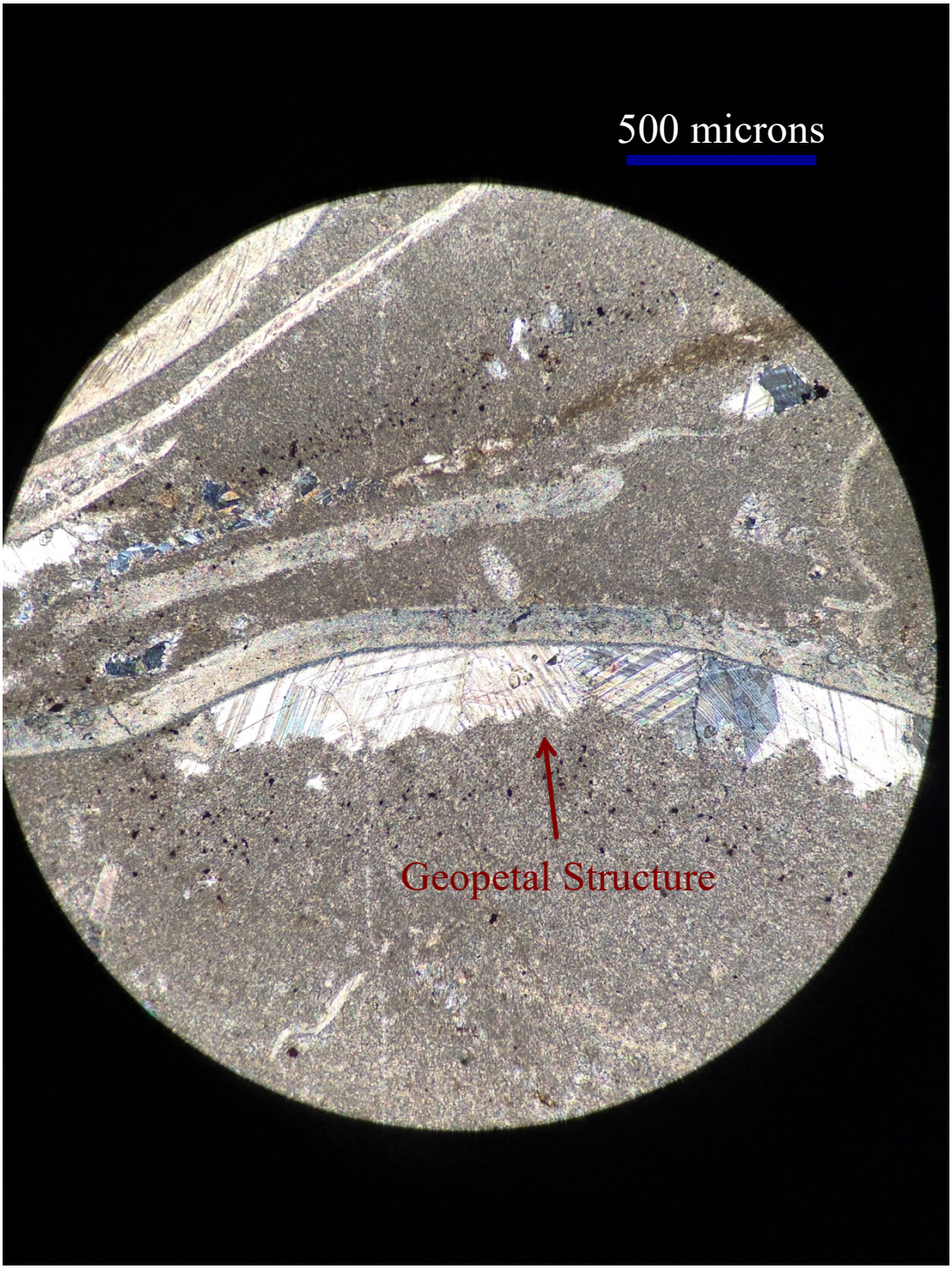
500 microns
Geopetal Structure

Figure 9: Arrow indicating synsedimentary calcite cements radiating from bioclast from the Catlin Member. Slide stained with Alizerin Red.

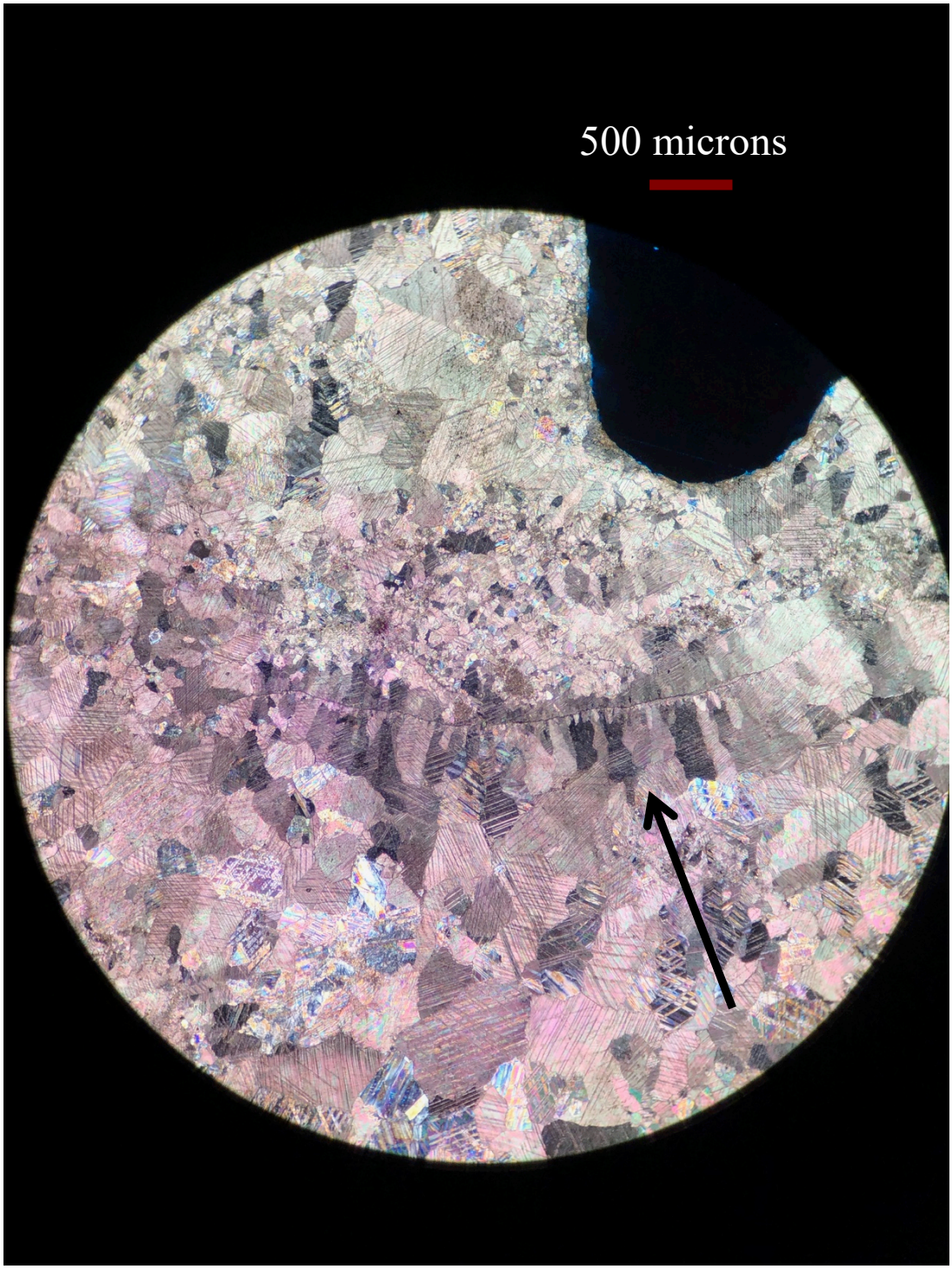
500 microns

Figure 10: Lithologic log for CHC-2. *Irvingella major* Zone occurs above CHC-2-216.95. Below is the Barton Canyon Limestone.

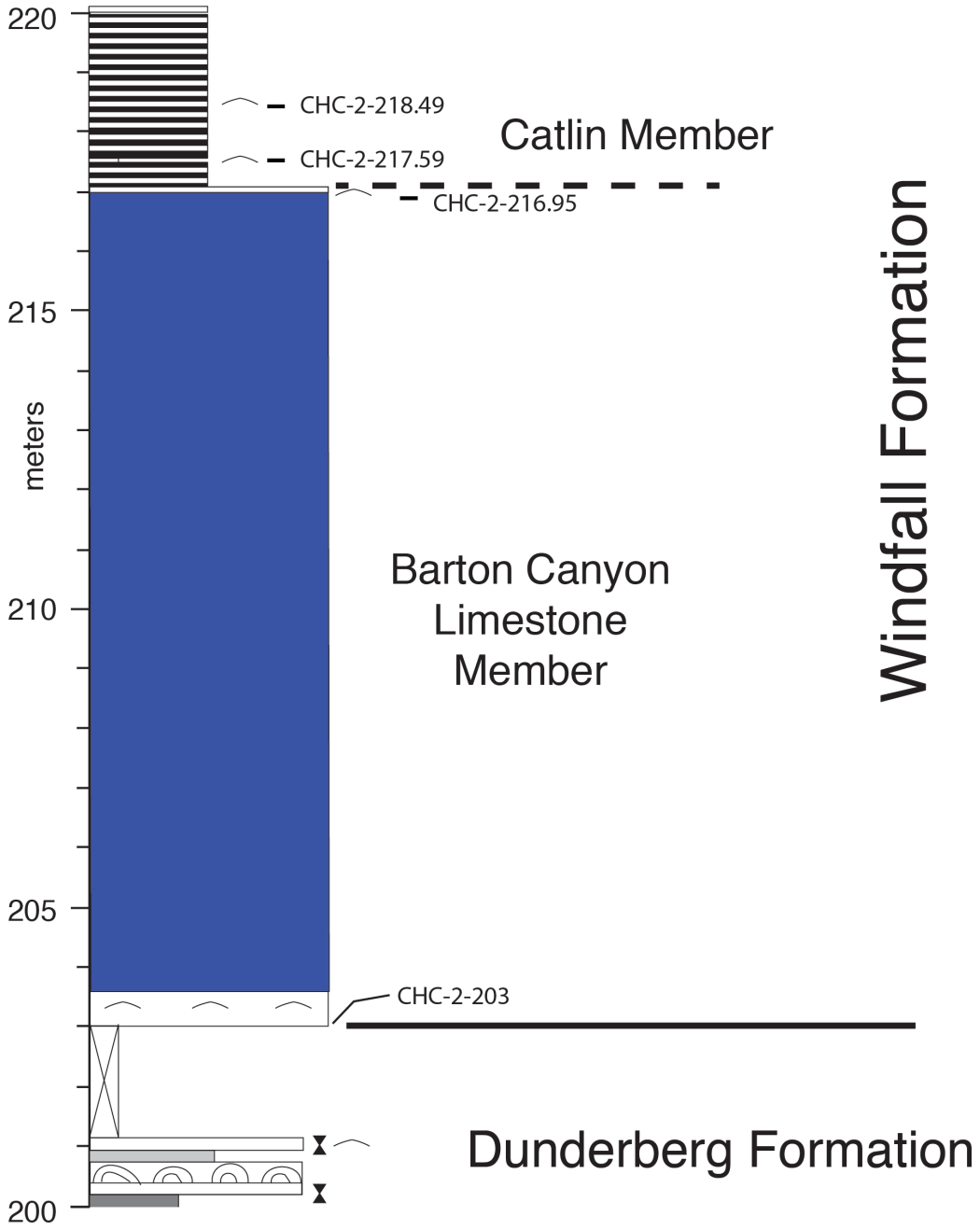

Thin-bedded, laminated, dark grey, silty (siliciclastic) lime and calcisiltite with thin shales.

Thick, stylo-bedded, mostly light grey, bioturbated lime wackestone with cm-thick bioclastic packstone. Cm- to dm-thick interbeds bioclastic grainstone and rudstone in lower half of Barton Canyon Member

Bioclastic grainstone or packstone

Sand-grade intraclasts

Thrombolitic microbial buildups

Figure 11: 1. Trilobite-echinoderm grainstone, lower Barton Canyon, section CHC–2, about 6 m above the base of the member. Lens cap scale.

2. Poorly exposed Catlin Member. Section STR; hammer is about 2.3 m above the base of the member.


1


2

References:

Adrain, J. M., and S. R. Westrop. 2004. A Late Cambrian (Sunwaptan) silicified trilobite fauna from Nevada. Bulletins of American Paleontology, 365:1–56.

Adrain, J. M., and S. R. Westrop. 2005. Late Cambrian ptychaspidid trilobites from western Utah: implications for trilobite systematics and biostratigraphy. Geological Magazine, 142:377–398.

Brady, M. J., and Rowell, A. J., 1976. An Upper Cambrian subtidal blanket carbonate, eastern Great Basin: Brigham Young University Geology Studies, 23:153–164.

Chatterton, B.D. and Gibb, S., 2016. Furongian (Upper Cambrian) Trilobites from the McKayGroup, Bull River Valley, Near Cranbrook, Southeastern British Columbia, Canada. Geological Association of Canada and the Canadian Society of Petroleum Geologists.

Chatterton, B.D. and Ludvigsen, R., 1998. Upper Steptoean (Upper Cambrian) trilobites from the McKay Group of southeastern British Columbia, Canada. Memoir, The Paleontological Society, 1-43.

Evans, K.R., J.F. Miller, and B.F. Datillo. 2003. Sequence stratigraphy of the Sauk Sequence: 40th anniversary field trip in western Utah, p. 17–35. In T. W. Swanson (ed.), Western Cordillera and adjacent areas. Geological Society of America Field Guide 4.

Hall, J., and R. P. Whitfield. 1877. Report of the Geological Exploration of the Fortieth Parallel. Part 2 Palaeontology. Professional Papers of the Engineer Department, US Army, 18:199–299.

Hintze, L.F. and Palmer, A.R., 1976. Upper Cambrian Orr Formation: Its subdivisions and correlatives in western Utah. United States Geological Survey Bulletin 1405 G, 1-25.

Merdith, A.S., Collins, A.S., Williams, S.E., Pisarevsky, S., Foden, J.D., Archibald, D.B., Blades, M.L., Alessio, B.L., Armistead, S., Plavsa, D. and Clark, C., 2017. A full plate global reconstruction of the Neoproterozoic. Gondwana Research, 50:84-134.

Merriam, C. W. 1964. Cambrian rocks of the Pioche Mining district Nevada. United States Geological Survey Professional Paper, 469:1–64.

Miller, J.F., Evans, K.R. and Dattilo, B.F., 2012. The Great American Carbonate Bank in the miogeocline of western central Utah: tectonic influences on sedimentation.

Nolan, T. B. 1962. The Eureka Mining District, Nevada. United Geological Survey Professional Paper, 406:1–78.

Osleger, D., and Read, J.F., n.d., Relation of Eustasy to Stacking Patterns of Meter-Scale Carbonate Cycles, Late Cambrian, U.S.A.: p. 28.

Palmer, A. R. 1955. Upper Cambrian Agnostidae of the Eureka district, Nevada. Journal of Paleontology, 29:86–101.

Palmer, A. R. 1965a. Biomere: A new kind of biostratigraphic unit. Journal of Paleontology, 39:149–153.

Palmer, A. R. 1965b. Trilobites of the Late Cambrian Pterocephaliid Biomere in the Great Basin, United States. U.S. Geological Professional Paper, 493: 1–154.

Palmer, A. R. 1984. The biomere problem: evolution of an idea. Journal of Paleontology, 58:599–611.

Saltzman, M. R., J. P. Davidson, P. Holden, B. Runnegar, and K. C. Lohmann. 1995. Sea-level-driven changes in ocean chemistry at an Upper Cambrian extinction horizon. Geology, 23:893–896.

Saltzman, M.R., B. Runnegar, and K. C. Lohmann. 1998. Carbon isotope stratigraphy of Upper Cambrian (Steptoean Stage) sequences of the eastern Great Basin: Record of a global oceanographic event. Geological Society of America Bulletin 110:285-297.

Stitt, J. H. 1971a. Repeating evolutionary pattern in Late Cambrian trilobite biomeres. Journal of Paleontology, 45:178–181.

Stitt, J. H. 1971b. Late Cambrian and earliest Ordovician trilobites, Timbered Hills and lower Arbuckle Groups, western Arbuckle Mountains, Murray County, Oklahoma. Oklahoma Geological Survey Bulletin, 110:1–83.

Taylor, M.E. and Cook, H.E., 1976. Continental shelf and slope facies in the Upper Cambrian and Lowest Ordovician of Nevada.

Walcott, C. D. 1884. Paleontology of the Eureka District. U.S. Geological Survey Monograph, 8:1–298.

Westrop, S R., and M. B. Cuggy. 1999 Comparative paleoecology of Cambrian trilobite extinctions. Journal of Paleontology, 73:337-354

Westrop, S.R., and Adrain, J.M., 2013, Biogeographic shifts in a transgressive succession: the Cambrian (Furongian, Jiangshanian; Latest Steptoean–earliest Sunwaptan) agnostoid arthropods *Kormagnostella* Romanenko and *Biciragnostus* Ergaliev in North America: Journal of Paleontology, 87:804

Zecchin, M., 2007. The architectural variability of small-scale cycles in shelf and ramp clastic systems: the controlling factors. Earth-Science Reviews, 84:21-55

Zecchin, M. and Catuneanu, O., 2013. High-resolution sequence stratigraphy of clastic shelves I: units and bounding surfaces. Marine and Petroleum Geology, 39: 1- 25.

Chapter II: Biostratigraphy, Trilobite Biofacies and Carbon Isotope Stratigraphy

Introduction

Palmer's (1960, 1962, 1965) landmark papers remain the most comprehensive studies of Steptoean trilobite and agnostoid arthropod faunas of the Great Basin, and established the current biostratigraphic zonation for the region. A recent program of new field work is the basis for a major revision of the faunas, but published work so far has focused on individual genera (Westrop and Adrain, 2007, 2009a, b, 2013, 2016; Westrop et al., 2007, 2008, 2010; Armstrong et al., 2020). This field work led to the discovery of previously unknown latest Steptoean faunas from Cherry Creek and Steptoe Ranch, Nevada, and Orr Ridge, Utah, which are the subject of this thesis. Each fauna lies immediately below the trilobite extinction at the end of the Steptoean Stage. This event, which occurs at the base *Irvingella major* Zone, serves as a marker that correlates the Barton Canyon Member of the Windfall Formation and the Sneakover Member. These members were deposited in distal and more proximal ramp settings, respectively, and their new faunas provide a perspective on biofacies differentiation along a depth gradient immediately prior to the onset of the extinction. Carbon isotope data provide an independent means of correlating the strata, and also offer evidence for changes in carbon cycling in the oceans during a time of major faunal turnover.

This chapter will evaluate the age and correlation of the faunas and will document the trilobite associations of the Barton Canyon Limestone and the Sneakover Member. Biofacies analysis will compare relative abundances and diversity between study sites ramp, as well as with previously published studies. Finally, carbon isotope data from the

Barton Canyon Member is compared to previously published information for the Sneakover Member (Saltzman et al., 1998) and to a new curve for the latest Steptoean and earliest Sunwaptan of Oklahoma.

Age and correlation of the faunas

Seventy years ago, Wilson and Frederickson (1950) showed that the *Irvingella major* Zone was one of the most widely correlatable biostratigraphic units in the Cambrian succession of Laurentian North America. Subsequent studies (e.g., Stitt, 1971, 1977; Westrop, 1986; Pratt, 1992; Taylor et al., 1994; Westrop and Adrain, 2007) have confirmed and elaborated on this earlier work. Although the *I. major* Zone marks the onset of the extinctions, it is a conventional zone defined by the entry of species into the succession, rather than by the disappearance of elements of the underlying faunas. Species of *Comanchia* Frederickson, in Wilson and Frederickson, 1950, and *Bartonaspis* Adrain and Westrop, 2007 have their lowest occurrences at the base of the zone across Laurentia. Within the Great Basin, *B. palmeri* Westrop and Adrain and *B. wilsoni* Westrop and Adrain are both present in the *I. major* Zone at Orr Ridge and at Barton Canyon (see Westrop and Adrain, 2007 for further discussion), providing a species-level correlation between the successions. New material described in this thesis shows that *Stenambon paucigranulus* Palmer 1965 also characterizes the zone at both of these localities.

From their positions immediately below the *I. major* Zone, the new *Elvinia* faunas from the Barton Canyon and Sneakover should be coeval. Shared species provide support for this correlation. *Labiocephalus cassia* n. gen and n. sp. occurs in both

collections CHC-2-216.95 and ORR 59.4, as does *Labiostria westropi* Chatterton and Ludvigsen 1998 and *Anechocephalus ralphi* n. sp.

Outside of the study area, *Labiocephalus* is known only from the Royer Ranch section in Oklahoma (collection RR 140) and also occurs immediately below (60 cm) the base of the *I. major* Zone (collection RR 142; Stitt, 1971, p. 66). Chatterton and Gibb (2016) showed that *Labiostria westropi* occurs in the upper *Elvinia* Zone (their *Wujiajiania lyndasmithae* and *W. sutherlandi* subzones) in the McKay Group of the Bull River Valley of southeastern British Columbia. The youngest subzone of the *Elvinia* Zone in the McKay Group, the *W. ricksmithi* Subzone, lacks *L. westropi* but it contains only three species of trilobites and agnostoids, and there are no published quantitative data to determine whether the apparent drop in diversity indicated in the range chart (Chatterton and Gibb, 2016, fig. 2) is simply a function of sample size or a genuine drop in the number of species. *Birciragnostus viator* Westrop and Adrain, 2013, which occurs in the uppermost *Elvinia* Zone with *L. westropi* at Barton Canyon and Steptoe Ranch, is recorded from the *W. ricksmithi* Subzone, confirming the assignment of that subzone to the latest Steptoean.

In conclusion, species range data support the conclusion that the new faunas from the Barton Canyon and Sneakover Limestone members are coeval and represent the youngest Steptoean assemblages in the Great Basin. These faunas are assigned to a new *Labiocephalus cassia* Zone, whose base is defined by the lowest occurrences of the eponymous species and *Anechocephalus ralphi*. *Birciragnostus viator* Westrop and Adrain, 2013 is confined to the zone.

Trilobite Biofacies

Upper Cambrian trilobite biofacies in Laurentian North America have been documented extensively over the four decades (e.g., Ludvigsen and Westrop, 1983; Westrop, 1986; Westrop and Cuggy, 1999; Taylor et al., 1999), typically with multivariate statistical analysis. For this study, there are only three collections and the sample sizes are small, but they point to differences in composition between inner and outer parts of the ramp. Abundances were calculated using the minimum number of individuals method (Gilinsky and Bennington, 1994) and was generally equivalent to the maximum number of cranidia for each genus in the collection.

Pterocephalia-Iddingsia Biofacies

Collection ORR 59.4 from the Sneakover yielded 51 individuals, but includes 9 genera (Fig 1. *Elvinia* (7%), *Iddingsia* (5%), *Pterocephalia* (7%), and "*Morosa"* (15%); other, less common genera are *Anechocephalus Deckera*, *Labiocephalus*, *Labiostria*, and *Dokimocephalus*. Species diversity is slightly higher than in the *Labiostria–Anechocephalus* Biofacies that occurs down-ramp in Nevada (9 species versus 7 species in a sample rarefied to 50 individuals; Fig. 2).

Labiostria-Anechocephalus Biofacies

This biofacies occurs in the more distal sites on ramp in the Barton Canyon Member. At Barton Canyon, 60 individuals yielded 8 genera. Two-thirds of the individuals were represented by the two nominate genera, *Anechocephalus* and *Labiostria*, with *Elvinia* and *Noelaspis* together comprising 22% of individuals (Fig. 1). At Steptoe Ranch, a

smaller collection of 28 individuals and 6 genera had *Elvinia* ranked first (46%) with *Labiostria* and *Anechocephalus* accounting for a combined of 32% (Fig. 1). Rarefaction curves (Fig. 2) for the two collections are virtually identical, and confirm that species diversity is slightly lower than in the *Pterocephalia-Iddingsia* Biofacies.

Comparison of Biofacies.—Elvinia is the only genus that is common in both the *Pterocephalia-Iddingsia* biofacies and the *Labiostria-Anechocephalus* biofacies, but this is not surprising as it is reported widely across North America (see Occurrence section for *E. roemeri* in Chapter III). The two biofacies differ in associated taxa. In the more proximal ramp settings, *Iddingsia*, *Pterocephalia*, and "*Morosa"* are confined to the *Pterocephalia-Iddingsia* biofacies. *Labiostria*, and *Anechocephalus* are abundant in the more distal biofacies in the Barton Canyon Limestone that bears their name, but both of these genera are rare up-ramp in the Sneakover Member.

Comparisions with biofacies in other regions.— Chatterton and Ludvigsen (1998) published abundance data for a deep water biofacies in the McKay Group of southeastern British Columbia that was subsequently named the *Wujiajiania* Biofacies by Chatterton and Gibb (2016). The olenid *Wujiajiania* (51%) and *Labiostria* (37%) are the dominant genera in a sample of more than 3600 trilobite and agnostoid individuals, and the latter is shared with the *Labiostria–Anechocephalus* Biofacies. Indeed, *Labiostria* is abundant only in deeper water lithofacies in Laurentia. Other genera, including *Pterocephalia* (6%), *Irvingella* (1%), and *Elvinia* (1%), are minor components of the *Wujiajiania* Biofacies. Although it is absent from the *Labiostria–Anechocephalus* Biofacies,

Wujiajiania does occur in the overlying Catlin Member at Barton Canyon and at Steptoe Ranch, suggesting that the *Wujiajiania* Biofacies occupied deeper and possibly less oxygenated water environments (Westrop, unpublished).

Chatterton and Gibb (2020) established two other biofacies in the McKay Group based on a qualitative assessment of their collections and they did not present any quantitative data. Their *Labiostria–Pterocephalia* Biofacies is perhaps closest to the *Labiostria–Anechocephalus* Biofacies of the Barton Canyon Member, although sclerites of *Pterocephalia* have yet to be found the latter. Based on the stratigraphic occurrences of *Labiostria* and *Wujiajiania* at the Barton Canyon and Steptoe Ranch sections, the *Labiostria–Pterocephalia* Biofacies of the McKay Group probably occupied sites father up-ramp than the *Wujiajiana* Biofacies. A *Proceratopyge* Biofacies has been reported from deep water facies in both the McKay Group (Chatterton and Gibb, 2020) and the Rabbitkettle Formation of northwestern Canada (Pratt, 1992). *Proceratopyge* is not present in the study interval in both Nevada and Utah, and Chatteron and Gibb (2020, p. 20) noted that the *Proceratopyge* Biofacies occurred in older strata than their *Labiostria–Pterocephalia* Biofacies.

Westrop and Cuggy (1999) included collections from uppermost *Elvinia* Zone strata in their quantitative analysis of biofacies distribution patterns at trilobite extinction events. Their data from shallow subtidal carbonates were from Stitt's (1971, 1977) abundance counts from the Honey Creek Formation of Oklahoma, including collections from the Royer Ranch section that were analyzed for carbon isotopes as part of this thesis (see below). All of the *Elvinia* collections from the Honey Creek Formation formed a cluster that was assigned to the *Camaraspis* Biofacies, and were dominated by the

eponymous genus (Westrop and Cuggy, 1999, fig. 14). *Camaraspis* is absent from all of the collections used in this study. Indeed, it has yet to be recovered from any *Elvinia* Zone succession in the Great Basin (Palmer, 1960, 1965; Westrop, unpublished), but it is abundant in the inner shelf siliciclastic facies of the Upper Mississippi Valley in Minnesota and Wisconsin (Eoff, 2012). *Pterocephalia-Iddingsia* Biofacies of the Sneakover Limestone does share some genera with the *Camaraspis* Biofacies, including "*Morosa", Pterocephalia* and *Elvinia*. The two biofacies record ecological differentiation between shallower inner shelf and deeper subtidal, outer shelf settings.

Conclusions

Quantitative analysis of Upper Cambrian collections from across North America has highlighted changes in trilobite distribution before, during, and after trilobite extinction events (Ludvigsen and Westrop, 1983; Westrop, 1986, 1996; Westrop and Cuggy, 1999). A general pattern is a shift from a well-differentiated spectrum of environmentally related biofacies prior to the extinctions, to widespread associations of trilobites whose distribution cuts across several lithofacies boundaries. This study provides new information on trilobite distribution prior to the onset of the end-Steptoean extinction, and provides further evidence of strong faunal differentiation along a depth gradient. The more distal *Labiostria-Anechocephalus* Biofacies is generally similar to other deep water biofacies reported from western Canada. The more proximal *Pterocephalia-Iddingsia* biofacies is compositionally distinct from shallower inner shelf trilobite associations.

Figure 1: Bar charts with relative abundance of trilobite genera for each location: Orr Ridge (ORR), Cherry Creek (CHC), and Steptoe Ranch (STR).

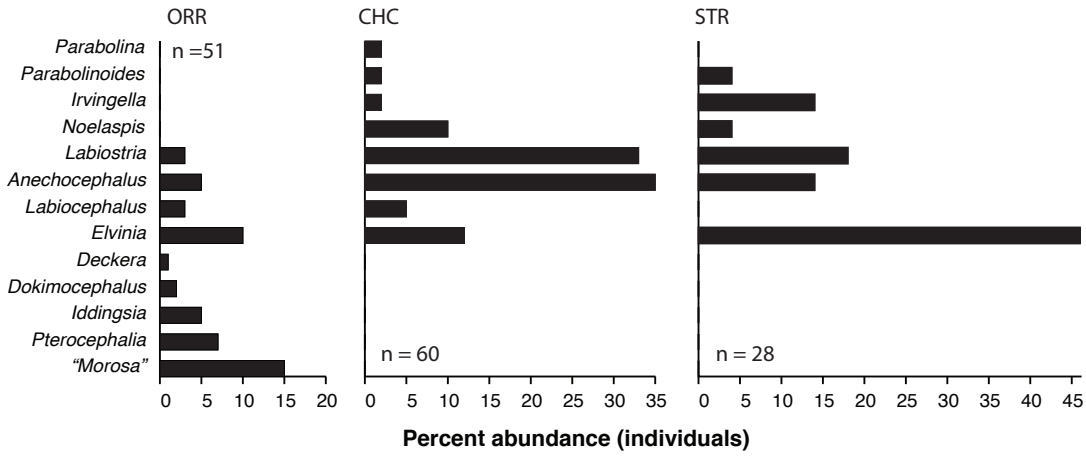
ORR
CHC
STR
Parabolina
Parabolinoides
Irvingella
Noelaspis
Labiostria
Anechocephalus
Labiocephalus
Elvinia
Deckera
Dokimocephalus
Iddingsia
Pterocephalia
"Morosa"
n =51
n = 60
n = 28
0 5 10 15 20
0 5 10 15 20 25 30 35
0 5 10 15 20 25 30 35 40 45
Percent abundance (individuals)

Figure 2: Rarefaction curves for each location (ORR, CHC, STR) showing the estimated number of species relative to the number of individuals collected. The Orr Ridge fauna (ORR) is represented by red stars, and has the highest number of expected species. The Barton Canyon fauna from the Cherry Creek range (CHC) is represented by black circles. The fauna from Steptoe Ranch (STR) is represented with blue crosses.

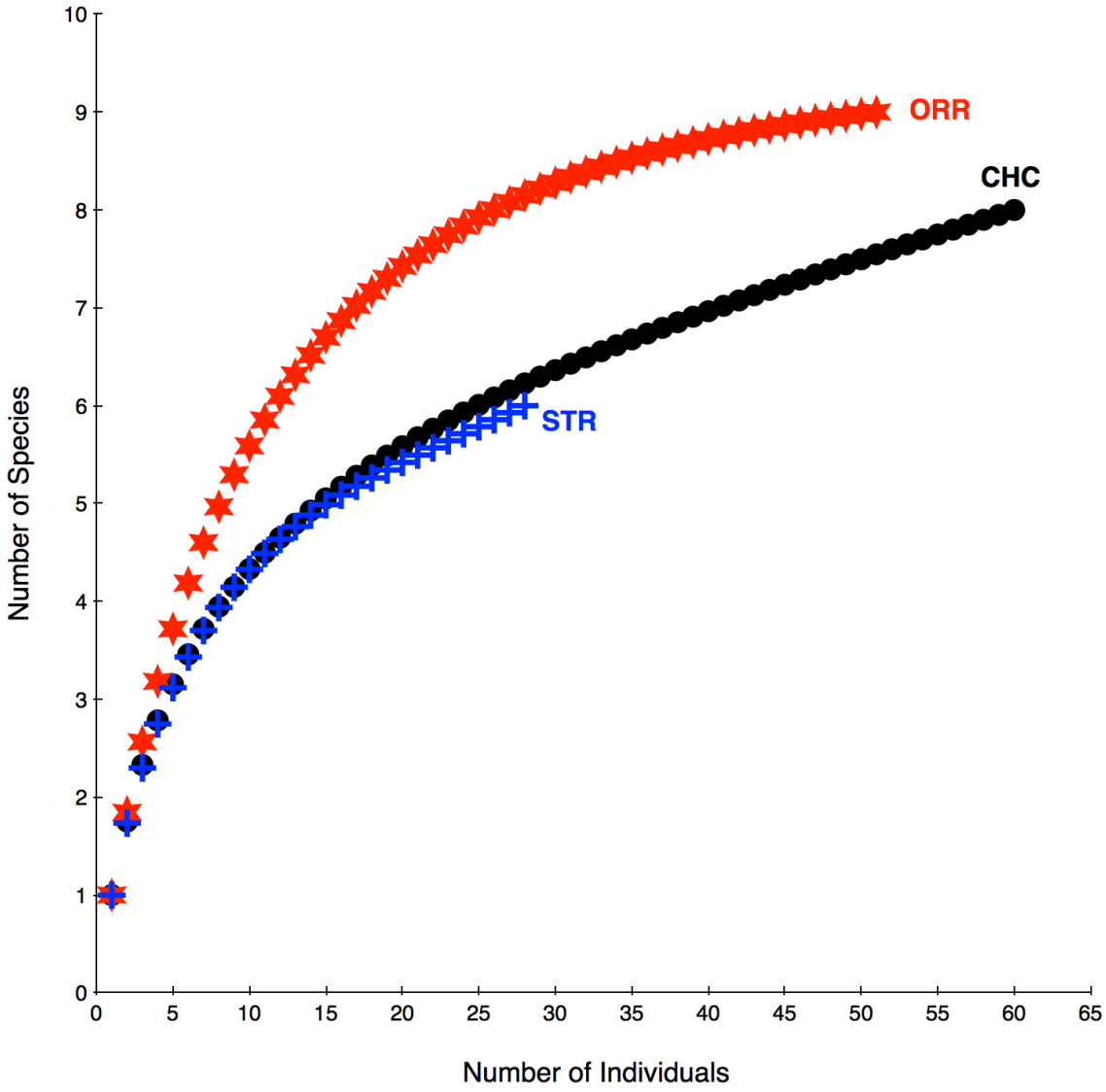
ORR
CHC
STR
Number of Species
Number of Individuals
0
1
2
3
4
5
6
7
8
9
10
0
5
10
15
20
25
30
35
40
45
50
55
60
65

Carbon isotope stratigraphy across the Steptoean–Sunwaptan boundary

Carbon isotope stratigraphy is a valuable tool for correlation of marine carbonate rocks and can be applied to rocks as old as Archean (Saltzman and Thomas, 2012). Carbonate rocks record past perturbations in the global carbon cycle as excursions in $\delta^{13}C_{carb}$ (Gill et al., 2011). Positive excursions of $\delta^{13}C$ reflect the burial of organic carbon as a result of enhanced preservation due to anoxic conditions, high sedimentation rates, or increased productivity (Saltzman et al., 2004). During the Late Cambrian to Early Ordovician, there are five modest to high positive $\delta^{13}C$ excursions that are associated with trilobite extinction events (Saltzman et al. 2015, fig. 1). In the study area of Nevada and Utah, positive excursions have been reported from the extinction intervals at the base of the Sunwaptan Stage (Saltzman et al., 1995; peaks at +2.8‰), base of the Steptoean (Paibian) Stage (Saltzman et al., 1998; lower part of the Steptoean Positive Carbon Isotope Excursion [SPICE], that rises to about +4 ‰ in the *Dunderbergia* Zone), and base of the Ordovician Stairsian Stage (Saltzman et al., 2015; peaks at about +1.5‰). Concurrent positive excursions in $\delta^{34}S_{cas}$ (carbonate-associated sulphate) at the basal Steptoean and Stairsian extinctions have been used to infer a possible relationship between sea-level rise and incursions of anoxic water onto the outer part of the shelf (Gill et al., 2011; Saltzman et al., 2015).

In this study, samples from section CHC-2 and a correlative section in Oklahoma (section RR of Stitt, 1971; collections housed at the Sam Noble Oklahoma Museum of Natural History) were analyzed for carbon isotopes by Dr. Michael Engel (School of Geosciences, Univ. Oklahoma). Samples from a second locality in Oklahoma (section KR1; Westrop et al., 2010) were also analyzed but showed a strong positive correlation

between $\delta^{13}C$ and $\delta^{18}O$ (Pearson's correlation coefficient; $r = 0.71$; $p < .001$) suggestive of diagenetic resetting, and were not included in the study. Published $\delta^{13}C$ data from Orr Ridge, Utah (House Range section of Saltzman et al., 1998; GSA Data Repository item 9804) were available for comparison. This section was measured on the slopes of Little Horse Canyon, and is located no more than a kilometer north of our section ORR, which was measured on the ridge at the south side of Big Horse Canyon. The succession at section CHC-2 is of interest because the extinction at the base of the Sunwaptan is associated with a major flooding surface, and the *Irvingella major* Zone, which marks the onset of trilobite turnover (Westrop and Cuggy, 1999), is a thin condensed bioclastic interval at the top of the Barton Canyon Member (Westrop and Adrain, 2007, 2013; Westrop, unpublished data). As such, this locality is unusual in providing direct sedimentological evidence for sea level rise and environmental change at the extinction (Westrop, unpublished data).

Methods

Limestone samples were crushed into a fine powder using a mortar and pestle. Afterward, 200-300 μg of each sample was placed into a Labco 938 W 12 ml borosilicate exetainer vial. These vials were then sealed with butyl rubber septa caps and placed in a thermostated sample tray at 50℃. They were then flushed with ultra-high purity He (99.999%) using a ThermoGas Bench II equipped with a PAL auto sampler flushing needle. This process took 360 seconds and removed the air from the vials. Afterward, a syringe was used to manually inject 0.4 ml of 100% phosphoric acid into the vials; the following reaction occurred over the course of two hours at 50℃. A PAL measurement

needle was used to sample the vials and the headspace CO_2 was analyzed for $\delta^{13}C$ and $\delta^{18}O$ using a Thermo Delta V Plus isotope ratio mass spectrometer.

According to Coplen, 2011 the compositions of carbon and oxygen isotopes are expressed as:

$$\delta^{13}C_{VPDB} = [R(^{13}C/^{12}C)_P / R(^{13}C/^{12}C)_{VPDB}] - 1$$

and

$$\delta^{18}O_{VPDB} = [R/(^{18}O/^{16}O)_P / R(^{18}O/^{16}O)_{VPDB}] - 1$$

where $R(^{13}C/^{12}C)_P = N(^{13}C)_P / N(^{12}C)_P$, the ratio of the number of ^{13}C and ^{12}C atoms in sample P and equivalent parameters apply for VPDB (Vienna Pee Dee Belemnite); $R(^{18}O / ^{16}O)_P = N(^{18}O)_P / N(^{16}O)_P$, the ratio of the number of ^{18}O and ^{16}O atoms in sample P and equivalent parameters apply for VPDB.

Kim et al. (2015) reported $\delta^{13}C$ values relative to VPDB on a normalized scale in which $\delta^{13}C$ of N-bromosuccinimide (NBS) 18 is -5.01 per mil. Values of $\delta^{18}O_{VPDB}$ are reported on a normalized scale where $\delta^{18}O$ of Standard Light Antarctic Precipitation (SLAP) is -55.5 per mil relative to Vienna Standard Mean Ocean Water (VSMOW). According to Brand et al. (2014) using this $\delta^{18}O_{VPDB}$ scale, the values of NBS 18 and NBS 19 are -23.01 per mil and -2.2 per mil respectively. At 50℃, the oxygen isotope fractionation factor for calcite is 1.00934 (Kim et al., 2015). The IUPAC-recommended relation was used to convert the calcite $\delta^{18}O_{VSMOW-SLAP}$ values from the $\delta^{18}O_{VPDB}$ values (Kim et al., 2015), where the IUPAC-recommended relation is:

$\delta^{18}O_{VSMOW-SLAP} = 1.03092\ \delta^{18}O_{VPDB} + 30.92$ per mil.

Results

Section CHC-2.— Collections came from a 30 meter-thick interval through the Barton Canyon and lower Catlin members of the Windfall Formation (Fig. 3; the Barton Canyon-Windfall boundary corresponds to the top of the condensed *I. major* Zone). Samples from the Barton Canyon Member are mostly from biosclastic wackestone and packstone, but those from the Catlin Member are more diverse lithologically and include bioclastic grainstone and rudstone. The samples were not screened lithogically for diagenetic features. However, covariation between $\delta^{13}C$ and $\delta^{18}O$ would be expected if a major diagenetic resetting of carbon isotopic ratios had occurred. A cross-plot of $\delta^{13}C$ and $\delta^{18}O$ (Fig. 4.1) did not reveal a significant correlation (Pearson's correlation coefficient; $r = 0.21$; $p = .31$), so there is no evidence for pervasive diagenetic alteration.

The $\delta^{13}C$ values in the segment of the curve (Fig. 1) represented by samples from the Barton Canyon Member oscillates between +0.7‰ and +1.25‰. At the very top of the member, at the *I. major* Zone, values rise into the lower two meters of the Catlin Member, reaching a peak of 2.17‰. There is a gap of about 4 m in the section, above which, values drop back to a range of roughly zero to 0.64‰.

The overall pattern is one of a modest positive excursion that begins near the onset of extinctions, and continues beyond, and peaks above, the second phase of turnover (e.g. Westrop and Cuggy, 1999) at the top of the *I. major* Zone. This is congruent with the record of $\delta^{13}C$ through this interval documented by Saltzman et al. (1995) in Wyoming and at sites farther to the east of CHC in Nevada and Utah.

Section RR.—Collections from the Honey Creek Formation of Arbuckle Mountains of south-central Oklahoma published by Stitt (1971) are now housed at the Sam Noble Museum. The Royer Ranch section, Murray County (Stitt, 1971, p. 64) was selected for geochemical analysis because collections are closely spaced through the Steptoean—Sunwaptan boundary interval, and they yield abundant trilobites that are currently being revisited by S.R. Westrop. The sample interval extends from the upper *Elvinia* Zone into the *Idahoia lirae* Zone. The samples are skeletal pack- and grainstone and, while micrite was sampled wherever possible, this could not be done with grainstone beds. A cross-plot of $\delta^{13}C$ and $\delta^{18}O$ (Fig. 4.2) did not reveal a significant correlation (Pearson's correlation coefficient; r = -.17; p =.31).

The $\delta^{13}C$ curve (Fig. 5) in the pre-extinction interval (*Elvinia* Zone) is quite variable but there is a general trend through a 3.7 m interval (38.7–42.4 m above the base of the section) to more positive values from -0.19‰–1.16‰). Values decline into the *I. major* Zone, reaching a minimum at the base of the *Taenicephalus* Zone, and then rising steadily to a peak at +1.36‰ through 4.25 m of section.

In detail, the pattern of change through the upper *Elvinia* Zone and into the lower *Taenicephalus* Zone is one of two trends of increasingly positive values separated by a reversal into the extinction interval. However, excluding the most positive sample (+1.16‰ at 42.4 m) in the *Elvinia* Zone, one could make a case for a single overall trend towards increasingly positive values. A similar, essentially steady rise in $\delta^{13}C$ from the *Elvinia* Zone into the *Taenicephalus* Zone was recorded by Saltzman (1999, fig. 8) in the Open Door Formation and correlative Snowy Range Formation in northwest Wyoming. Like section RR, the peak values of $\delta^{13}C$ in Wyoming are lower (reaching +1.11‰ about

2 m above the base of the *Taenicephalus* Zone at Warm Springs Peak; Saltzman, 1999, table 1) than maxima recorded in Nevada and Utah (Saltzman et al., 1995, 1998; this thesis).

Correlation and interpretation of the $\delta^{13}C$ curves.— The curves for CHC-2, RR and Saltzman et al.'s (1998) section at Orr Ridge are aligned using the base of the *Irvingella major* Zone (Fig. 6). As discussed earlier (see Biostratigraphy, above), this thin zone can be correlated across Laurentia at very high resolution. A feature of all three curves is a trend towards increasingly positive $\delta^{13}C$ values that begins in the vicinity the *I. major* Zone (either just below the base, as at Orr Ridge, or immediately above, as at RR). As noted above, a similar rise starting in the *Elvinia* Zone is apparent in the Steptoean-Sunwaptan boundary interval in Wyoming (Saltzman, 1999). Below the *Irvingella major*, there is no clear trend at CHC-2 and Orr Ridge, whereas at RR, there is a "noisy" positive trend that could, as noted above be interpreted as part of a longer-term rise into the *Taenicephalus* Zone.

As noted by Saltzman (1999), the trend towards increasingly more positive $\delta^{13}C$ values across the top of the Steptoean reflects, at a shorter temporal scale, the early part of the SPICE excursion (Saltzman et al., 1998) at the base of the stage. Saltzman et al. (1995) interpreted the positive trend across the Steptoean–Sunwaptan boundary as the result of increased carbon burial due to upwelling of anoxic water, possibly in response to a sea level rise, and Gerhardt and Gill (2016) offered a similar interpretation of the early part of the SPICE event. A role for anoxia is supported for the latter by the $\delta^{34}S$ record. Gill et al. (2011) documented a positive $\delta^{34}S_{cas}$ (carbonate-associated sulphate) excursion

that paralleled the $\delta^{13}C$ excursion of the SPICE in Laurentian North America and Australia, as well as a similar excursion in pyrite ($\delta^{34}S_{pyr}$) in Sweden (Baltica). They interpreted these coupled excursions as the product of increased burial of organic carbon and pyritic sulphur under anoxic and euxinic conditions. They proposed that the extinction was the result of anoxic waters moving onto the shelf during a sea level rise.

The changes in $\delta^{13}C$ across the Steptoean–Sunwaptan boundary are consistent with upwelling of anoxic waters. However, it remains to be seen exactly how anoxia may have caused these extinctions or, for that matter, the extinction at the base of the Steptoean Stage. There is independent evidence for sea level rise and environmental change at section CHC-2, where the deep water facies of the Catlin Member appear above the shallower carbonates of the Barton Canyon Limestone Member. However, anoxia is unlikely to spread into shallow, wind-mixed waters of the shelf interior. There is no independent sedimentary evidence for anoxia in the Honey Creek Formation of Oklahoma, which was deposited in shallow water, a tidally influenced setting in an archipelago of rhyolite islands (Donovan et al., 2000; McElmoyl and Donovan, 2000). And yet, the extinctions are clearly documented both in the Arbuckle (Stitt, 1971) and Wichita (Stitt, 1977; Westrop, unpublished data) mountains. An alternative possibility is that cascading ecological effects resulted (e.g., reduced population sizes and geographic ranges; invasive species) in response to the spread of anoxic and dysoxic waters in the outer part of the shelf (e.g., Westrop and Ludvigsen, 1987; Saltzman et al., 2015).

Figure 3: Carbon isotope curve for the Barton Canyon Limestone (CHC-2).

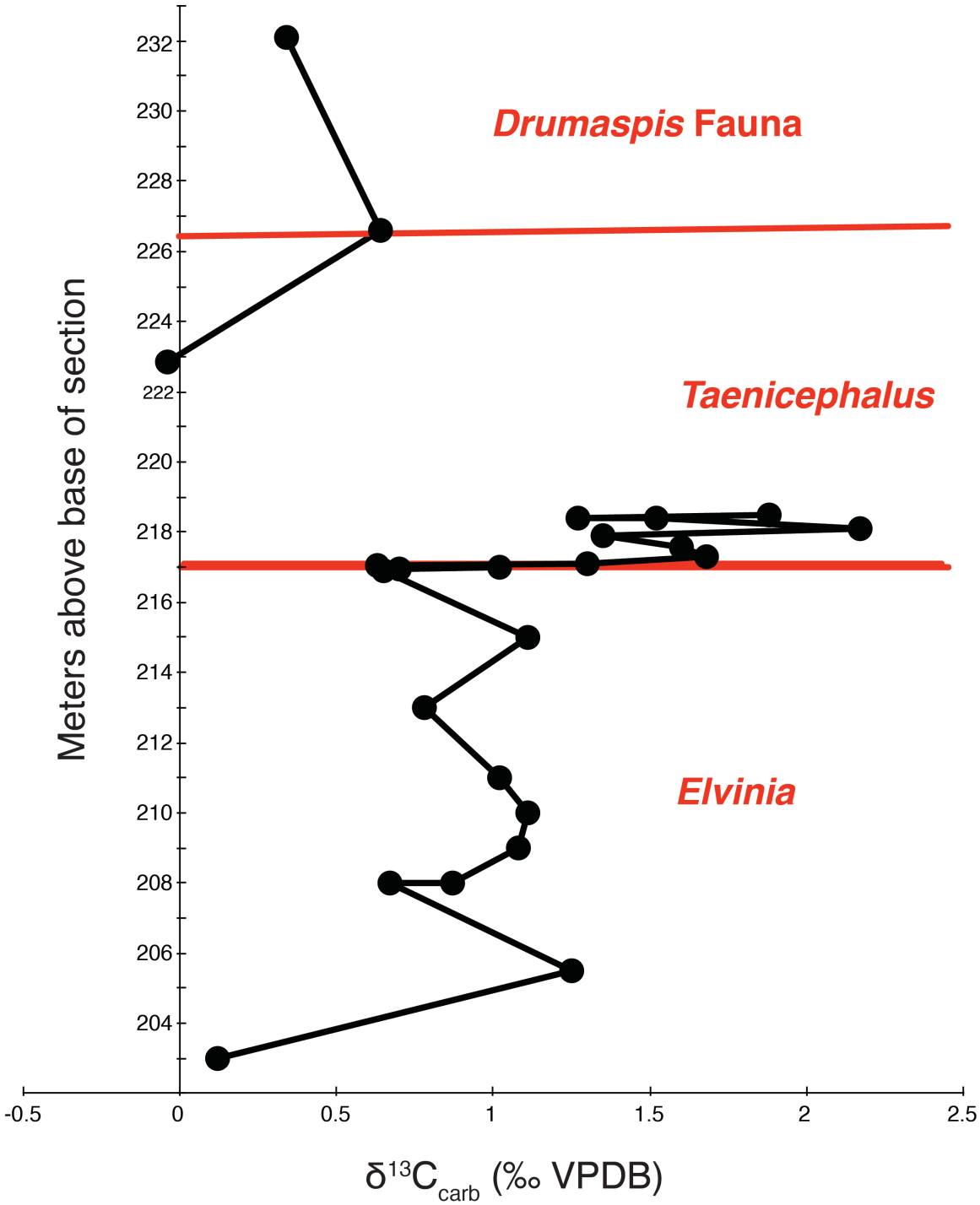
Drumaspis Fauna
Taenicephalus
Elvinia
Meters above base of section
232
230
228
226
224
222
220
218
216
214
212
210
208
206
204
-0.5
0
0.5
1
1.5
2
2.5
δ13Ccarb (‰ VPDB)

Figure 4: Top) Cross-plot of $\delta^{13}C$ and $\delta^{18}O$ for the Barton Canyon Limestone (CHC-2). There is no correlation; Pearson's correlation coefficient; r = 0.21; p =.3. Bottom) Cross-plot of $\delta^{13}C$ and $\delta^{18}O$ for the Honey Creek Formation (RR). Again, there is not a strong correlation, with Pearson's correlation coefficient; r = -.17; p =.31.

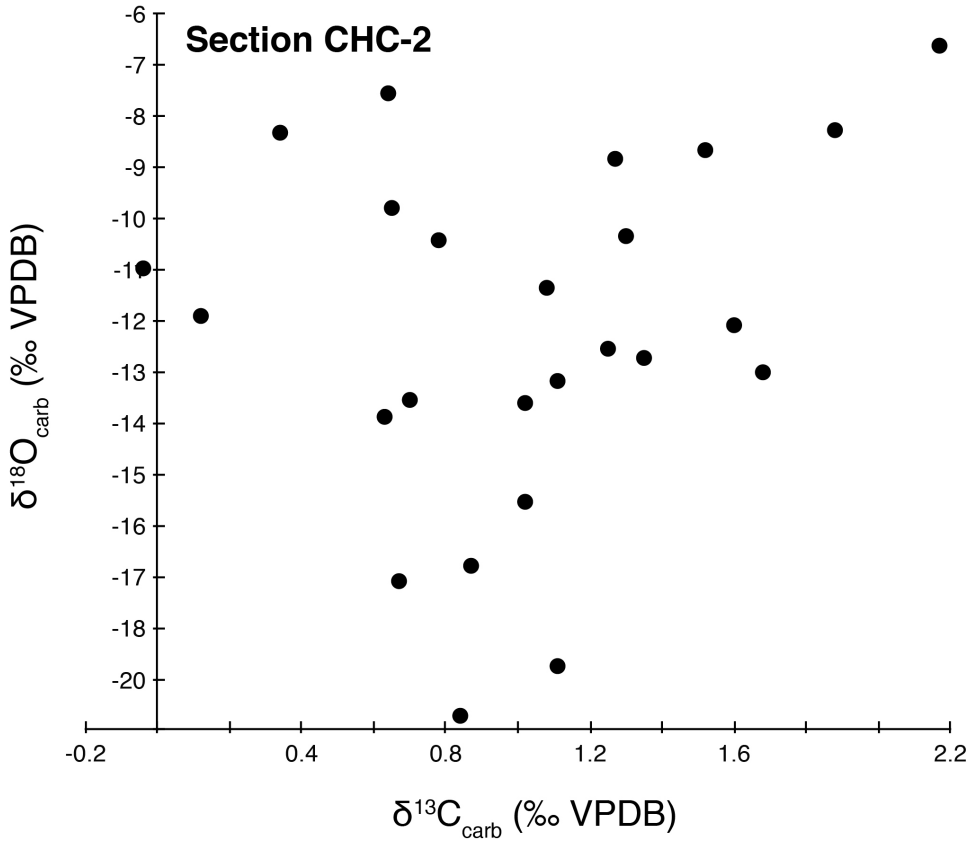
Section CHC-2
-6
-7
-8
-9
-10
-12
-13
-14
-15
-16
-17
-18
-20
-0.2
0.4
0.8
1.2
1.6
2.2
δ18Ocarb (‰ VPDB)
δ13Ccarb (‰ VPDB)

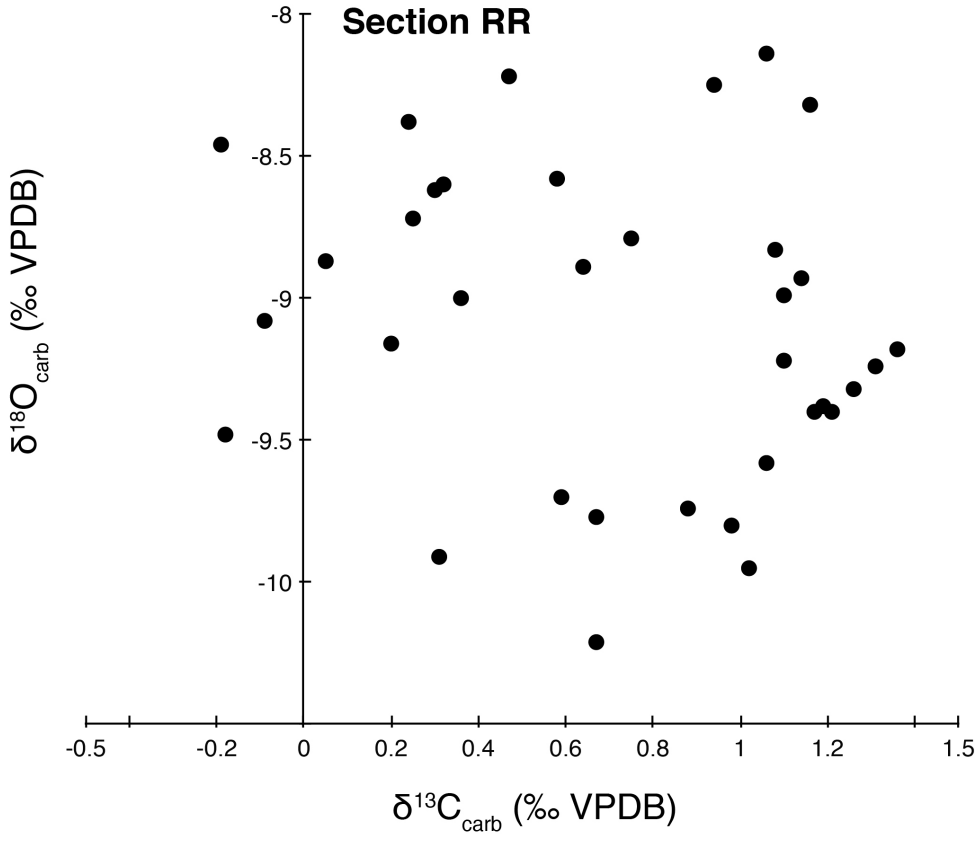
Section RR
-8
-8.5
-9
-9.5
-10
-0.5
-0.2
0
0.2
0.4
0.6
0.8
1
1.2
1.5
δ18Ocarb (‰ VPDB)
δ13Ccarb (‰ VPDB)

Figure 5: Carbon isotope curve for the Honey Creek Formation (RR).

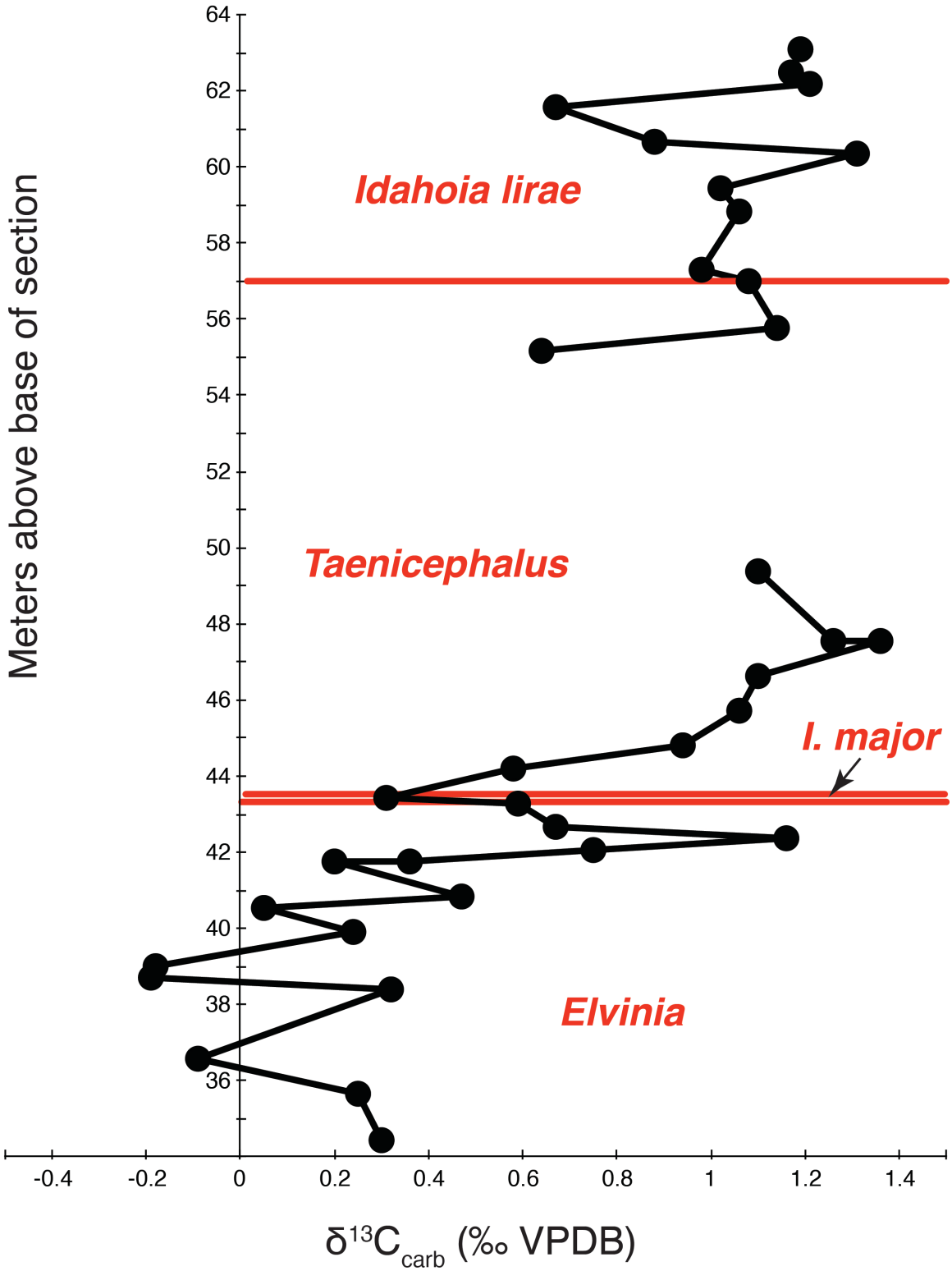
Meters above base of section
64
62
60
58
56
54
52
50
48
46
44
42
40
38
36
Idahoia lirae
Taenicephalus
I. major
Elvinia
-0.4
-0.2
0
0.2
0.4
0.6
0.8
1
1.2
1.4
δ13Ccarb (‰ VPDB)

Figure 6: Carbon isotopic curves for CHC-2, RR and Saltzman et al.'s (1998) section at Orr Ridge correlated using the base of the *Irvingella major* Zone.

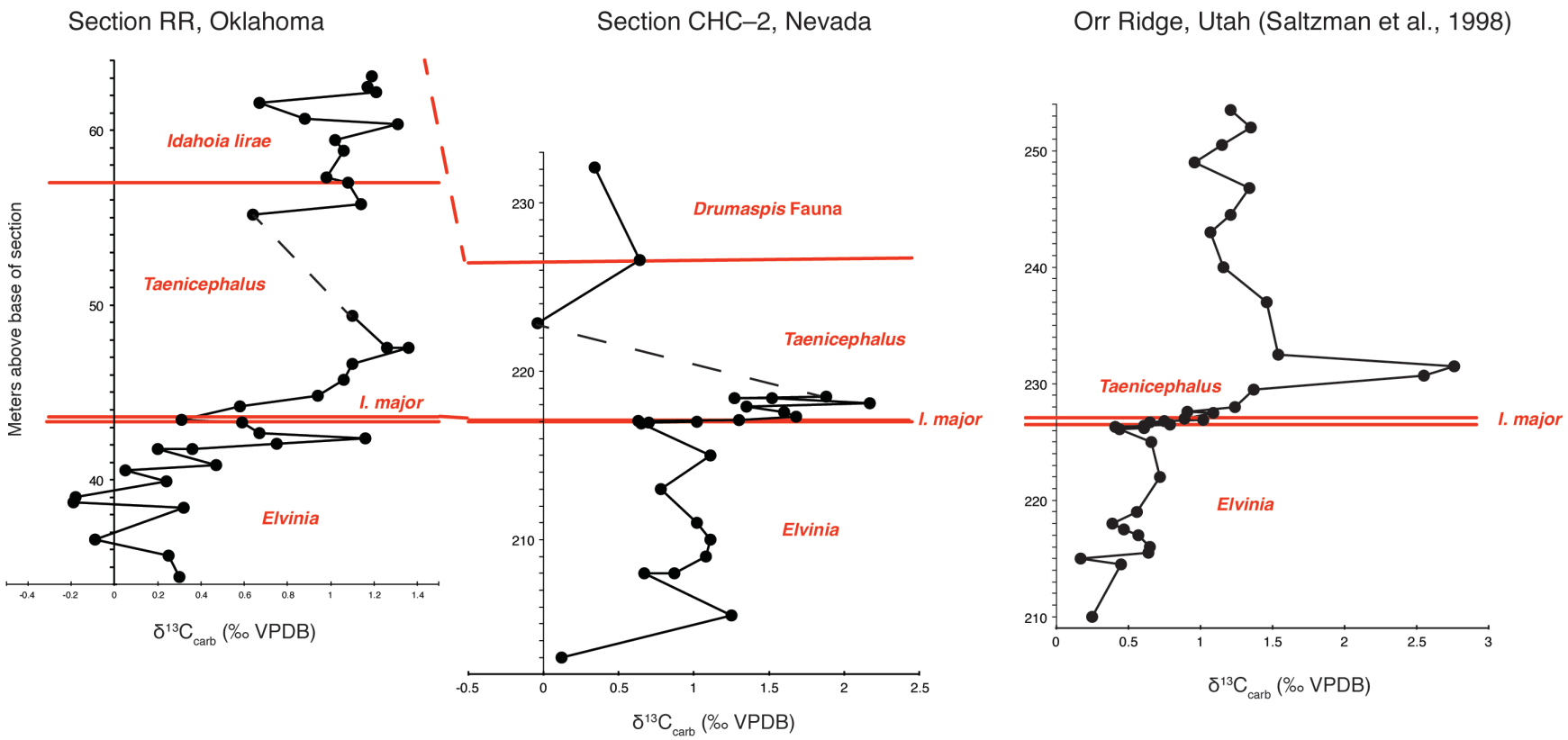
Section RR, Oklahoma
Section CHC–2, Nevada
Orr Ridge, Utah (Saltzman et al., 1998)
Meters above base of section
Idahoia lirae
Taenicephalus
I. major
Elvinia
Drumaspis Fauna
Taenicephalus
I. major
Elvinia
Taenicephalus
I. major
Elvinia
δ13Ccarb (‰ VPDB)
δ13Ccarb (‰ VPDB)
δ13Ccarb (‰ VPDB)

References

Armstrong, M., S. R. Westrop, and J. D. Eoff. 2020. Systematics of a survivor: the Cambrian kingstoniid trilobite *Blountia* Walcott, 1916 across the Marjuman Steptoean (Guzhangian–Paibian) extinction interval in Laurentian North America. Zootaxa, 4804:179.

Brand, W.A., Coplen, T.B., Vogl, J., Rosner, M. and Prohaska, T., 2014. Assessment of international reference materials for isotope-ratio analysis (IUPAC Technical Report). Pure and Applied Chemistry, 86.3: 425-467.

Chatterton, B.D. and Gibb, S., 2016. Furongian (Upper Cambrian) Trilobites from the McKayGroup, Bull River Valley, Near Cranbrook, Southeastern British Columbia, Canada. Geological Association of Canada and the Canadian Society of Petroleum Geologists.

Chatterton, B.D. and Ludvigsen, R., 1998. Upper Steptoean (Upper Cambrian) trilobites from the McKay Group of southeastern British Columbia, Canada. Memoir, The Paleontological Society, 1-43.

Coplen, T.B., 2011. Guidelines and recommended terms for expression of stable-isotope-ratio and gas-ratio measurement results. Rapid communications in mass spectrometry, *25*.17: 2538-2560.

Donovan, R. N., and A. K. Bucheit. 2000. Marine Facies and Islands in the Reagan Formation (Upper Cambrian) in the Slick Hills, Southwestern Oklahoma. Oklahoma Geological Survey Circular, 103:25–37.

Eoff, J. D. 2014. Sequence stratigraphy of the Upper Cambrian (Furongian; Jiangshanian and Sunwaptan) Tunnel City Group, Upper Mississippi Valley:

Transgressing assumptions of cratonic flooding. Sedimentary Geology, 302:87–101.

Gerhardt, A. M., and B. C. Gill. 2016. Elucidating the relationship between the later Cambrian end-Marjuman extinctions and SPICE Event. Palaeogeography, Palaeoclimatology, Palaeoecology, 461:362–373

Gilinsky, N.L., Bennington, J.B., 1994. Estimating numbers of whole individuals from collections of body parts: a taphonomic limitation of the paleontological record. Paleobiology, 20: 245–258.

Gill, B.C., Lyons, T.W., Young, S.A., Kump, L.R., Knoll, A.H. and Saltzman, M.R., 2011. Geochemical evidence for widespread euxinia in the Later Cambrian ocean. Nature, 469.7328: 80-83.

Kim, S.T., Coplen, T.B. and Horita, J., 2015. Normalization of stable isotope data for carbonate minerals: Implementation of IUPAC guidelines. Geochimica et cosmochimica acta, 158: 276-289.

McElmoyl, C., and R. N. Donovan. 2000. Unconformity in the Lower Part of the Cambrian Honey Creek Limestone, Slick Hills, Oklahoma: Candidate for a Grand Cycle Boundary. Oklahoma Geological Survey Circular, 101:65–78.

Palmer, A.R., 1960, Trilobites of the Upper Cambrian Dunderberg Shale, Eureka District, Nevada. Shorter contributions to geology: Geological Survey Professional paper 334C: 109 p.

Palmer, A.R. 1962. Glyptagnostus and associated trilobites in the United States. United States Geological Survey, Professional Paper 374F: 1-49, pls. 1-6.

Palmer, A. R. 1965b. Trilobites of the Late Cambrian Pterocephaliid Biomere in the

Great Basin, United States. U.S. Geological Professional Paper, 493: 1–154.

Saltzman, M.R., Runnegar, B. and Lohmann, K.C., 1998. Carbon isotope stratigraphy of Upper Cambrian (Steptoean Stage) sequences of the eastern Great Basin: Record of a global oceanographic event. Geological Society of America Bulletin, 110.3: 285-297.

Saltzman, M. R. 1999. Upper Cambrian Carbonate Platform Evolution, *Elvinia* and *Taenicephalus* Zones (Pterocephaliid--Ptychaspid Biomere Boundary), Northwestern Wyoming. Journal of Sedimentary Research, 69: 1–13.

Saltzman, M.R., Cowan, C.A., Runkel, A.C., Runnegar, B., Stewart, M.C. and Palmer, A.R., 2004. The Late Cambrian SPICE (δ13C) event and the Sauk II-Sauk III regression: new evidence from Laurentian basins in Utah, Iowa, and Newfoundland. Journal of Sedimentary Research, 74.3: 366-377.

Saltzman, M. R., and E. Thomas. 2012. Chapter 11 - Carbon Isotope Stratigraphy. In Felix M. Gradstein, James G. Ogg, Mark Schmitz and Gabi Ogg (eds.) The Geological Time Scale 2012, 207–232.

Saltzman, M. R., C. T. Edwards, J. M. Adrain, and S. R. Westrop. 2015. Persistent oceanic anoxia and elevated extinction rates separate the Cambrian and Ordovician radiations. Geology, 43:807–810

Saltzman, M. R., J. P. Davidson, P. Holden, B. RUNNEGAR, and K. C. Lohmann. 1995. Sea-level-driven changes in ocean chemistry at an Upper Cambrian extinction horizon. Geology, 23:893–896.

Stitt, J. H. 1977. Late Cambrian and Earliest Ordovician Trilobites, Wichita Mountains Area, Oklahoma. Oklahoma Geological Survey Bulletin, 124:1–79.

Stitt, J. H. 1971b. Late Cambrian and earliest Ordovician trilobites, Timbered Hills and lower Arbuckle Groups, western Arbuckle Mountains, Murray County, Oklahoma. Oklahoma Geological Survey Bulletin, 110:1–83.

Westrop, S. R., and J. M. Adrain. 2007. *Bartonaspis* new genus, a trilobite species complex from the base of the Upper Cambrian Sunwaptan Stage in North America. Canadian Journal of Earth Sciences, 44:987–1003.

Westrop, S. R., and J. M. Adrain. 2009a. The Late Cambrian (Furongian; Steptoean) Trilobite Genus *Xenocheilos* Wilson, 1949: Systematics and Biostratigraphic Significance. Australasian Palaeontological Association Memoirs, 37:351–368.

Westrop, S. R., and J. M. Adrain. 2009b. The Late Cambrian (Steptoean; Furongian) trilobite *Pseudokingstonia* Palmer, 1965 in North America. Canadian Journal of Earth Sciences, 46:355–360.

Westrop, S. R., J. D. Eoff, T.-W. Ng, A. A. Dengler, and J. M. Adrain. 2008. Classification of the Late Cambrian (Steptoean) trilobite genera *Cheilocephalus* Berkey, 1898 and *Oligometopus* Resser, 1936 from Laurentia. Canadian Journal of Earth Sciences, 45:725–744.

Westrop, S. R., and J. M. Adrain. 2013. Biogeographic Shifts in a Transgressive Succession: The Cambrian (Furongian, Jiangshanian; Latest Steptoean–Earliest Sunwaptan) Agnostoid Arthropods Kormagnostella Romanenko and Biciragnostus Ergaliev in North America. Journal of Paleontology, 87:804–817.

Westrop, S. R., and J. M. Adrain. 2016. Revision of *Irvingella tropica* Öpik 1963 from Australia and related species from North America: implications for correlation of the

base of the Jiangshanian Stage (Cambrian, Furongian). Australasian Palaeontological Association Memoirs, 49:395–432.

Westrop, S R., and M. B. Cuggy. 1999 Comparative paleoecology of Cambrian trilobite extinctions. *Journal of Paleontology* 73:337-354

Westrop, S. R., and R. Ludvigsen. 1987. Biogeographic control of trilobite mass extinction at an Upper Cambrian“ biomere” boundary. Paleobiology, 13:84–99.

Westrop, S. R., R. A. W. Poole, and J. M. Adrain. 2010. Systematics of *Dokimocephalus* and related trilobites from the Late Cambrian (Steptoean; Millardan and Furongian Series) of Laurentian North America. Journal of Systematic Palaeontology, 8:545–606.

Wilson, J.L and E.A. Frederickson. 1950. The *Irvingella major* (‘‘Ptychopleurites’’) faunizone of the upper Cambrian. American Journal of Science, 248:891–902.

Chapter III: Systematic Paleontology

Figured specimens are housed at the Oklahoma Museum of Natural History, University of Oklahoma (OU) and at the National Museum of Natural History (USNM). All measurements were made on digital images to the nearest tenth of a millimeter using the Measure Tool of Adobe Photoshop ™. To maximize depth of field, all digital images were rendered from stacks of images focused at 100 micron intervals using Helicon Focus 4.0 for the Macintosh <http://www.heliconsoft.com>.

Family Idahoiidae Lochman 1956

Discussion.—Following Westrop (1995), Loganellidae Rasetti, in Moore, 1959 is considered to be a junior synonym of Idahoiidae.

Genus *Noelaspis* Ludvigsen and Westrop, in Ludvigsen et al., 1989

Type Species— Noelaspis bilobata Ludvigsen and Westrop, in Ludvigsen et al., 1989 from the Shallow Bay Formation, Cow Head Group, western Newfoundland (by original designation)

Noelaspis primitiva n. sp.

Pl. 1 figs. 1–11, Pl. 2 figs. 1-11

Diagnosis.— Long preglabellar field that is twice the length of the anterior border. Anterior branches weakly divergent. Palpebral area of fixed cheeks broad (tr.), equal to about 52% of glabellar width at L2.

Etymology.— From *primitivus* (L), first, early, in reference to its status as the oldest known species of *Noelaspis*

Holotype.—A pygidium (OU 237966; Pl. 2, figs. 1–3) from the Barton Canyon Member, Windfall Formation, Barton Canyon, Cherry Creek Range, Nevada

Occurrence.— Barton Canyon Member, Windfall Formation, Barton Canyon, Cherry Creek Range (CHC-2-216.95) Nevada.

Description.— Cranidium nearly quadrate, length approximately 98% (95-100) of width across palpebral area. Axial and pre-glabellar furrows well defined. Convex glabella tapered slightly, truncated anteriorly, occupies about 75% (74-77) of cranidial length, and 50% (48-52) of width across palpebral lobes; glabellar width at occipital furrow equals 76% (74-80) of glabellar length. Three pairs of weakly defined, wide glabellar furrows. S1 longest, S2 and S3 progressively shorter and shallower. Both S1 and S2 posteriorly directed at approximately 40°, S3 transverse. Occipital furrow broad, well defined, shallowest medially. Occipital ring upturned abaxially, occupies about 10% of cranidial length. Gently sloping frontal area, with preglabellar field accounting 16% (13-18) of cranidial length and 67% (64-69) of frontal area length. Gently convex anterior border

arched slightly in anterior view. Anterior border furrow pitted, well defined. Palpebral area of fixed cheek wide and nearly flat, equal to 52% (49-57) of glabellar width at L2 and 26% (25-27) of cranidial width across palpebral lobes. Palpebral lobe equal about 34% of glabellar length, centered opposite L2, extending posteriorly to L1. Arcuate palpebral furrow broad, shallow. Palpebral ridge weakly convex, extends to S3. Anterior branches of facial suture diverge anteriorly only slightly. Posterior branch of facial suture slopes approximately 17 degrees posteriorly. Posterior area nearly transverse, slightly flexed downward abaxially; posterolateral projection narrow but wide (tr.). Posterior border convex, widens abaxially, length about 71% of glabellar width. Posterior border furrow well defined, shallowest adaxially Very faint, widely spaced granules scattered throughout lower half of glabella, occipital ring, and preglabellar field.

Pygidium nearly semicircular, widest anteriorly, length, excluding incomplete articulating half ring equal to 50% (48-52) of width; median indentation produces bilobed posterior margin. Axis convex, standing well above pleural field, length occupies 87% (85-90) of pygidial length and 43% (41-46) of width. Post-axial ridge extends from terminal piece to border. Three transverse axial rings and terminal piece present, with three well-defined ring furrows; terminal piece composed of two segments. Pleural field nearly flat, with broad, shallow pleural furrows. Border furrow weak. Border broad, raised only slightly above pleural field.

Discussion.— Ludvigsen and Westrop (in Ludvigsen et al., 1989) established *Noelaspis* for Sunwaptan idahoiids that differ from *Loganellus* Devine, 1863 in pygidial morphology. The pygidium of *Noelaspis* has a distinctive median indentation that

produced a bilobed posterior margin (e.g., Westrop, 1995, pl. 9, figs 3, 4, 7), whereas *Loganellus* has a broad pygidium with an evenly rounded margin (e.g., Ludvigsen et al., 1989, pl. 5, figs. 8, 13, 14, 17). The sclerites from the Barton Canyon Limestone record a new species, *N. primitiva*, which is the oldest representative of the genus, and the only one known from Steptoean strata. The pygidia resemble those of the type species, *N. bilobata* Ludvigsen and Westrop (in Ludvigsen et al., 1989, pl. 9, figs. 5, 6, 9) from the Cow Head Group of western Newfoundland, differing only in having wider pleural fields (e.g. Pl. 2, figs. 1–3, 11). All previously described species of both *Noelaspis* (Ludvigsen et al., 1989, pl. 9, figs. 3, 4, 7, 8, 10, 11, 13, 15; Westrop, 1995, pl. 9, figs. 1, 2, 5, 8, 9, pl. 10, figs. 1–6, 8–11) and *Loganellus* (Ludvigsen et al., 1989, pl. 5, figs. 8–12, 15, 16, pl. 6, figs. 1–3, 8, 9; Westrop, 1995, pl. 8, fig. 1) have cranidia with short preglabellar fields that are no longer than the anterior border, and strongly divergent anterior branches of the facial sutures. Cranidia of *N. primitiva* (Pl. 1, figs. 1–11) have weakly divergent sutures and an unusually long preglabellar field that is about twice the length of the anterior border. In addition, the palpebral area of the fixed cheek is very wide, so that the palpebral lobe is located far from the glabella.

Family Dokimocephalidae Kobayashi, 1935

Discussion.— Dokimocephalidae is a mostly Laurentian family with some representatives in, for example, Gondwana (e.g., Shergold, 1980), South China (e.g., Peng, 1992), and North China (e.g., Choi et al., 2008). Westrop et al. (2010) revised a subset of Laurentian genera that comprised *Dokimocephalus* Walcott, 1924 and related

taxa, including *Iddingsia* Walcott, 1924, *Plataspella* Wilson, 1949, *Burnetiella* Lochman, 1958, *Edithiella* Kurtz, 1975, and *Stittella* Westrop et al., 2010, that they referred to as Dokimocephalidae sensu strictu. Several other genera that likely belong to Dokimocephalidae, including *Sulocephalus* Wilson, 1948, *Kindbladia* Frederickson, 1948, *Dellea* Wilson, 1949, *Pseudosaratogia* Wilson, 1951 and *Calocephalites* Kurtz, 1975, await modern treatment. *Deckera* Frederickson, 1949 is revised in this thesis, and a new genus, *Labiocephalus* is established for material from the Great Basin and Oklahoma.

Genus *Iddingsia* Walcott, 1924

Type species.—*Ptychoparia similis* Walcott, 1884 from Dunderberg Formation, Eureka District, Nevada (by original designation)

Iddingsia n. sp. 1

Pl. 3, figs. 1-11

Occurrence— Sneakover Member, Orr Formation, Orr Ridge, northern House Range, Utah (ORR 59.4)

Material.—Five incomplete cranidia.

Description.— Cranidium wedge-shaped in outline, length 100% (91-105) of width across palpebral lobes. Axial furrows deep, preglabellar furrow shallow groove. Strongly convex, subovate glabella, subrounded anteriorly. Glabella accounts for 71% (67-74) of length. At S1, glabella occupies 51% (42-55) of width across palpebral lobes. Glabellar width at S0 74% (67-77) of glabellar length. Two pairs of broad, shallow glabellar furrows; S2 shorter than S1, nearly imperceptible on some specimens. S0 deeply incised, shallowest medially. L0 upturned and narrow abaxially, accounts for 9% (6-10) of cranidial length and 12% (8-14) of glabellar length. Slightly convex, gently sloping pre-glabellar field 20% (17-22) of cranidial length and 68% of frontal area length. Anterior border short, forms a broad pointed arch in outline; slope of anterior border shallower than that of preglabellar field. Anterior border furrow deep groove, deepest abaxially. Palpebral area of fixed cheek narrow, gently upsloping; width of one palpebral area is 34% (30-40) of glabellar width at S1 and 17% of cranidial width across palpebral lobes. Palpebral lobe long, upsloping, and arcuate, occupies approximately 34% of glabellar length, centered opposite L2. Palpebral furrow arcuate, well defined, Palpebral weakly convex, extends beyond S2. Anterior branches of facial suture diverge approximately 15 degrees abaxially between palpebral lobe and anterior border furrow. Posterior branches of facial suture diverge sharply. Posterior border furrow deep, narrowest adaxially. Posterior border narrow, posterolateral projection flexed downward.

Discussion.— A few cranidia from the Sneakover Limestone differ from previously described species of *Iddingsia* (e.g., Westrop et al., 2010, figs. 15A, L, P, 16A, D, H) in

possessing a much shorter anterior border. They probably represent a new species, but more material will be needed to name it formally.

Genus *Deckera* Frederickson 1949

Type species.— *Deckera aldenensis* Frederickson 1949 from the Honey Creek Formation, Arbuckle and Wichita mountains, Oklahoma (by original designation).

Diagnosis.— Subrectangular cranidium with broad fixed cheeks; cranidium much wider than long with broad. Glabella convex, tapered, and subrounded anteriorly; glabella long, occupying at least 70% of cranidial length. Glabellar furrows weak, expressed clearly near axial furrow. Preglabellar field short. In all but basal species, palpebral area of fixed cheek steeply upsloping, with top near level of crest of glabella. Coarse granules on external surface on cranidium and pygidium. Margin of pygidium strongly flexed in posterior view. Long, multisegmented axis.

Discussion.—The original diagnosis of *Deckera* by Frederickson (1949) included the strongly inflated fixed cheeks and elevated palpebral lobes. The discovery of a new species in the Dunderberg Formation (*Deckera* n. sp. 1, below) necessitates a modification to accommodate species with gently inflated fixed cheeks and, consequently, palpebral lobes that are not elevated.

Deckera aldenensis Frederickson 1949

Pl. 4, figs. 1-10, Pl. 7, figs. 10-15

1949 *Deckera aldenensis* Frederickson, p. 350, pl. 68, figs. 22–24.

Holotype—A cranidium (OU 4305; Pl. 4, fig. 1) from the Honey Creek Formation exposed on an isolated hill one-third mile west of HW 58, Blue Creek Canyon, Comanche County, Oklahoma (Frederickson, 1949 locality 6).

Occurrence.—Honey Creek Formation, Wichita Mountains region, Oklahoma; Frederickson (1949) localities 6 (Comanche County) and 9 (Kiowa County); Ring Top Mountain, section KR2 (Westrop et al., 2010), KR2 49.4, 50.3 (Comanche County).

Diagnosis.—Palpebral area upsloping at about 25°, rising just above level of crest of glabella. Palpebral lobe short (exsag.), upturned flap opposite L1 glabellar lobe, length equal to 24% of glabellar length. Palpebral furrow shallow; palpebral lobe separated from palpebral area largely by change in slope. Coarse granules on entire external surface, including borders; well developed on crest of glabella and posterior half of occipital ring, augmented by fine granules, but limited to scattered tubercles on lateral lobes; reduced density of coarse granules on adaxial part of palpebral area.

Description.— Cranidium subrectangular and broad (tr.), width across palpebral lobes 163% (140-176) of cranidial length. Axial and preglabellar furrows deeply incised. Convex, tapered, anteriorly rounded glabella occupies approximately 35% of width

across palpebral lobes and about 75% of cranidial length; width of glabella at S0 is approximately 78% (76%-80%) of glabella length. Occipital ring occupies about 14% (13%-15%) of cranidial length and 19% (17%-21%) of glabellar length. Occipital furrow widest medially, turns anteriorly and tapers abaxially. Two pairs of faint, oblique glabellar furrows. S1 gently impressed but more distinct and extends farther inward than S2. Palpebral area of fixed cheeks upsloping at an angle of about 25°, rising slightly above glabella; broad, equal to about 70% of glabella width at anterior end of S1. Convex palpebral ridge present, extending from palpebral lobe to just beyond S2. Palpebral lobe small, semicircular in outline and upsloping, length equal to 24% of glabellar length; situated opposite L1. Frontal area short, occupying roughly 25% of cranidial length and 36% of glabellar length. Preglabellar field steeply sloping, and convex; occupies 44% (40-46) of frontal area length. Deeply incised border furrow, nearly transverse, curved only slightly forward in dorsal view. Anterior border widest medially, tapers abaxially, weakly crescent shaped in outline. Anterior branches of facial suture nearly parallel, directed inward slightly. Posterior border flexed steeply downward. Posterior border furrow widens abaxially. Coarse granules scattered over fixigenae, including row on posterior border; density of granules reduced adaxially on palpebral area; coarse and fine granules developed on crest of glabella, including occipital ring, with single rows of widely spaced granules on L1 and L2 glabellar lobes. Density of granules apparently increases with size of cranidia (compare Pl. 4, figs. 1 and 5).

Pygidium with strongly curved anterior margin, widest at corner opposite terminal piece. Narrow, convex axis occupies about 31% of maximum pygidial width; at least five transverse axial rings and terminal piece separated by faint ring furrows. Pleural and

interpleural furrows finely etched grooves, curved downward and backward to disappear at border; separate anterior and posterior pleural bands of roughly equal length, Pleural field flexes downward to upturned border, forming "valley" in lateral view (Pl. 7, fig. 12), but distinct, independently incised border furrow absent. Border flexes downward medially in posterior view. Small granules present throughout the pleural field; single large granule on posterior bands.

Discussion.— Deckera completa Wilson, 1951, (Pl 6. figs. 1-10) from the Ore Hill Member of the Gatesburg Formation has a longer border than *D. aldenensis* (e.g., Pl.4 fig. 1) accounting for 57% of frontal area length, versus 46% in the latter. Also, the fixed cheeks of *D. completa* are more steeply inclined and are elevated higher above the glabella. The palpebral lobe of *D. aldenensis* is equal to only about a quarter of glabellar length (Pl.4 fig.1), whereas the palpebral lobe of *D. completa* is more than a third (37%) of glabellar length (Pl.6 fig.10). The well-defined palpebral furrow of *D. completa* differs from the more gently impressed furrow of *D. aldenensis*; however, *D. completa* is often preserved as an internal mold, which may have accentuated the difference in definition. *Deckera aldenensis* has coarser granules on the fixigenae that are more abundant than those of *D. completa*. The latter species also has small, closely packed fine granules on the glabella (aside from furrows), whereas the glabella of *D. aldenensis* has fine granules augmented by larger, more widely scattered granules. Futhermore, the anterior border of *D. completa* is covered by very fine granules (Pl. 6 fig. 10), whereas the anterior border of *D. aldenensis* has coarse granules that are expressed on the external surface and internal molds (e.g., Pl.4 figs.1-10).

Kurtz (1975, p. 1025, pl. 2, fig. 23) identified cranidia from the Davis Formation of Missouri as *D.* cf. *D. aldenensis*. Like *D*. *aldenensis*, the fixed cheeks are upsloping, and the proportions of the anterior border and preglabellar field are comparable. However, as noted by Kurtz, the anterior border *D.* cf. *D. aldenensis*is is nasute, whereas the anterior border of *D. aldenenis* is rounded, and the former appears to have a higher density of granular sculpture.

Deckera completa Wilson 1951

Pl. 6, figs. 1–10, Pl. 7, figs. 4-6

1951 *Deckera completa*, Wilson, p. 634, pl. 90, figs. 10-17

non 1971b *Deckera completa*, Stitt, p. 18, pl. 1, fig. 16 [= *Deckera* sp. indet.]

Diagnosis.— Crescent-shaped anterior border longer than preglabellar field, occupying approximately 57% of frontal area length. Glabellar furrows faint, defined largely by absence of sculpture on external surface (Pl. 6 fig. 10). Palpebral area slopes steeply upward at about 45°, rising above crest of glabella. Palpebral lobe equal to 37% of glabella and located opposite L1 glabellar lobe, posterior tip extending back to level of S0. Sculpture of fine granules with scattered coarser granules on glabella except for furrows. Sparsely distributed larger granules on fixed cheeks, better expressed on internal mold; anterior border smooth.

Holotype.— Cranidium (YPM 18565) from north side of Potter Creek, 55 above the base of the Orr Hill member, Gatesburg Formation, Pennsylvania.

Occurrence.— Ore Hill Member, Gatesburg Formation, Pennsylvania.

Material.- Two cranidia (YPM 18564, YPM 18557) from south side of an asphalt township road west of Drab-Beavertown, Pennsylvania. Free cheek (YPM 18568) from the south of Potter Creek. A pygidium (YPM 18566) from north side of Potter Creek, 55 above the base of the Orr Hill member

Description.—Cranidium sub-rectangular and broad. Cranidial width across the palpebral lobes equal to 157% (153%-161%) of length. Well incised axial and preglabellar furrows. Glabella convex, elliptical in outline, and rounded anteriorly; Glabella width 36% (36%-37%) of cranidial width. Glabellar length occupies 71% (70%-72%) of cranidial length. Occipital ring length 15% (14%-16%) of cranidial length and 21% (19%-23%) of glabellar length. Occipital furrow shallowest medially, deeply incised and curved forward abaxially. S1 and S2 faint and oblique; S1 extends further inward. Palpebral area of fixed cheeks steeply sloping upward, cresting above glabella. Width of palpebral area 71% (65%-75%) of glabellar width at L1. Gently convex palpebral ridge visible, extending from just in front of S2 to the top of the palpebral lobe. Palpebral lobe semicircular in outline and situated opposite L1; length 37% (36%-37%) of glabellar length. Frontal area occupies 28% of cranidial length and 40% of glabellar length. Pre-glabellar field short and steeply sloping, accounting for 12% (11%-13%) of the cranidial length and 43% (39-

47%) of the frontal area. Border furrow firmly impressed and gently curved. Anterior border arcuate, broad, and the nearly flat. Anterior branches of facial suture nearly parallel, flexed slightly abaxially. Posterior branches angled sharply outward. Posterolateral projection flexed backward and downward. Posterior border narrow, wide and rounded abaxially. Posterior border furrow firmly impressed groove, shallowest medially. Scattered, large granules present along the preglabellar field and fixed cheeks. A combination of finer and scattered coarse granules present on the glabella; glabellar furrows lack granules. Anterior border smooth.

Librigenal field of free cheek convex. Lateral border of free cheek broad near base of genal spine, tapers anteriorly. Genal spine stout and short; curved inward slightly. Border furrow shallow throughout, but becomes very faint toward base of genal spine. Posterior border well defined and broad. Granules present throughout, coarser granules present on librigenal field.

Pygidium subtrapezoidal in outline. Anterior margin transverse, then flexed backward, with maximum width opposite fourth axial ring at distinct "corner". Pygidial length approximately 53% of maximum pygidial width. Axis convex, occupying about 90% of pygidial length and 48% of pygidial width. Seven axial rings and short terminal piece. Axial ring furrows firmly impressed. Pleural furrows well incised; pleural furrows more finely etched. Pleural bands roughly equal in length (exsag.), slightly oblique near axial furrow but curved strongly backward abaxially. Pleural field flexes downward to upturned border. Border defined largely by absence of pleural and interpleural furrow; narrows posteriorly. Posterior margin downward medially in posterior view. Very small granules present on axis, pleural bands, and border.

Discussion.— Stitt (1971b, pl. 1, fig. 16) assigned an incomplete cranidium from the Honey Creek Formation of southern Oklahoma to *Deckera completa*. As recognized by Kurtz (1975, p. 1026), this specimen is unusual in displaying a transverse posterior margin, whereas other species, including *D. aldenensis* (Pl. 4 fig. 1), *D. completa* (Pl. 6 fig. 5), and *D.* cf. *D. aldenensis* from Nevada (Pl. 5 fig. 9) all possess lateral margins that show distinct backward deflection.

Deckera cf. *D. aldenensis* Frederickson 1949

Pl. 5, figs. 1–11

cf. 1949 *Deckera aldenensis* Frederickson, p. 350, pl. 68, figs. 22–24.

non 1975 *Deckera* cf. *D. aldenensis* Kurtz, p. 1025, pl. 2, fig. 23

Occurrence.— Barton Canyon Member, Windfall Formation, Barton Canyon, Cherry Creek Range (CHC-2-203.1) and the Corset Spring Shale Member, Orr Formation, Orr Ridge, northern House Range (ORR 7.5).

Discussion.— Cranidia from Nevada and Utah are related to the type species, *D. aldenensis* (Pl. fig.), sharing coarse granulose sculpture over most of the cranidium, including the anterior border, and a conical, anteriorly rounded, glabella. They differ from *D. aldenensis* in that the palpebral lobes are centered farther forward, opposite S1, rather than L1. Additionally, the preglabellar field of *D.* cf. *D. aldenensis* occupies 57%

(52%-62%) of the frontal area length, whereas the preglabellar field of *D. aldenensis* is approximately 46% of the frontal area length. The posterolateral projection of *D.* cf. *D. aldenensis* is deflected more strongly backward than in *D. aldenensis* (compare Pl. 4 fig. 1 and Pl. 5 fig. 9), and the palpebral area of the former is more steeply upsloping at an angle of about 30º, rather than 25º.

The free cheek of *D.* cf. *D. aldenensis* has a long, slender genal spine that is deflected downwards in lateral view, producing a distinct curve in the lateral margin. The librigenal field is convex, rising steeply from the border furrow. Well defined anteriorly, the lateral border furrow becomes shallower posteriorly, and does not join the posterior border. A row of granules is present of the posterior border as well. The lateral border is of nearly equal thickness, until it reaches the base of the genal spine, where it thickens; posterior border narrows slightly towards the genal spine. The borders and genal spine have fine granules; larger, low granules are present on the upper part of the librigenal field.

The free cheek of *D. completa* (Pl. 6 fig. 8) has a stouter genal spine than *D.* cf. *D. aldenesis* that also lacks the downward deflection. In addition, the anterior border (e.g., Pl. 6 fig. 1) is longer than in *D.* cf. *D. aldenensis* (e.g., Pl. 5 fig. 1) and lacks the coarse granulose sculpture. The palpebral lobe is farther back on the cranidium in *D. completa*, opposite L1, rather than S1 as in *D.* cf. *D. aldenensis*.

Deckera cf. *D. completa* Wilson 1951

Pl. 7, figs. 1–3, 7-9

cf. 1951 *Deckera completa* Wilson, p. 634, pl. 90, figs. 10-17

non 1960 *Deckera* sp. cf. *D. completa* Wilson; Lochman and Hu, p. 812, pl. 96, fig. 34 [= *Deckera* sp. indet.]

Occurrence.— Sneakover Limestone Member, Orr Formation, Orr Ridge, northern House Range (ORR 59.4)

Discussion.— An incomplete cranidium and pygidium from ORR 59.4 resemble *D. completa* from Pennsylvania (Pl. 6 figs. 1-10). In particular, the cranidia share a long anterior border, which separate them from *D. aldenensis* (Pl. 4 figs. 1-10). However, the cranidium of *D*. cf. *D. completa* has unusually deep glabellar furrows that distinguish it from all other species (e.g. Pl 7. figs. 1-3). *Deckera* cf. *D. completa* and *D. completa* are clearly different in the pygidial anatomy. The latter species (Pl. 7 figs. 4-6) is widest posteriorly, opposite the fourth axial ring, whereas the widest portion of *D*. cf. *D. completa* is situated anteriorly, opposite the second ring furrow. Additionally, in posterior view, the *D*. cf. *D. completa* is not as strongly flexed downward in the axial region. The pygidial sculpture of the *D*. cf. *D. completa* consists of closely packed fine granules augmented by scattered coarser granules, whereas the pygidium of *D. completa* lacks the coarser granules. *Deckera* cf. *D. completa* likely represents a new species, but more specimens are needed in order to name it.

A single cranidium from the Wind River Mountains of Wyoming was described by Lochman and Hu, 1960 as resembling *D. completa* and was labeled as cf. *D. completa*. Lochman and Hu state that Wyoming specimen has a preglabellar field to anterior border ratio of 1:1; the ratio seen in the Orr Ridge specimen is slightly less than 2:3.

Additionally, it appears that the glabellar furrows of the Wyoming specimen are not as deep.

Deckera n. sp. 1

Pl. 26, figs. 1-3

1965 Genus and species undetermined 3 Palmer, p. 92, pl. 3, fig. 18.

Occurrence.—Dunderberg Formation, Barton Canyon, Cherry Creek Range (CHC-2-138.5); Bastian Peak, Nevada, USGS collection 3009–CO (Palmer, 1965)

Description.—Cranidum subrectangular in outline; width across palpebral lobes about 205% of cranidial length (excluding occipital ring). Axial and preglabellar furrows well defined. Glabella convex, tapered, and bluntly-rounded anteriorly. Glabellar length occupies approximately 80% of cranidial length. Oblique S1 and S2 glabellar furrows present, deepest abaxially. S1 extends further inward than S2, curving towards occipital furrow. Very faint S3 expressed as a slight indentation of glabellar margin. Palpebral area of fixed cheeks nearly flat, lying well below crest of glabella; width about 70% of glabellar width at anterior tip of .L2. Palpebral lobe semicircular in outline, upturned, and situated opposite L2; length is about 40% of glabellar length. Palpebral furrow narrow, deeply etched groove. Palpebral ridge extends obliquely forward, reaching axial furrow opposite S3. Frontal area short, about 22% of cranidial length and 28% of glabellar length. Preglabellar field occupies about 32% of frontal area length. Preglabellar field

weakly convex and gently sloping. Border furrow distinct and nearly transverse, bends toward glabella medially. Anterior border convex, widest medially, tapers abaxially, and nearly transverse. Anterior branches of facial suture directed slightly inward anteriorly. Posterior border flexed downward. Fixed cheeks evenly coated with both large and small granules. Smaller granules present on glabella, except for furrows. Granules on anterior border larger than those on fixed cheeks and glabella.

Discussion.— Palmer (1965, p. 92, pl. 3, fig. 18) described a single cranidium from the *Dunderbergia* Zone at Bastian Peak, Nevada, that he compared to *Deckera*. He recognized that all previously described species of *Deckera* had elevated palpebral lobes located farther back on the cranidia at the crests of tall, strongly upsloping fixed cheeks, whereas his "Genus and species undetermined 3" had more anteriorly placed palpebral lobes set on nearly flat fixed cheeks. An additional cranidium of what appears to be the same species was recovered from the *Dunderbergia* Zone at Barton Canyon. It shares several characters with other species of *Deckera*, including a wide, subrectangular cranidium with broad fixed cheeks and a short anterior border. As in other species, there is coarsely granulose external surface, although the granules are more densely packed than in species such as *D. aldenensis* and *D. completa*. The tapered, anteriorly rounded glabella with relatively shallow S1 and S2 furrows resembles those of *D. completa* and *D. aldenensis*. The cranidia from the *Dunderbergia* Zone is interpreted as a basal species of *Deckera*, which possesses some, but not all, of the characters of the genus. The diagnosis of the genus is revised above. *Deckera* n. sp. 1 is also the oldest known species, and the only one that occurs below the *Elvinia* Zone.

Genus *Labiocephalus* gen. nov.

Type species.—*Labiocephalus cassia* sp. nov. from uppermost Steptoean strata, Nevada and Utah.

Diagnosis.— Tapered, anteriorly rounded glabella with lateral glabellar furrows faint to absent. Anterior border weakly nasute; in anterior view, border and border furrow nearly horizontal medially but flexed steeply downward abaxially, producing lip-like appearance. Palpebral lobe posteriorly positioned, with rear tip extending back to L1; palpebral ridge strongly oblique. Convex pygidium with axis of two distinct segments and terminal piece. Pleural field flexed steeply downward distally; border narrow, down sloping.

Etymology.—From labium (L), lip and kephale (G), head, in reference to the lip-shaped anterior border as seen in anterior view.

Discussion.— Collections from Nevada and Utah yield sclerites of a new dokimocephalid genus that is also represented in Oklahoma by a single cranidium. The nature of the anterior border is the most compelling candidate for a synapomorphy of *Labiocephalus* gen. nov. It is relatively short, weakly nasute, and transverse medially but flexed strongly downward abaxially (Pl. 8 figs. 1, 5, 7, 9). In anterior view, the flexure gives the border a distinctly lip-shaped appearance (Pl. 8 figs. 4, 10). Species of genera of

Dokimocephalidae s.s., as revised by Westrop et a. (2010), typically have long borders without strong abaxial flexure (e.g., Westrop et al., 2010, figs. 7A, 9D, 12F, 16B, J, 17C, D, 22C, E, 26B, 29A). Where borders are short, in such genera as *Kindbladia*, *Dellea* and *Sulcocephalus*, abaxial flexure is also absent (e.g., Westrop, 1986, pl. 28, figs. 2, 5, 7, 11).

Effacement of glabellar furrows is present in species within (e.g., *Plataspella*; e.g., Westrop et al. 2010, fig. 19A-L) and outside (e.g. *Dellea*; e.g. Westrop, 1986, pl. 28, figs. 1–5) Dokimocephalidae s.s, suggesting that this character state has originated independently, and may also provide support for monophyly of *Labiocephalus*. *Labiocephalus cassia* has an occipital spine (Pl. 8 fig. 5) but the occipital ring is broken in *L*. sp. 1, so that this character state cannot yet act as a synapomorphy for the genus. Moreover, in *Plataspella* (e.g., Westrop, 2010, fig. 19A–M) and *Kindbladia* (e.g., Resser, 1942, pl. 15, figs. 26, 30, pl. 16, fig. 10; Palmer, 1960, pl. 11, figs. 19, 20), individual species differ in the presence or absence of an occipital spine.

The convex pygidium of *Labiocephalus* (Pl. 8 figs. 13-15) is most like *Iddingsia* (e.g., Westrop et al., 2010, fig. 15E, F), sharing an axis of two rings and a terminal piece, and a down-sloping border. The pleural field is more strongly down sloping in *Labiocephalus*, and the border is very narrow. Because the pygidium is known for only one of the two species assigned to the genus, it is not known whether these characters are also synapomorphies, but they are included provisionally in the diagnosis. *Dellea* (e.g., Wilson, 1951, pl. 91, figs. 22. 23) has a broad, concave border, whereas *Kindbladia* (e.g. Hohensee and Stitt, 1989, fig. 4.2, 4.3) has an unusually short and wide pygidial outline, and an axis with only one distinct ring in front of the terminal piece. Other

dokimocephalid genera, including *Dokimocephalus* (e.g., Westrop, et al., 2010, figs. 10L–Q), *Plataspella* (e.g., Westrop et al., 2010, figs. 19M, N), and *Burnetiella* (e.g., Westrop et al. 2010, fig. 21H, I), are characterized by relatively flat pygidia.

Westrop et al. (2010) identified a free cheek with a long, outwardly curved genal spine as a derived character state that united Dokimocephalidae s.s. The free cheek of *Labiocephalus* is unknown, but other characters indicate that the genus most closely allied with Dokimocephalidae s.s. For example, species belonging to this grouping share a posterior palpebral lobe position in which the posterior tip reaches L1 and, consequently, a strongly deflected palpebral ridge (e.g., Westrop et al., 2010, figs. 4A, N, 7C, 15A, L, 16A, 19C, I, J, 23A, E, 26A, F, 27A, 29B) with *L.cassia* and *L.* sp. 1 (Pl. 8 figs. 1, 5).

Labiocephalus cassia sp. nov.

Pl. 8, figs. 1-15

Diagnosis. *Labiocephalus* with smooth external surface; small specimens with scattered granules, particularly on posterior half of glabella and posterior border.

Holotype.— An incomplete cranidium (OU 237977, pl. 8, figs. 8-10) from the Barton Canyon Limestone.

Etymology.— Named after Cassidy Jones.

Material and occurrence.—Three cranidia and one pygidium from the Barton Canyon Member, Windfall Formation, Barton Canyon, Cherry Creek Range (collections CHC-1-0, lower layer; CHC-2-216.95). One cranidium and one pygidium from the Sneakover Member, Orr Formation, Orr Ridge, Utah (collection ORR 59.4).

Description.—Cranidium strongly arched, width across the palpebral areas is 97% (92–103) of cranidial length. Axial and preglabellar furrows shallow. Glabella tapered forward, rounded anteriorly, and convex; occupies 61% (58-65) of the width across palpebral areas, and glabellar length is 79% (78-79) of cranidial length. Occipital ring with strongly upturned occipital spine; accounts for 15% (13-17) of glabellar length. Occipital furrow shallow, nearly transverse medially but curved forward abaxially. Glabellar furrows barely perceptible or absent; when visible, S1 and S2 are oblique and oriented inward and backward. Frontal area steeply sloping and short, occupying 21% (19-23) of the cranidial length; preglabellar field occupies 11% (10-13) of the cranidial length. Anterior border is weakly nasute, narrowing arched downward abaxially; lip-like appearance in anterior view. Border furrow is finely etched groove. Palpebral lobe equal to 32% of pre-occipital glabellar length; centered slightly behind glabellar midlength, and extending posteriorly to L1. Palpebral ridge weakly convex, terminating just beyond S2, at which point, width of upsloping palpebral area is 32% (26-36) of glabellar width. Anterior branches of the facial suture diverge anteriorly before converging abruptly inward along anterior border; posterior branches diverge along nearly straight path. Posterior area flexed downward; posterolateral projection roughly triangular in outline. Posterior border furrow firmly impressed groove, becomes deeper along posterolateral

projection. Convex border expands abaxially, length (exsag.) near sutural margin about 150% of length near axial furrow. Larger cranidia with smooth external surface; smaller specimens with scattered granules, particularly on posterior half of glabella and posterior border.

Strongly arched pygidium widest anteriorly, with length (excluding incompletely preserved articulating half ring) 42% (41-44) of width; subtriangular in outline, with posterior margin curved medially. Gentle median arch in posterior view. Convex axis stands well above pleural field; occupies 71% (68-75) of the pygidial length. Two deep, transverse axial ring furrows separate two rings and terminal piece. Terminal piece composed of at least two, and probably three, segments, as indicated by faint furrow at anterior third. Pleural field curves downward, steepening distally. Finely etched shallow border furrow and narrow, down-sloping border. Pleural furrows wide, well defined; interpleural furrows not expressed.

Discussion.— *Labiocephalus cassia* differs from *L*. sp. 1 from the Honey Creek Formation, Oklahoma, in the surface sculpture. *Labiocephalus* sp. 1 has dense granulose sculpture over the entire external surface except for smooth glabellar furrows, along with a network of caecal markings on the preglabellar and preocular areas. Large cranidia of *L. cassia* are smooth (e.g., Pl. 8 figs. 1-3). Smaller specimens of comparable size to *L*. sp. 1 have far more widely scattered granules particularly on the posterior part of the glabellar and posterior border (e.g., Pl. 8 figs. 7, 9).

Labiocephalus sp. 1

Pl. 26, figs. 4-6

Material and occurrence.— One cranidium from collection RR 140, Royer Ranch section, Murray County, Oklahoma (Stitt, 1971b).

Discussion.—A single cranidium provides the only record of *Labiocephalus* outside the Great Basin. As noted above, it differs from *L. cassia* in the nature of the external sculpture, but more material is needed to evaluate this species fully.

Family Elviniidae Kobayashi, 1935

Genus *Elvinia* Walcott, 1924

Type species: *Dikelocephalus roemeri* Shumard 1861 from the Wilberns Formation, central Texas (by original designation).

Elvinia roemeri (Shumard, 1861)

Pl. 9, figs. 4-10, Pl. 10, figs. 4-7

1861 *Dikelocephalus roemeri* Shumard, p. 220.

1924 *Elvinia roemeri* (Shumard); Walcott, p. 56, pl. 11, fig. 3.

1965 *Elvinia roemeri* (Shumard); Palmer, p. 44, pl. 3, figs. 9, 11, 14, 16 (synonymy to date).

1986 *Elvinia roemeri* (Shumard); Westrop, p. 62, pl. 30, figs. 14-16 (synonymy to date).

Occurrence.— Barton Canyon Limestone Member, Windfall Formation, Barton Canyon, Cherry Creek Range [CHC-1-0, CHC-2-216.95] and Steptoe Ranch, North Egan Range [STR 9.5, STR 10.9-11.1], Nevada; Sneakover Member, Orr Formation, Orr Ridge, northern House Range [ORR 59.4], Utah. Species documented across North America, including Texas (Bridge and Girty, 1937; Wilson, 1949), Pennsylvania (Wilson, 1951), Nevada and Utah (Palmer, 1965), Missouri (Kurtz, 1975), South Dakota (Hu, 1979), Indiana (Palmer, 1982), and Alberta, Canada (Westrop, 1986).

Diagnosis.— External surface of cranidium smooth. Preglabellar field occupies 54% of frontal area length. Axis has two distinct rings.

Description.— Cranidium subtrapezoidal, width across palpebral lobes 123% (110%-133%) of length. Axial and preglabellar furrows deep. Glabella convex, rising well above palpebral lobes; tapered forward, truncated anteriorly; occupies 78% (72%-90%) of cranidial length. Glabella width at narrow, well-defined occipital furrow is 75% (64%-89%) of glabella length; glabella occupies 43% (38%-54%) of cranidial width across the palpebral lobes. Roughly u-shaped S1 furrows well defined, connected across glabella by deep transverse furrow. S2 and S3 faint when visible, oriented backward; S2 slightly longer (tr.) than S3. Occipital ring widest medially, curves forward abaxially; accounts for 15% (10%-18%) of glabellar length and 12% (9%-14%) of cranidial length. Anterior profile of glabella and frontal area gently sloping. Anterior border furrow well defined, transverse to slightly arched forward. Anterior border convex, widest medially, gently arcuate in shape. Preglabellar field accounts for 12% (9%-18%) of cranidial length and

54% (42%-66%) of frontal area length. Palpebral area of fixed cheek equals 54% (44%-63%) of glabellar width at L2. Long, arcuate palpebral lobe centered approximately midway between S1 and S2; length 43% (35%-51%) of glabellar length. Palpebral ridge faint, oblique, intersects axial furrow opposite anterior tip of S3. Anterior branches of facial sutures diverge slightly. Posterior branches of facial suture flare sharply outward. Posterior border furrow broad and deep, transverse. Posterior border narrowest at axial furrow, widens abaxially, flexed slightly downward. Posterolateral projection continues flexure, narrows abaxially to truncate termination.

Free cheek with broad, convex librigenal field; separated from narrow, flat lateral border by a shallow, broad border furrow. Border furrow curves inward to meet deeper posterior border furrow. Lateral border widest anteriorly, gently curved inward. Base of genal spine thickest at junction with borders. Genal spine short and slender.

Pygidium semicircular in outline, length 44% (34%-55%) of pygidial width, excluding articulating half ring (not preserved on most specimens). Anterior border forms low raised rim; border furrow well defined, broad. Pygidial axis strongly convex, occupying 85% (78%-90%) of pygidial length and 38% (31%-49%) of width. Axis has two distinct transverse ring furrows. Incomplete ring divides terminal piece into two segments. Articulating half ring long, equal to 86% (78%-93%) of anteriormost ring. Pleural fields flat, with two posteriorly-deflected pleural furrows. Interpleural furrows not expressed.

Discussion: In separating *Elvinia granulata* Resser, 1942 (Palmer, 1965, pl. 3, fig. 12; Ludvigsen and Westrop, 1983, pl. 3, figs. 1–11, pl. 4, figs. 17, 18; pl. 5, figs. 10–13) from

E. roemeri , Palmer (1965) emphasized the difference in cranidial sculpture: the latter is smooth, rather than granulose. In their study of specimens from the Hoyt Formation of New York, Ludvigsen and Westrop (1983, p. 21) also noted that *E. granulata* differs in having more firmly impressed S2 furrows, S3 furrows that are expressed on internal molds, longer in genal spines, and a relatively wider pygidium.

Elvinia sp. 1

Pl. 9, figs. 1-3

Occurrence.— Barton Canyon Member, Windfall Formation, Barton Canyon, Cherry Creek Range (collection CHC-2-216.95), Nevada.

Discussion: A single cranidium differs from *E. roemeri* in possessing a very short preglabellar field that occupies, occupying only 41% of the frontal area length, versus 54% (44%-63%) in *E. roemeri*. Additionally, the palpebral lobes of *E.* sp. indet. 1 are located farther forward than the palpebral lobes of *E. roemeri*.

Elvinia sp. 2

Pl. 10, figs. 1-3

-

Occurrence. —Barton Canyon Limestone Member, Windfall Formation, Steptoe Ranch, North Egan Range [STR 9.5], White Pine County, Nevada.

Discussion.— A cranidium from the Steptoe Ranch section has a glabella that is subrounded anteriorly, rather than truncate, as in *E. roemeri*. Additionally, furrows S2 and S3 clearly visible, and of equal depth as S1. Compared to similarly-sized specimens of *E. roemeri*, the palpebral area is much wider, equal to about 65% of the glabella width at the palpebral lobe, versus about 54% in *E. roemeri*. Finally, the palpebral lobes are very long, extending from the mid-point L1 to beyond S3, and the palpebral ridge is better defined than in *E. roemeri*. More material is needed to evaluate the significance of these differences.

Family Aphelaspididae Palmer, 1960

Genus *Anechocephalus* Palmer, 1960

Type species.— *Anechocephalus trigranulatus* Palmer, 1960 from the Dunderberg Formation, Eureka District, Eureka County, Nevada (by original designation).

Diagnosis: Axial furrows distinct, preglabellar furrow shallow. Fixed cheeks upsloping. Palpebral lobes large, arcuate. One pair of pygidial spines. Short, strongly convex axis with transverse ring furrows. Pleural furrows broad, deeper anteriorly, curved downward.

Discussion.— Chatterton and Gibb (2016) proposed that that *Dicanthopyge* Palmer, 1965 is a junior synonym of *Anechocephalus*, noting that the two genera share pygidia with short axes and a pair of marginal spines. Indeed, Chatterton and Gibb (p. 46) argued that,

aside from shorter preglabellar fields, species of *Anechocephalus* match all of the characters included in Palmer's (1965) diagnosis of *Dicanthopyge*.

Anechocephalus ralphi n. sp.

Pl. 11, figs. 1-11, Pl. 12, figs. 1-15, Pl. 13, figs. 1-10

Diagnosis.— Preglabellar field short, occupying 7% of cranidial length. Axial length 78% of pygidial length. Slender, short pygidial spines spaced far apart.

Holotype.— A pygidium (OU 237992, Pl.12, figs. 4-6) from the Barton Canyon Member of the Orr Formation, Cherry Creek Range, (CHC-2-216.95).

Etymology.— Named for Ralph Welch.

Occurrence.—Barton Canyon Member, Windfall Formation, Barton Canyon, Cherry Creek Range (CHC-1-0, lower layer; CHC-2-216.95) and Steptoe Ranch, South Egan Range (STR 9.5), White Pine County, Nevada.

Description.—Cranidium weakly arched, width across palpebral lobes is 121% (108%-131%) of cranidial length. Axial furrows deep, preglabellar furrow shallow. Glabella tapered forward, weakly rounded anteriorly, and convex; occupies 47% (42–51) of the width across the palpebral lobes, and 81% (79-85) of cranidial length. Occipital ring accounts for 13% (11-15) of glabellar length. Occipital furrow deep, transverse medially

but curved forward abaxially. Glabellar furrows weakly incised at best, but identifiable as smooth areas on external surface of exoskeleton. S1 and S2 are oblique and oriented inward and backward. Frontal area steeply sloping and short, occupying 19% (15-21) of cranidial length; preglabellar field occupies 7% (5-9) of cranidial length. Anterior border convex, nearly transverse, widest medially. Border furrow deep. One palpebral area of fixed cheek 32% (24-37) of glabellar width at L2 and 15% (12-17) of width across palpebral lobes. Palpebral lobe equal to 46% (42-49) of glabellar length; centered at opposite L2 lobe, extending posteriorly to L1. Anterior branches of the facial suture diverge weakly~~;~~ posterior branches diverge gradually along faintly sigmoid path. Posterolateral projection short (exsag.), tapers abaxially. Posterior border furrow firmly impressed grove, depth stays constant along posterolateral projection; posterior border convex, expands abaxially before being truncated at sutural margi~~n.~~ Scattered granules on external surface of glabella (except for lateral furrows), and palpebral and postocular areas; anterior border carries terrace ridges.

Lateral border of free cheek gently curved downward and flat. Posterior border broad, tapers slightly approaching genal spine. Border furrow most distinct anteriorly, faint at the base of genal spine. Librigenal field strongly convex, broad; tapers at base of genal spine. Genal spine broad, short, curved slightly inward. Smooth exterior.

Pygidium widest anteriorly, with length (sag.) 48% (44-55) of width; subtrapezoidal in outline, excluding widely separated slender spines; between spines, posterior margin gently concave. Convex axis stands well above pleural field; occupies 78% (72-82) of pygidial length not including articulating half ring; axial length 70% (68-73) including articulating half ring. Axial furrows very shallow. Deep, transverse articulating furrow.

One well-defined axial ring separated from terminal piece of at least two segments by well incised, transverse ring furrow. Faint, incomplete furrows on terminal piece. Pleural field curves downward. Border furrow defined in part by change in slope at edge of pleural field. Border widest at spines and narrows posteriorly. Pleural furrows wide and shallow; interpleural furrows not expressed.

Discussion: The type material of *Anechocephalus spinosus* Palmer, 1965 comes from three different collections from the Dunderberg Formation of Nevada and, as Palmer (1965, p. 78) recognized, the pygidia in each of these collections are strikingly different. He concluded that the species (1965, p. 78) "is either unusually variable or else composed of two or more closely related forms." He chose the former interpretation because his collections were from the same general stratigraphic interval (upper *Elvinia* Zone). However, new material from the very top of the *Elvinia* Zone at Barton Canyon includes equally distinctive pygidia that show very little variation. They suggest that Palmer's second interpretation was correct, and *A. spinosus* almost certainly is a composite of at least two distinct species.

The holotype cranidium of *A. spinosus* (Palmer, 1965, pl. 20, fig. 3) is associated with a pygidium that has short spines and a relatively short axis (Palmer, 1965, pl. 20, fig. 4) that occupies barely half of pygidial length (sag). Axes of pygidia of *A. ralphi* (Pl.11 figs.1, 11, Pl. 12, fig. 4) are proportionately longer and terminate much closer to the anterior margin, and the marginal spines are more slender, and are spaced farther apart. Additionally, Palmer (1965) stated that the frontal area of *A. spinosus* is between one-third and one-half of the glabellar length whereas the frontal area of *A. ralphi* is about

24% (18%-27%) of glabellar length. Two other pygidia attributed to *A. spinosus* (Palmer, 1965, pl. 20, figs. 7, 12) have wider, longer spines than both the specimen associated with the holotype and *A. ralphi*, and they differ from each other in the width (tr.) of the embayment between the spines.

Anechocephalus trigranulatus Palmer, 1960, the type species and also from the Dunderberg Formation, has an abbreviated frontal area on the cranidium (Palmer, 1965, pl. 20, figs. 5, 8, 9) that is even shorter than in *A. ralphi*. Although the pygidium has a median embayment, marginal spines are not developed, and the posterior corners are rounded (e.g., Palmer, 1965, pl. 20, fig. 13).

Articulated specimens of *Anechocephalus* from the McKay Group, southern British Columbia (Chatterton and Gibb, 2016), provide valuable information on the complete exoskeleton. However, they are variably compacted, and that can influence the apparent lengths of various parts of the anatomy (e.g., compare apparent lengths of the preglabellar field in Chatterton and Gibb, 2016, pl. 20, figs. 1 and 2). Consequently, comparisons with three-dimensionally preserved specimens must be made carefully. *Anechocephalus intermedius* Chatterton and Gibb (2016, pl. 18, figs. 2, 7, pl. 20, figs. 1–7, pl. 21, figs. 1–4) differs from *A. ralphi* in having a relatively narrower axis that occupies only 38% of pygidial width (Chatterton and Gibb, 2016, p. 45), versus 34% (28-37) in the latter, and broader marginal spines. Cranidia of *A. intermedius* have far deeper S1 and S2 glabellar furrows , although these could be exaggerated by compaction. *Anechocephalus rebeccaae* Chatterton and Gibb (2016, pl. 22, figs. 1–4) possesses pygidial spines that are much longer than those of *A. ralphi*. Furthermore, Chatterton and Gibb (2016, p. 47) note that the pygidial axis of *A. rebeccaae* is well over half the pygidial length (approximately

67%). This differs from *A. ralphi* with a pygidial axis that occupies 80% of the pygidial length. Like *A. intermedius*, *A. rebeccaae* also has distinct glabellar furrows.

Anechocephalus aphelodermus Rucker, in Stitt et al., 1994, from the Collier Shale of west-central Arkansas, has a very short occipital ring (Stitt et al, 1994, fig. 3.6). In addition, the palpebral lobe is smaller than in *A. ralphi*, and the posterior tip does not extend as far backward. According to Stitt et al. (1994, p. 522), the external surface of the cranidium of *A. aphelodermus* is smooth, whereas most of the surface of *A. ralphi* is granulose.

Species assigned previously to *Dicanthopyge*, *A. convergens* (Palmer, 1965), *D. quadratus* (Palmer, 1965) and *D. reductus* (Palmer, 1965), are characterized by much longer preglabellar fields than *A. ralphi* (e.g., see Palmer, 1965, pl. 9, figs. 1-3, pl. 10, fig. 19), and also have wider palpebral areas of the fixed cheeks, so that the eyes are located farther from the glabella. Both *A. convergens* and *A. reductus* have narrower pygidia and, consequently, far more closely spaced margin spines than *A. ralphi* (compare Pl. 11, figs. 1, 11, pl. 12, fig. 4, with Palmer, 1965, pl. 9, figs. 4, 6, pl. 10, fig. 20). *Anechocephalus quadratus* resembles *A. ralphi* in that the spines of the pygidium are spaced farther apart, and the pleural fields are relatively wide (Palmer 1965, pl. 9, figs. 5, 7, 8, 9). The spines of *A. quadratus* increase in length during ontogeny, but they become much longer than those of *A. ralphi* in the holaspis stage.

Family Pterocephaliidae Kobayashi 1935

Subfamily Pterocephaliinae Kobayashi 1935

Genus *Pterocephalia* Roemer 1849

Type species.—*Pterocephalia sanctisabae* Roemer, 1849 from the Wilberns Formation of Texas (by original designation).

Pterocephalia sp. indet.

Pl. 14, figs. 1-9

Occurrence.— Sneakover Member, Orr Formation, Orr Ridge, northern House Range, Utah (ORR 59.4).

Material.— Six incomplete cranidia and one incomplete pygidium

Discussion.— New material from Orr Ridge, Utah is unlike previously described species of *Pterocephalia*. Although none of the specimens is complete, some show that the anterior border is flat to weakly concave and is slightly shorter than the glabella. In the type species, *P. sanctisabae* Roemer 1849, the border is relatively longer, and there is a distinct ridge near the anterior margin, beyond which the border is more strongly concave. Bridge and Girty's (1937, pl. 68, fig. 7) illustration of Roemer's types shows that this feature is evident on both the dorsal and ventral surface of the exoskeleton, and is also expressed clearly on cranidia attributed to *P. sanctisabae* from Oklahoma (Frederickson, 1949, pl. 69, fig. 3), Nevada (Palmer, 1960, pl. 9. fig. 7) and Alberta (Westrop, 1986, pl. 27, figs. 19, 20). It continues onto the free cheek (Palmer, 1960, pl. 9. fig. 13; Westrop, 1986, pl. 27, fig, 17). However, a ridge is barely perceptible at best on

cranidia from Orr Ridge (Pl. 14, fig. 1-9). Chatterton and Gibb (2016) reported *P. sanctisabae* from the McKay Group in southern British Columbia. Unfortunately, all of the exoskeletons are strongly compacted (Chatterton and Gibb, 2016, pl. 14) and the cephala do not show any trace of the ridge that is so conspicuous on cranidia preserved in full relief. As a result, there is some doubt about the identification of these specimens.

The associated pygidium is incomplete but has pleural fields with well-incised pleural furrows (Pl. 14 fig. 3). This clearly differentiates it from the pygidium of *P. concava* Palmer (1960, pl. 9, fig. 9), from older *Dunderbergia* Zone strata in Nevada, in which the pleural field is largely effaced. Compared to the cranidia from Orr Ridge, *P. concava* has shallow glabellar furrows. Pygidial morphology also separates the species from Orr Ridge from *P. norfordi* Chatterton and Ludvigsen (1998) from the McKay Group of British Columbia. Although likely exaggerated by compaction, the latter species has a very broad pygidium that is noticeably wider (compare Pl. 14 fig. 3) with Chatterton and Gibb, 2016, pl. 15, figs. 8, 9), and the cephala have palpebral lobes are smaller, and more anteriorly positioned (e.g., Chatterton and Gibb, 2016, pl. 16, figs. 1, 6). In contrast, *P. elongata* Palmer, 1960 is diagnosed by a relatively long and narrow pygidium (Palmer, 1960, p. 88, pl. 9, figs. 17–19) that is striking different in outline from the specimen from Orr Ridge. In addition, the palpebral lobes are located closer to the glabella in *P. elongata* (compare Pl. 14, figs. 1, 4, 7 with Palmer, 1960, pl. 9, figs. 14, 16 and Palmer, 1965, pl. 17, fig. 9).

According to Palmer (1965), *Pterocephalia*? *punctata* Palmer 1965 has short palpebral lobes that occupy one-third to one-half of the glabellar length ((pl. 17, figs. 8, 12, 13), whereas those of the Orr Ridge material range from 45% to 61% of the glabellar

length. In addition to the difference in relative length of the palpebral lobes, they are also placed positioned farther forward in *P. punctat*a. Finally *P. punctata* has pitted external surfaces, and a glabella that is truncated anteriorly, rather than more rounded, as in the species from Orr Ridge.

Genus *Labiostria* Palmer, 1954

Type species.—*Labiostria conveximarginata* Palmer, 1954 from the Riley Formation of central Texas (by original designation).

Diagnosis.— Large palpebral lobes with firmly impressed palpebral furrows. Well incised anterior border furrow and convex border. Pygidium roughly elliptical in outline, maximum width opposite the posterior end of the axis, and smooth posterior margin or with weak median indentation

Discussion.—Palmer (1954) originally proposed *Labiostria* for species from the Riley Formation of Texas that differed from *Aphelaspis* Resser, 1935 in possessing a well-defined anterior border furrow on the cranidium. He later (Palmer, 1962) decided that species assigned to these genera actually overlapped in morphology and treated *Labiostria* as a junior subjective synonym of *Aphelaspis*. However, from a study of silicified sclerites from the Rabbitkettle Formation that he assigned to *L. conveximarginata* Palmer, 1954, Pratt (1992, p. 57, pl. 14, figs. 16–30) argued that

Labiostria should be resurrected because it had median suture separating the free cheeks, rather than a rostral plate as in *Aphelaspis* (e.g., Palmer, 1962, pl. 6, figs. 16–19).

In their study of the fauna of the McKay Group of British Columbia, Chatterton and Ludvigsen (1998) followed Pratt's lead and retained *Labiostria* as a distinct genus. The McKay Group is unusual in that that large numbers of trilobites are preserved as complete, albeit variably compacted, exoskeletons that include carcasses and molts. Many of the molts of *Labiostria* have cheeks that were yoked (i.e., no rostral or median suture) and shed as a single unit (e.g., Chatterton and Ludvigsen, 1998, fig. 19.4–19.6). However, they also argued that some specimens may have had a rostral suture, although their evidence is weak. Fractures that Chatterton and Ludvigsen interpreted as rostral sutures could equally well be the products of compaction (e.g. Chatterton and Ludvigsen, 1998, fig. 18.9), and displacement of cheeks that Chatterton and Ludvigsen attributed to independent movement due to a sutural contact (e.g., Chatterton and Ludvigsen, 1998, fig. 19.2) could be the result of taphonomic processes. In short, there is clear evidence for yoked cheeks in their specimens, but the case for rostral sutures is less than compelling.

Chatterton and Gibb (2016, pl. 23) illustrated more exoskeletons of *L. westropi* from the McKay Group and concluded that it actually possessed a ventral median suture. Once again, this seems to be based on cracks in the doublure in compacted material. The two specimens that they cite in support of their interpretation (Chatterton and Gibb, 2016, pl. 23, figs. 2, 3) do have cracks at the midline that could be regarded as ventral median sutures, but additional cracks are visible in images of both specimens. For example, the cephalon illustrated in their pl. 23, fig. 3 has a crack on the right side that crosses the

doublure just inside (adaxial to) the point where the dorsal suture passes beneath (in this inverted specimen) the doublure; another crosses the doublure on the left side, a little farther inside the intersection point between the dorsal suture. A large crack crosses the doublure on the left lateral margin, and on the right side, a long crack running parallel to the margin splits the doublure; several other cracks are developed in, or propagate from, the glabella. The evidence for ventral sutures on the doublure is less than compelling, and does not overturn the clear case for yoked cheeks in Chatterton and Ludvigsen's (1998) material of *L. westropi*.

The free cheek illustrated by Pratt (1992, pl. 14, figs. 16–30) does seem to have a median suture, and if the paratype free cheek of *L. platifrons* Palmer from Texas (Pl. 16, figs. 5, 6) preserves an intact sutural margin, a case can also be made for a median suture in this species. These observations mean that there is variation in the nature of the ventral sutures in *Labiostria*. Chatterton and colleagues (Chatterton and Ludvigsen, 1998, p. 23; Chatterton and Gibb, 2016) argued for intraspecific variability within *L. westropi*, with a functional suture in some specimens and yoked cheeks in others. As noted above, the evidence for functional sutures in that species is equivocal. Instead, variation is more likely to be inter-specific, with *L. westropi* possessing yoked cheeks, whereas other species had functional median sutures.

As noted by Chatterton and Gibb (2016, p. 47), the presence of median sutures in at least some species has implications for the classification of *Labiostria*. Although Pratt (1992) placed the genus questionably to Aphelaspididae Palmer, 1960, they recognized that the presence of a functional median suture in at least some species indicated an assignment to Pterocephaliidae Kobayashi, 1935. However, in what seems to have been

an editorial error, they listed it under Aphelaspididae, although this apparent lapse was perpetuated by Chatterton (2020, p. 670). To be clear, the arguments of Chatterton and Gibb (2016, p. 47) are followed here, and *Labiostria* is included in Pterocephaliidae.

Revision of *Labiostria* by Pratt (1992) and Chatterton and Ludvigsen (1998) was based on new material from western Canada, and did not involve restudy of the type material of the three species from the Riley Formation of Texas that were originally included in the genus by Palmer (1954). These specimens are reillustrated (Pl. 15, figs.1-8 and Pl. 16, figs.1-9), and were used to develop the provisional diagnosis presented above. Full evaluation of *Labiostria* is difficult because there are other similar pterocephaliid genera, including *Taenora* Palmer, 1960 and *Listroa* Palmer, 1962, that also need revision. Characters that seem likely to be diagnostic of *Labiostria* include large palpebral lobes with firmly impressed palpebral furrows (e.g., Pl. 16, figs. 1–3, 7–9; Pl. 18, figs. 6, 14), well incised anterior border furrow and convex border (e.g., Pl. 15, figs. 1–6), and pygidia that are roughly elliptical in outline, with maximum width opposite the posterior end of the axis, and a posterior margin that is smooth or with a weak median indentation (Palmer, 1954, pl. 86, fig. 1; Pl. 16, figs. 4; Pl. 21). Further progress will require a comprehensive phylogenetic analysis of Pterocephaliidae, but this is beyond the scope of this thesis.

Labiostria westropi Chatterton and Ludvigsen, 1998

Pl. 17, figs. 1-10, Pl. 18, figs. 1-15, Pl. 19, figs, 1-13, Pl. 20, figs. 1-18, Plate 21, figs. 1-6

1998 *Labiostria westropi* Chatterton and Ludvigsen, p. 25, 28, figs. 1, 5, 6.7-6.10, 17-20

?2007 *Labiostria westropi* Chatterton and Ludvigsen, Sundberg et al., p. 796, fig. 3.2

2016 *Labiostria westropi* Chatterton and Ludvigsen, Chatterton and Gibb p. 47, pl. 23, fig. 1-9, pl. 83, fig. 4; pl. 84, fig. 2

2020 *Labiostria westropi* Chatterton and Ludvigsen, Chatterton, fig. 9.1

Diagnosis.— See Chatterton and Ludvigsen (1998, p. 25).

Holotype.— A complete exoskeleton (UA11196) from the McKay Group, Tanglefoot Creek, south-eastern British Columbia illustrated by Chatterton and Ludvigsen (1998, fig. 20.1)

Occurrence.— Lower McKay Group, southeastern British Columbia (Chatterton and Ludvigsen, 1998; Chatterton and Gibb, 2016). Barton Canyon Member, Windfall Formation, Barton Canyon, Cherry Creek Range (CHC-1-0, lower layer; CHC-2-216.95) and Steptoe Ranch, South Egan Range (STR 9.5), White Pine County, Nevada. Sneakover Limesone Member, Orr Ridge, Northern House Range (ORR 59.4), Millard County, Utah. Questionably, Emigrant Formation, Goldfield Hills, southwestern Nevada (Sundberg et al., 2007).

Description.— Cranidium strongly arched (sag.; tr.), with width across palpebral lobes equal to 96% (91–101) of cranidial length. Axial and preglabellar furrows shallow grooves. Glabella slightly tapered forward, gently rounded anteriorly, and moderately

convex; occupies 69% (64–72) of cranidial length and 51% (48–52) of width across palpebral lobes. Occipital ring accounts for 12% (9–17) of glabellar length; posterior margin curved gently backwards. Occipital furrow firmly impressed, widest medially, and bifurcates weakly abaxially. Three pairs of lateral glabellar furrows. S1 and S2 well defined on external surface and, particularly, internal mold, oriented obliquely inward and backward, and faintly bifurcate. S3 barely expressed on external surface, faint on internal mold, and nearly transverse. Frontal area divided into steeply sloping preglabellar and preocular fields and convex, gently down-sloping anterior border by well incised border furrow; furrow also marked by row of pits on external surface, also expressed as small tubercles on internal mold. Preglabellar field occupies 59% (46–70) of frontal area length. Anterior border crescentic in outline, narrowing abaxially. Palpebral area of fixed cheek narrow (tr.), equal to about 31% (24–39) of glabellar width at L2; slopes up steeply from axial furrow. Palpebral lobe long, arcuate in outline and gently upturned; centered opposite anterior tip of S1, and with length equal to 38% (32—45) of glabellar length. Palpebral furrow firmly impressed groove. Anterior branches of facial sutures diverge forward from palpebral lobes before curving inward along anterior cranidial margin; posterior branches more abruptly divergent, following gently curved path. Posterior area flexed downward abaxially, traversed by broad, well defined posterior border furrow; posterior border furrow convex, widens slightly abaxially, maximum length equal to 69% (59-79) of glabellar width. Posterolateral projection wide (tr.) but short (exsag.), tapering to pointed distal termination. Preocular and preglabellar field with anastomosing network of caecal markings on external surface; more clearly expressed on internal molds. Remainder of external surface and internal mold smooth.

Free cheek with genal spine and clearly defined lateral and posterior furrows; broad, nearly flat lateral border about twice width of posterior border. Librigenal field slopes upward and capped by eye socle. Faint caecal markings extend from librigenal field onto lateral border.

Pygidium convex, subrectangular in outline, with gently curved lateral margins and more strongly curved posterior margin; length equal to 62% (55–67). Axis stands well above pleural field and occupies 65% (57–73) of pygidial length; divided into three axial rings and long terminal piece composed of at least two segments. Ring furrows transverse; first two well-defined, third shallower. Articulating half ring about half of length of anteriormost ring; articulating furrow well-incised. Post-axial ridge convex, narrow (tr.), terminating before reaching pygidial margin. .Pleural field curves downward and lacks border furrows; border expressed only by flattening of profile and shallowing of pleural and interpleural furrows. Interpleural furrows wide, clearly defined; pleural furrows absent. .External surface of some specimens with faint terrace ridges; internal mold smooth.

Discussion.—The type material of *Labiostria westropi* from British Columbia (Chatterton and Ludvigsen (1998, figs. 18–20) shares several features with sclerites from the Barton Canyon Member (Pls. 17-21), including a long preglabellar field with conspicuous caecal markings, and a subrectangular pygidium. Cranidia from British Columbia have relatively smaller palpebral lobes (e.g., Chatterton and Ludvigsen, 1998, figs. 18.5, 18.6, 19.6. 19.7, 20.7) than those from Nevada (e.g., *Labiostria* pl. 2, figs. 6, 14).

Labiostria sigmoidalis from the Riley Formation, Texas is known only from the holotype cranidium (Pl. 16. figs. 1–3). This species shares the well-developed caecal markings of *L. westropi* but the glabellar furrows are noticeably deeper. In lateral view (Pl. 16, fig. 2), the preglabellar field of *L. sigmoidalis* becomes almost vertical distally, whereas the preglabellar field of *L. westropi* is more gently sloping.

Labiostria conveximarginata Palmer, 1954, also from the Riley Formation of Texas, includes the holotype and paratype cranidia (Pl. 15, figs. 1–6), a free cheek (Pl. 15, figs. 7, 8) and a pygidium (Palmer, 1954, pl. 86, fig. 1) from the same collection from the White Creek section. The pygidium is broadly similar in outline to those from Nevada, but has more rounded lateral margins and a relatively longer axis. The holotype (Pl. 15, figs. 1–3) is weathered anteriorly, but apparently lacks caecal markings on the preglabellar field, and the glabellar seems to have lacked lateral furrows. The anterior border has a distinct plectrum, which is absent in *L. westropi*. The other cranidium illustrated by Palmer (Pl. 15, figs. 4–6) is from a different section (Lion Mountain). Compared to the holotype, it lacks the plectrum, has a shorter anterior border and the palpebral lobes, although incompletely preserved, appear to have been smaller. It may not belong to the same species.

Pratt (1992) identified material from the Rabbitkettle Formation as *L. conveximmarginata*. Cranidia from the Rabbitkettle Formation tend to have shorter preglabellar fields than those of *L. westropi*. The slope of the preglabellar field seems to be steep as well (pl. 14, figs. 17, 26), while the slope of *L. westropi* is gentle. *L. conveximarginata* also differs from *L. westropi* in that it has a longer anterior border (pl. 14, figs. 16, 18, 21, 27). Additionally, the pygidia of *L. conveximarginata* appear to much

wider than they are long (pl. 14, figs. 22, 24, 28, 29). The pygidial axis of *L. westropi* only occupies about 65% of pygidial length; the axis of *L. conveximarginata* is much longer, terminating near the posterior margin.

A third species from Texas, *L. platifrons* Palmer, 1954 (Pl. 16, figs. 6–9) is clearly differentiated from *L. westropi* from Nevada by the relatively long anterior border, which is equal in length to the preglabellar field, and in the absence of caecal margins on the preglabellar field. The free cheek has faint lateral and posterior border furrows, which contrast with more firmly impressed furrows in *L. westropi*. Finally, the pygidium has shorter, straighter lateral margins and a more strongly curved posterior margin than in *L. westropi*.'

Chatterton (2020) described a new species, *Labiostria gibbae*, from the McKay Group of southeastern British Columbia, Canada. The type material consists of a carcass carapace from 180m above the base of section at Clay Creek as the holotype, and an incomplete carapace from the same location. There are a few characteristics that differentiate *L. gibbae* and *L. westropi*. For example, the glabella of *L. gibbae* is much less tapered than that of *L. westropi*, creating more of an oval-like appearance. Additionally, although the *L. westropi* of Utah and Nevada and *L. gibbae* both have large papebral lobes, the positioning is very different. The palebral lobes of *L. westropi* are centered at S1 and extend from the base of L1 to the base of L3. In the case of *L. gibbae*, the palpebral lobes extend from the midlength of L1 to the midlength of the frontal lobe.

The pygidia differ as well, with *L. gibbae* having a much shorter pygidum. Chatterton states that the axis is "distinctly less than one half (sag.) length of pygidium" and is made up of one axial ring and a terminal piece. The axis of the pygidium of *L. westropi* consists

of three rings and a terminal piece, and the axis is 65% of the pygidial length, or 62% (54-69) excluding the articulating half ring.

Genus *Stenambon* Palmer, 1965

Type species.—*Stenambon megagranulus* Palmer 1965 from the Dunderberg Formation, Eureka Mining District, Nevada (by original designation).

Diagnosis.—Well-developed granulose sculpture on cranidium, with sparse granules on pygidium. Anterior border short and convex; distinct anterior border furrow present. Glabella with three pairs of deeply incised lateral furrows. Palpebral lobe located opposite S1 glabellar furrow and strongly upturned. Free cheek with narrow articulating flange extending onto genal spine (Pl. 22, fig. 7) Pygidium sub-elliptical in outline with weak median embayment of posterior margin. (Modified from Palmer, 1965).

Discussion.— Among pterocephaliid genera, coarsely granulose sculpture is shared only by *Stenambon* and *Strigambitus*. Both genera have a short preglabellar field and a tapered, subrounded glabella with three pairs of glabellar furrows. Additionally, *Stenambon* and *Strigambitus* have distinct palpebral ridges that extend just above S3. The two genera differ most clearly in the position of the palpebral lobe. In *Stenambon* it is located farther backward, and centered opposite S1glabellar furrow (e.g. Pl. 22, figs. 1, 11). In contrast, palpebral lobe of *Strigambitus*, which is positioned opposite S2. A

notched posterior margin is seen on the pygidia of both *Stenambon* and *Strigambitus*. Photos of new material from Nevada show that the granulose sculpture is far better developed in *Strigambitus* (Westrop, unpublished data). Finally, the short anterior border of *Stenambon* is convex and defined posteriorly by a well-defined border furrow. In contrast, a border furrow is absent in *Strigambitus*, and the longer border is defined only by a gradual change in slope at the base of a down-sloping preglabella field, and by a change in sculpture from a caecal network on the preglabellar field to terrace ridges on the border (Hopkins 2011, fig. 13.4, 13.5; Westrop, unpublished photographs of new material from Nevada).

Stenambon paucigranulus Palmer 1965

Pl. 22, figs. 1-15, Pl. 23, 1-7

1965 *Stenambon paucigranulus* Palmer, p. 88, pl. 11, figs. 12, 16, 18 [fig. 16 is misnumbered on plate 20 as figs. 13 and 14; the plate caption is correct]

Diagnosis.—Glabella occupies 74% of length. S4 faint when present, directed anteriorly. Short, anteriorly directed S4 present on some specimens. Caecal markings distinct. Small, scattered granules cover majority of cranidium, aside from furrows. Posterior margin of pygidium has broad, shallow notch.

Occurrence.—*Irvingella major* Zone, Cherry Creek Range (collection CHC-1-0, "upper bed") and Orr Ridge, northern House Range, Utah (collection ORR 60.2). Palmer (1965) also reported the species from the Snake Range, Nevada.

Description.— Cranidium arcuate anteriorly. Width across palpebral lobes is 97% (93%-100%) of ~~l~~length. Axial furrows deep, preglabellar furrow shallow groove. Glabella tapered forward, rounded anteriorly, and convex; occupies 74% of cranidial length (73%-76%) and 52% (44%-55%) of width across palpebral lobes. Occipital ring accounts for 14% (12%-17%) of glabellar length, posterior margin gently curved; some specimens with posteriorly positioned median node. Occipital furrow deepest abaxially, very shallow medially. Three well- defined pairs of glabellar furrows. S1 and S2 angled obliquely inward and backward, S1 more steeply inclined. S3 nearly transverse, shallower than S1 and S2. Faint, short S4 directed forward from axial furrow on some specimens. Anterior half of glabella and frontal area gently sloping; preglabellar field and anterior border separated by moderately deep border furrow and abrupt change in slope. Preglabellar field occupies 64% (56%-70%) of frontal area length. Slightly convex anterior border weakly crescentic in outline Palpebral area of fixed cheek narrow, occupying 28% (21%-38%) of the glabellar width at L2. Palpebral lobe long, arcuate in outline; centered opposite of anterior tip of S1, length equal to 37% of glabellar length. Palpebral ridge well defined, oblique, intersects axial furrow opposite S3. Anterior branches of facial sutures diverge forward from palpebral lobes. Posterior branch of facial suture angled downward. Posterior area curved downward; posterolateral projection nearly transverse and narrowing sharply abaxially. Narrow, shallow posterior

border furrow. Posterior border expands abaxially; low ridge on crest Except for furrows, glabella, palpebral area, and posterior area with closely-spaced granules. On preocular and preglabellar fields, granules superimposed on conspicuous network of anastomosing caeca; anterior border with fine granules.

Free cheek with genal spine Weakly convex librigenal field separated from broad, flat lateral border by shallow border that curves inward to merge with posterior border. Low ridge extends onto posterior border and also present on outer edge of genal spine. Libri genal field with fine granules mounted on caecal markings; borders with scattered fine granules.

Pygidium convex, subtrapezoidal in outline with gently curved lateral margins. Posterior margin has broad, shallow median notch. Pygidial length is 65% of pygidial width (60%-70%). Earlier ontogenetic stages shorter, pygidial length 58% of width. Standing well above the pleural field, the axis occupies 72% (68%-75%) of pygidial length and 47% (44%-50%) of maximum pygidial width. Axis with three ring furrows and terminal piece comprised of two segments. Ring furrows transverse, the first two more distinct than the third. Articulating half-ring short, equal to less than half of length of anterior ring. Low post-axial ridge terminates at pygidial margin. Pleural field flexed downward distally. Three pleural furrows bend backward; interpleural furrows not expressed. Border furrow not sharply defined, but faint paradoublural furrow present on most specimens. External surface with scattered, faint granules.

Discussion.— *Stenambon paucigranulus* Palmer (1965, pl. 11, figs. 12, 16, 18) is a rare species whose types are restricted to a pygidium and an incomplete cranidium from the

Irvingella major Zone (uppermost *Elvinia* Zone of Palmer, 1965). New material from the same horizon at Barton Canyon in the Cherry Creek Range (Pl. 22, figs. 1-15, Pl. 23, figs.1-7) allows the species to be documented more thoroughly. The cranidia are generally similar to Palmer's specimen, although most have longer frontal areas and several have glabellas that are more tapered anteriorly. Palmer (1965, p. 88) described the granules of the cranidium as scattered, but specimens from Barton Canyon have closely spaced granules. Only one specimen, from Orr Ridge, matches Palmer's diagnosis. *Stenambon paucigranulus* differs from the type species, *S. megagranulus* Palmer (1965, pl. 11, figs. 17, 19), in having smaller granules, particularly on the cranidium. Additionally, *S. megagranulus* has four axial ring furrows in front of the terminal piece, whereas *S. paucigranulus* has three. The median pygidial notch of *S. megagranulus* is deeper than that of *S. paucigranulus*, giving it a more strongly bilobed appearance.

Family Uncertain

Genus "*Morosa"* Palmer 1960

Type species.— "*Morosa" longispina* Palmer, 1960 from the Dunderberg Formation, Eureka Mining District, Nevada (by original designation).

Discussion.— "*Morosa"* Palmer was named for a species of small, rather non-descript trilobites that shared anteriorly positioned palpebral lobes (e.g., Palmer, 1960, pl. 10, fig. 15; Palmer, 1965, pl. 20, figs. 16, 18). Stitt (1971) added two new species from Oklahoma (Pl. 24, figs. 1-6) that differ from the species from Nevada that have much

larger, more posteriorly positioned palpebral lobes, and it is far from clear that they have been identified correctly. A revision of "*Morosa"* should include restudy of the type material, but COVID restrictions on loans have prevented this. Material from the Sneakover Limestone is assigned to "*Morosa"* with reservation, and with the recognition that the genus as currently used is unlikely to be monophyletic.

"*Morosa"* cf. *bothra*, Stitt 1971

Pl. 25, figs. 1-14

cf. 1971 "*Morosa"*? *bothra* Stitt, p. 50, pl. 17–19.

Occurrence: Sneakover Member, Orr Formation, Orr Ridge, northern House Range, Utah (ORR 59.4).

Description.—Cranidium ovate, width across palpebral lobes approximately 106% of cranidial length. Axial furrows deep, preglabellar furrow shallow. Glabella convex, ovate, tapered slightly; occupies about 80% of cranidial length. Rises well above palpebral lobes. Glabella width at S0 approximately 68% of glabellar length. Glabella width at L2 approximately 47% of cranidial width across palpebral lobes. Two pairs of shallow glabellar furrows; S1 slightly deeper and longer than S2. Both sets of furrows angled about 45 degrees postermedially. L0 widest medially, upturned and narrow abaxially; accounts for approximately 11% of cranidial length and 14% of glabellar length. S0 deep, narrow groove. Frontal area gently sloping, short, 27% of glabellar

length. Anterior border furrow shallow, broad, arcuate. Anterior border widest medially, narrowed abaxially, arcuate in shape. Preglabellar field occupies 10% of cranidial length and 51% (49-54) of frontal area length. Palpebral area of fixed cheeks narrow; one palpebral area accounts for about 15% of cranidial width across palpebral lobes, 31% of glabellar width at L2, and 29% of glabellar width at S0. Long palpebral lobe centered at L2, about 40% of glabellar length. Palpebral ridge gently convex, meets axial furrow at frontal lobe. Anterior branches of facial suture diverge slightly. Posterior branches of facial suture diverge sharply. Posterior border furrow shallow, transverse. Posterior border widens abaxially, transverse.

Pygidium subtrapezoidal in outline, length 46% (44-48) of width, excluding articulating half ring (not preserved on most specimens). Anterior border forms convex rim; border furrow deep, broad. Pygidial axis strongly convex, 86% (83-91) of pygidial length and 40% (37-44) of pygidial width. Axis has two to three distinct ring furrows; furrows somewhat sinuous, flexing downward medially. Shallow, incomplete ring furrow bisects truncated terminal piece. Deep axial furrows separates axis from pleural field. When present, articulating half ring equal to about 90% of anteriormost ring. Interpleural furrows deep, pleural furrows gently curved posteriorly. Pleural field slopes downward, to a broad border furrow.

Discussion.— The specimens from the Orr Ridge location closely match the description of "*Morosa*" *bothra* provided by Stitt (1971), and the pygidia are virtually identical. Both the Utah and Oklahoma specimens have a slightly tapered, convex glabella with two pairs of shallow glabellar furrows. Additionally, the "*M.*" cf. *bothra* specimens share the deep

axial furrows and shallow preglabellar furrows of the Oklahoma sclerites. The pygidia (Stitt, 1971, pl. 1, fig. 19; Pl.25, figs.1-8) are similar in that specimens from both locations exhibit a down-sloping pleural field and elevated border. According to Stitt 1971, the anterior pleural furrow of "*M*." *bothra* is firmly impressed; other pleural furrows are faint. This is comparable to what is seen in "*M*." cf. *bothra*. Stitt (1971) described cranidal sculpture of fine granules but this is not evident in new, high–resolution digital images of the types (Pl. 24, figs.1-6). Cranidia of "*M."* cf. *bothra* differ minimally in being more ovate in outline rather than quadrate, with anterior borders that are wider and more arcuate in outline (pl. 25, figs. 9-13). Furthermore, the anterior border furrows of the Oklahoma specimens are deeper and narrower than those from Orr Ridge. Although the pygidia are almost identical, the differences in cranidial characteristics create some uncertainty regarding the placement of the Orr Ridge specimens within "*M".* *bothra*.

When compared to "*M*." *simplex* from the Honey Creek Formation (Pl. 24, figs. 7-9), the specimens of "*M*." cf. *bothra* have noticeably different frontal areas. For example, the anterior border furrow of "*M*." *simplex* is nearly straight, and the anterior border is downsloping, whereas "*M*." cf. *bothra* has a curved border furrow and a convex, slightly upturned border (pl. 25, fig.9-13). The surface of "*M*." cf. *bothra* is smooth, whereas the cranidium of *M. simplex* was described by as pitted, although new images (pl. 24, figs. 7-9) show that the pits are barely perceptible.

Species of "*Morosa"* from Nevada, including "*M." brevispina*, "*M." longispina*, and "*M." extensa* are differentiated clearly from "*M*." cf. *bothra* by their much smaller, more

anteriorly positioned palpebral lobes (e.g., Palmer, 1960, pl. 10, fig. 15; Palmer, 1965, pl. 20, figs. 16, 18).

References:

Bridge, J. and Girty, G.H., 1937. A redescription of Ferdinand Roemer's Paleozoic types from Texas (No. 186-M).

Chatterton, B.D.E. 2020. Mid-Furongian trilobites and agnostids from the *Wujiajiania lyndasmithae* Subzone of the *Elvinia* Zone, McKay Group, southeastern British Columbia, Canada. Journal of Paleontology, 94:653–680.

Chatterton, B.D. and Ludvigsen, R., 1998. Upper Steptoean (Upper Cambrian) trilobites from the McKay Group of southeastern British Columbia, Canada. Memoir, The Paleontological Society, 1-43.

Chatterton, B.D. and Gibb, S., 2016. Furongian (Upper Cambrian) Trilobites from the McKay Group, Bull River Valley, Near Cranbrook, Southeastern British Columbia, Canada. Geological Association of Canada and the Canadian Society of Petroleum Geologists.

Choi, D. K., E. Y. Kim, and J. G. Lee. 2008. Upper Cambrian polymerid trilobites from the Machari Formation, Yongwol, Korea. Geobios, 41:183–204.

Devine, T. 1863. Description of a new trilobite from the Quebec Group. Canadian Naturalist and Geologist, 8:95-998.

Frederickson, E.A. 1948. Upper Cambrian trilobites from Oklahoma. Journal of Paleontology, 22: 798-803, pl. 123.

Frederickson, E.A., 1949. Trilobite fauna of the Upper Cambrian Honey Creek Formation. Journal of Paleontology, 341-363.

Hopkins, M.J., 2011. Species-level phylogenetic analysis of pterocephaliids (Trilobita, Cambrian) from the Great Basin, western USA. Journal of Paleontology, 85:1128 1153.

Kobayashi, T. 1935a. The *Briscoia* fauna of the late Upper Cambrian in Alaska with descriptions of a few Cambrian trilobites from Montana and Nevada. Japanese Journal of Geology, 12:40-57.

Kurtz, V.E., 1975, Franconian (upper Cambrian) trilobite faunas from the Elvins Group of southeast Missouri: Journal of Paleontology, 49:1009–1043.

Lochman, C., 1956. The evolution of some Upper Cambrian and Lower Ordovician trilobite families. Journal of Paleontology, 445-462.

Ludvigsen, R. and Westrop, S.R. 1983. Franconian Trilobites of New York State. New York State Museum and Science Service Memoir, 23:1-83.

Ludvigsen, R., Westrop,S.R., and Kindle, C.H.,1989, Sunwaptan (upper Cambrian) trilobites of the Cow Head Group, western Newfoundland, Canada: Palaeontographica Canadiana, 6:175 p.

Moore, R.C., 1959. Treatise on Invertebrate Paleontology, Part O, Arthropoda 1, 560 pp. Univ. Kansas and Geol. Soc. Amer. Lawrence, Kansas.

Palmer, A.R., 1954. The fauna of the Riley Formation in central Texas. Journal of Paleontology, 28:709-786, pls. 76-92.

Palmer, A.R., 1960, Trilobites of the Upper Cambrian Dunderberg Shale, Eureka District, Nevada. Shorter contributions to geology: Geological Survey Professional paper 334-C:109 p.

Palmer, A.R. 1962. *Glyptagnostus* and associated trilobites in the United States. United States Geological Survey, Professional Paper 374F:1-49, pls. 1-6.

Palmer, A. R. 1965b. Trilobites of the Late Cambrian Pterocephaliid Biomere in the Great Basin, United States. U.S. Geological Professional Paper, 493:1–154.

Peng, S. 1992. Upper Cambrian Biostratigraphy and Trilobite Faunas of the Cili-Taoyuan Area, Northwestern Hunan, China. Australasian Association of Paleontologists Memoir, 13:1-119.

Pratt, B.R. 1992. Trilobites of the Marjuman and Steptoean stages (Upper Cambrian), Rabbitkettle Formation, southern Mackenzie Mountains, northwest Canada. Paleontographica Canadiana, 19:1-179.

Resser, C.E., 1935. Nomenclature of some Cambrian trilobites. Smithsonian Miscellaneous Collections.

Resser, C. E. 1942. New Upper Cambrian trilobites. Smithsonian Miscellaneous Collections, 103:1-136.

Roemer, F. 1849. Texas, mit besondered Rucksicht auf deutsche Auswanderung und die physischen Verhaltnisse des Landes. Bonn.

Shergold, J. H. 1980. Late Cambrian trilobites from the Chatsworth Limestone, Western Queensland. Bureau of Mineral Resources, Geology and Geophysics Bulletin, 186:1191.

Shumard, B. F. 1861. The Primordial Zone of Texas, with descriptions of new fossils. American Journal of Science, 2nd series, 32: 213-221.

Stitt, J. H. 1971b. Late Cambrian and earliest Ordovician trilobites, Timbered Hills and lower Arbuckle Groups, western Arbuckle Mountains, Murray County, Oklahoma. Oklahoma Geological Survey Bulletin, 110:1–83.

Sitt, J.H., Rucker, J.D., Boyer, N.D., and Hart, W.D. 1994. New Elvinia Zone (Upper Cambrian) trilobites from new localities in the Collier Shale, Ouachita Mountains, Arkansas. Journal of Paleontology, 68:518-523.

Sundberg, F.A., Kurkewicz, R. and Rooks, D.L., 2007. *Wujiajiania sutherlandi* Fauna (*Elvinia* Biozone, Paibian Stage, Furongian Series—"Upper" Cambrian) from the Emigrant Formation, Nevada. Journal of Paleontology, 81:794-796.

Walcott, C. D. Paleontology of the Eureka District. Monograph of the United States Geological Survey, 8:1-64, pls 1-24.

Walcott, C. D. 1924. Cambrian geology and paleontology V, no. 2, Cambrian and lower Ozarkian trilobites. Smithsonian Miscellaneous Collections, 75:53-60.

Westrop, S. R., 1995. Sunwaptan and Ibexian (Upper Cambrian-Lower Ordovician) trilobites of the Rabbitkettle Formation, Mountain River region, northern Mackenzie Mountains, northwest Canada. Palaeontographica Canadiana, 12:75 p

Westrop, S. R. 1986. Trilobites of the Upper Cambrian Sunwaptan Stage, southern Canadian Rocky Mountains, Alberta. Paleontographica Canadiana, 3:1-178

Westrop, S.R., Poole, R.A.W. and Adrain, J.M., 2010. Systematics of *Dokimocephalus* and related trilobites from the Late Cambrian (Steptoean; Millardan and Furongian series) of Laurentian North America. Journal of Systematic Palaeontology, 8:545-606.

Wilson, J. L. 1948. Two Upper Cambrian *Elvinia* Zone trilobite genera. Journal of Paleontology, 22:30-34.

Wilson, J. L. 1949. The trilobite fauna of the *Elvinia* Zone in the basal Wilberns Formation of Texas. Journal of Paleontology, 23:25-44.

Wilson, J.L., 1951. Franconian trilobites of the central Appalachians. Journal of Paleontology, 617-654.

Plate 1

Fig. 1-11. *Noelaspis primitiva* n. sp., from the Barton Canyon Member, Windfall Formation.

1, 2. Cranidium, dorsal and left lateral views, CHC-2-216.95 OU 237962 , x6.

3, 4, 5. Cranidium, right lateral, dorsal, and anterior views, CHC-2-216.95 OU 237963, x3.

6, 7, 8. Cranidium, anterior, right lateral, and dorsal views, CHC-2-216.95 OU 237964, x2.5.

9, 10, 11. Cranidium, dorsal, left lateral, and anterior views, CHCH-2-216.95 OU 237965, x6.

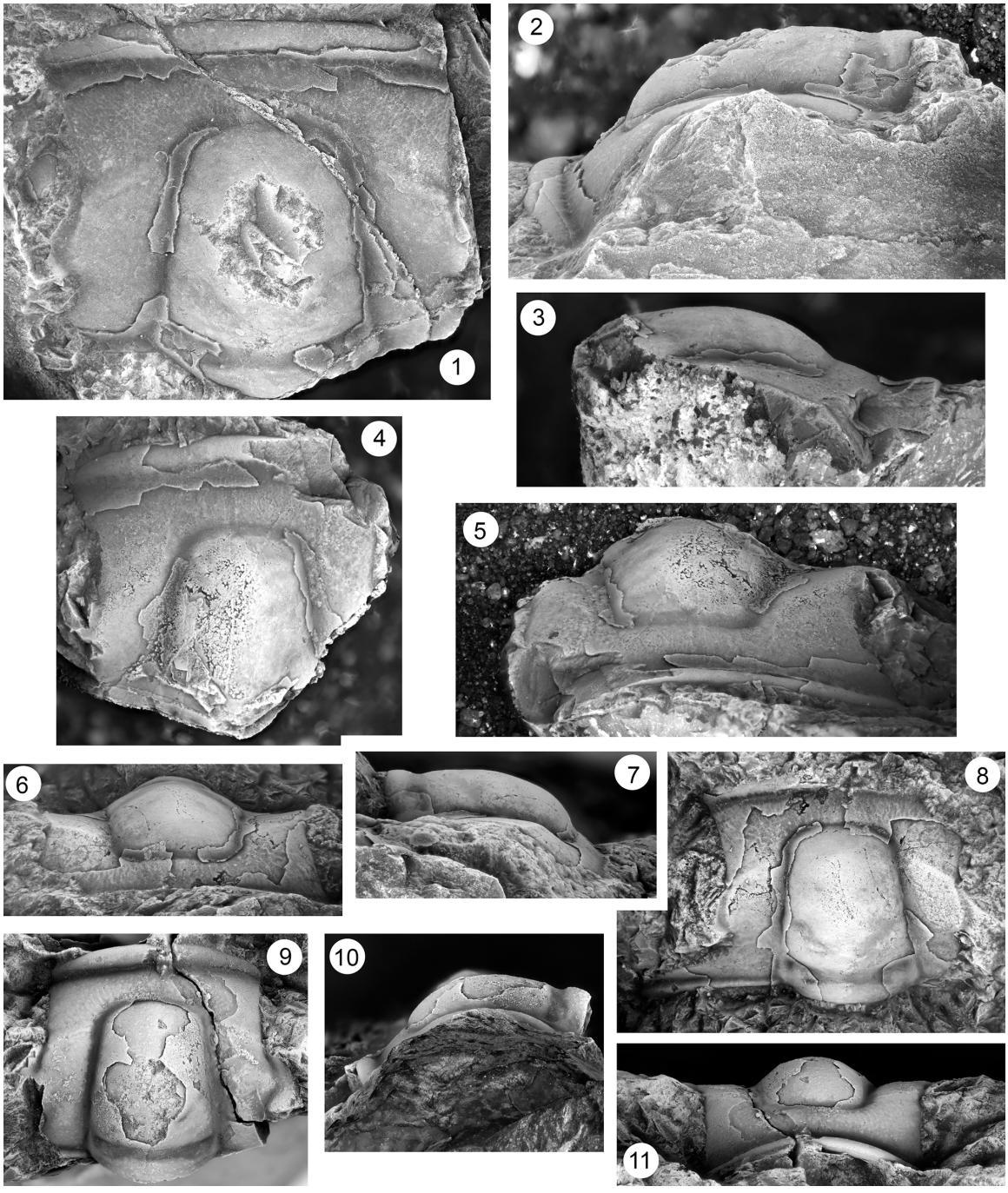
1
2
3
4
5
6
7
8
9
10
11

Plate 2

Fig. 1-12. *Noelaspis primitiva* n. sp., from the Barton Canyon Member, Windfall Formation.

1, 2, 3. Pygidium, dorsal, posterior, and left lateral views, CHC-2-216.95 OU 237966 (holotype), x6.

4, 5, 6. Cranidium, left lateral, dorsal, and anterior views, CHC-2-216.95 OU 237967, x3.5.

7, 8, 9. Cranidium, dorsal, right lateral, and anterior views, STR 9.5 OU 237968, x4.

10, 11. Pygidium, dorsal and posterior views, STR 9.5 OU237969, x3.5.

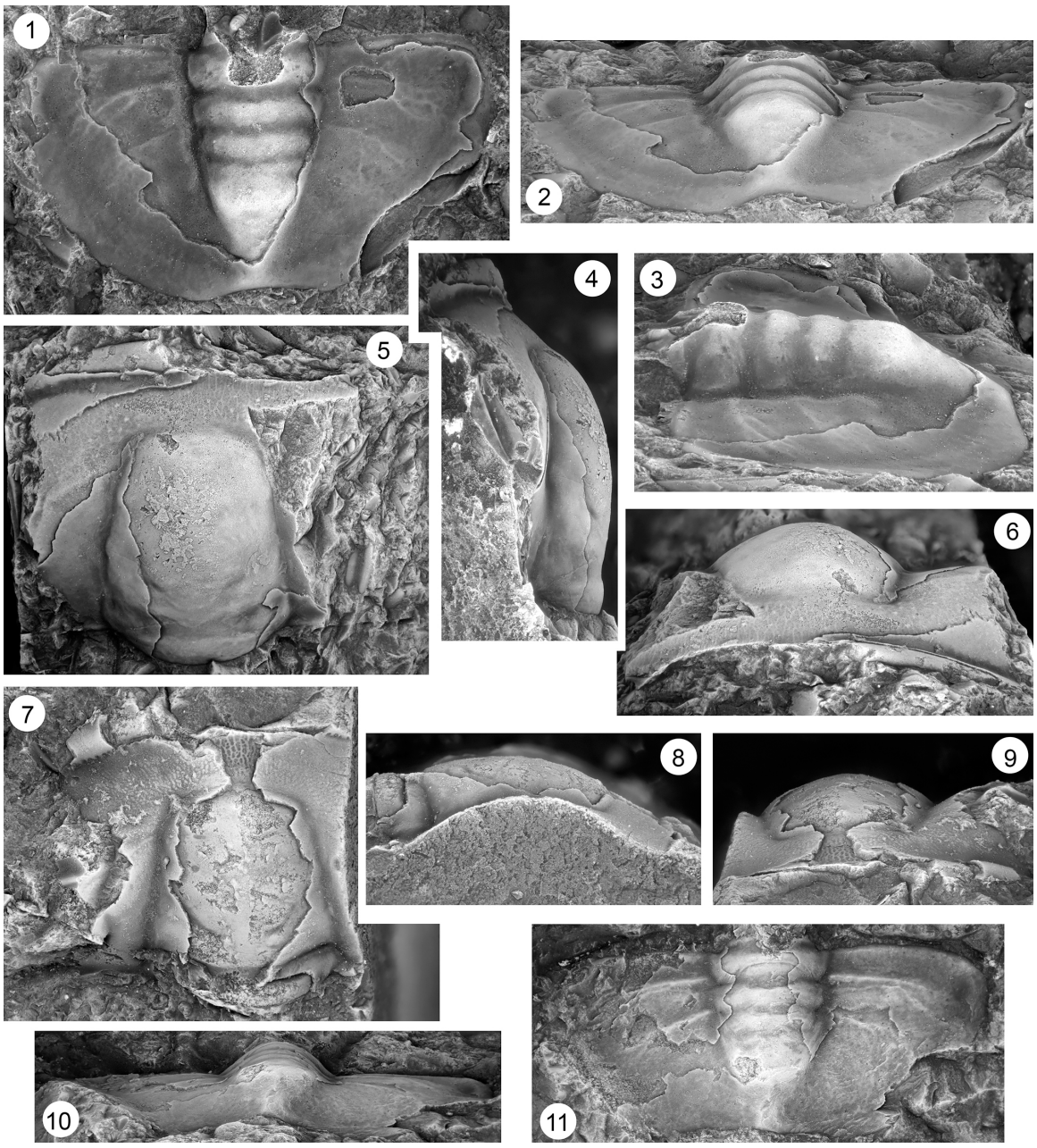
1
2
3
4
5
6
7
8
9
10
11

Plate 3

Fig. 1-11. *Iddingsia* n. sp. 1, Sneakover Member, Orr Formation.

1, 2, 3. Cranidium, dorsal, right lateral, and anterior views, ORR 59.4 OU 237970.

4, 5, 6. Cranidium, anterior, right lateral, and anterior views, ORR 59.4 OU 237971.

7, 8, 9. Cranidium, dorsal, right lateral, and anterior views, ORR 59.4 OU 237972.

10, 11, 12. Cranidium, anterior, and right lateral views, ORR 59.4 OU237973.

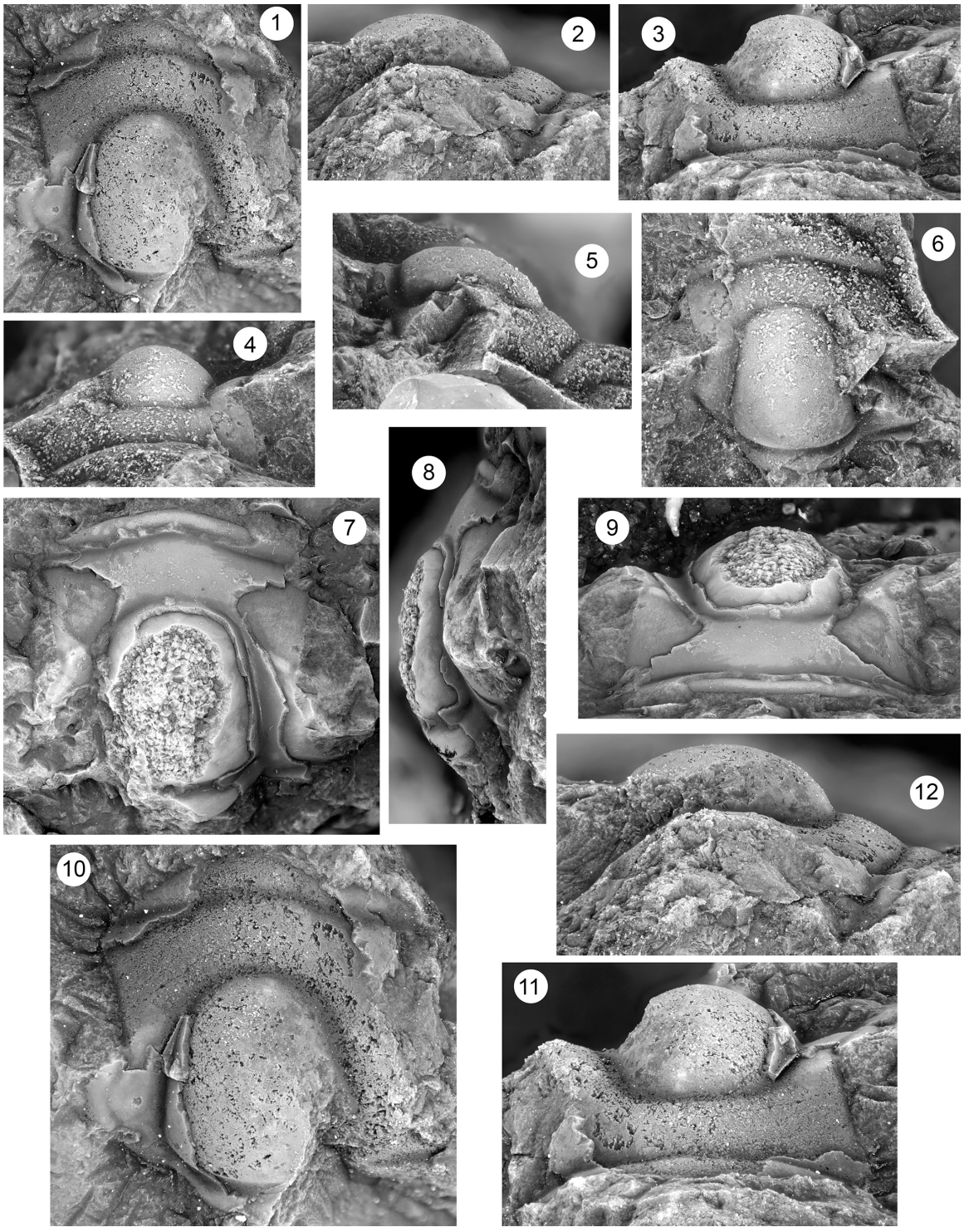
1
2
3
4
5
6
7
8
9
10
11
12

Plate 4

Fig. 1-10. *Deckera aldenesis* Frederickson 1949 from the Honey Creek Formation.

1, 2, 3, 4. Cranidium, dorsal, left lateral, posterior, and anterior views, OU 4305 (holotype), x12.

5, 6, 7. Cranidium, dorsal, anterior, and left lateral views, KR2 49.4 OU 12228, x16.

8, 9, 10. Cranidium, dorsal, right lateral, and anterior views, KR2 50.3 OU 12226, x16.

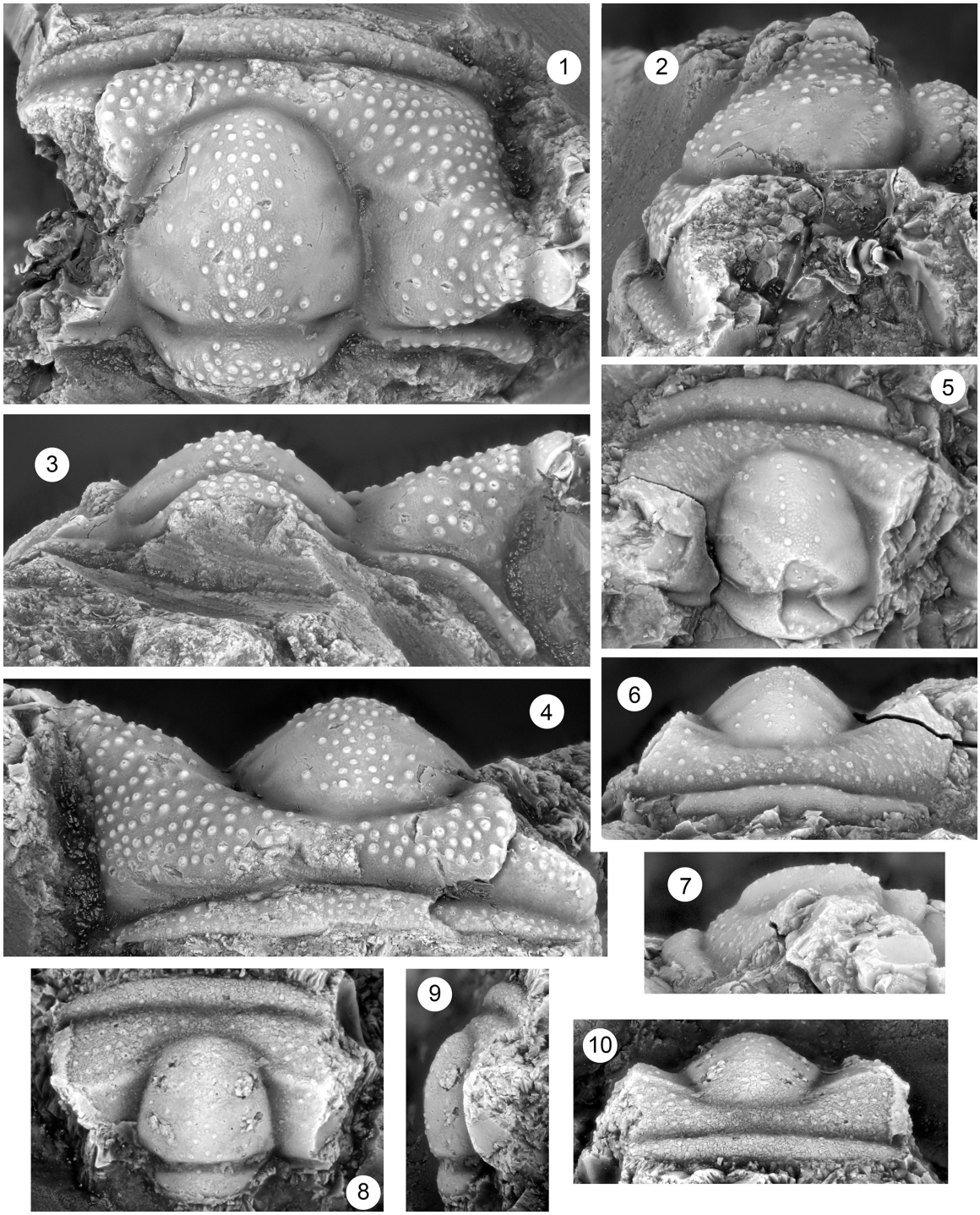
1
2
3
5
4
6
7
8
9
10

Plate 5

Fig. 1-11. *Deckera* cf. *D. aldenensis* Frederickson 1949 from the Barton Canyon Member, Windfall Formation.

1, 2, 3. Cranidium, dorsal, left lateral, and anterior views, CHC-2-203.1 OU 238137, x12.

4, 5, 6. Cranidium, dorsal, posterior, and anterior views, CHC-2-203.1 OU 238138, x12.

7, 8. Free cheek, left lateral and dorsal views, CHC-2-203.1 OU 238139, x7.5.

9, 10, 11. Cranidium, dorsal, left lateral, and anterior views, CHC-203.1 OU 238140, x12.

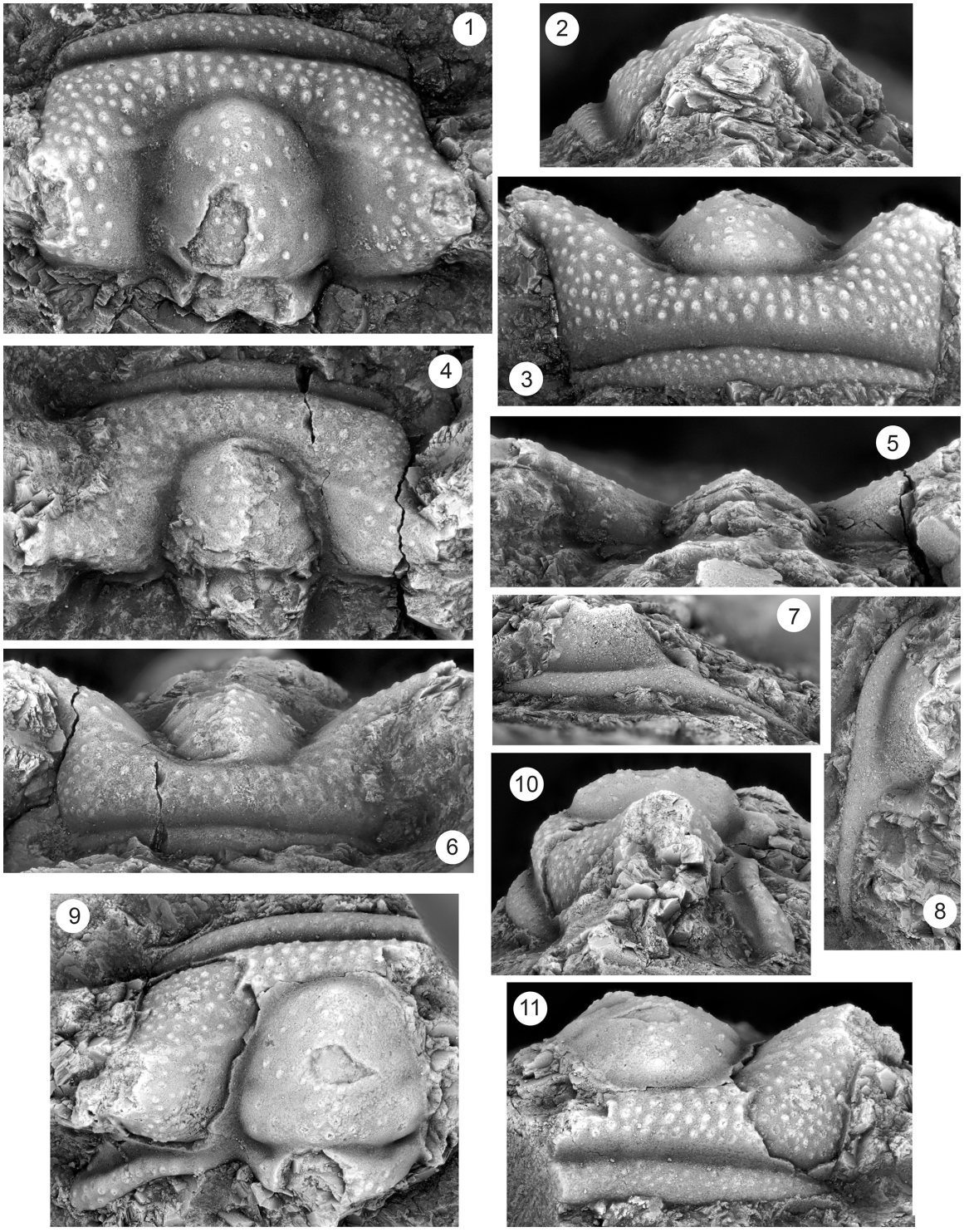
1
2
3
4
5
6
7
8
9
10
11

Plate 6

Fig. 1-10. *Deckera completa* Wilson 1951 from the Gatesburg Formation.

1, 2, 3. Cranidium, dorsal, right lateral, and anterior views, YPM 18565, x8.

4, 5, 6. Cranidium, anterior, dorsal, and posterior views, YPM 18567, x9.

7, 8. Free Cheek, dorsal and oblique (?) views, YPM 18568, x9.

9, 10. Cranidium, anterior and dorsal views, YPM 18564, x9.

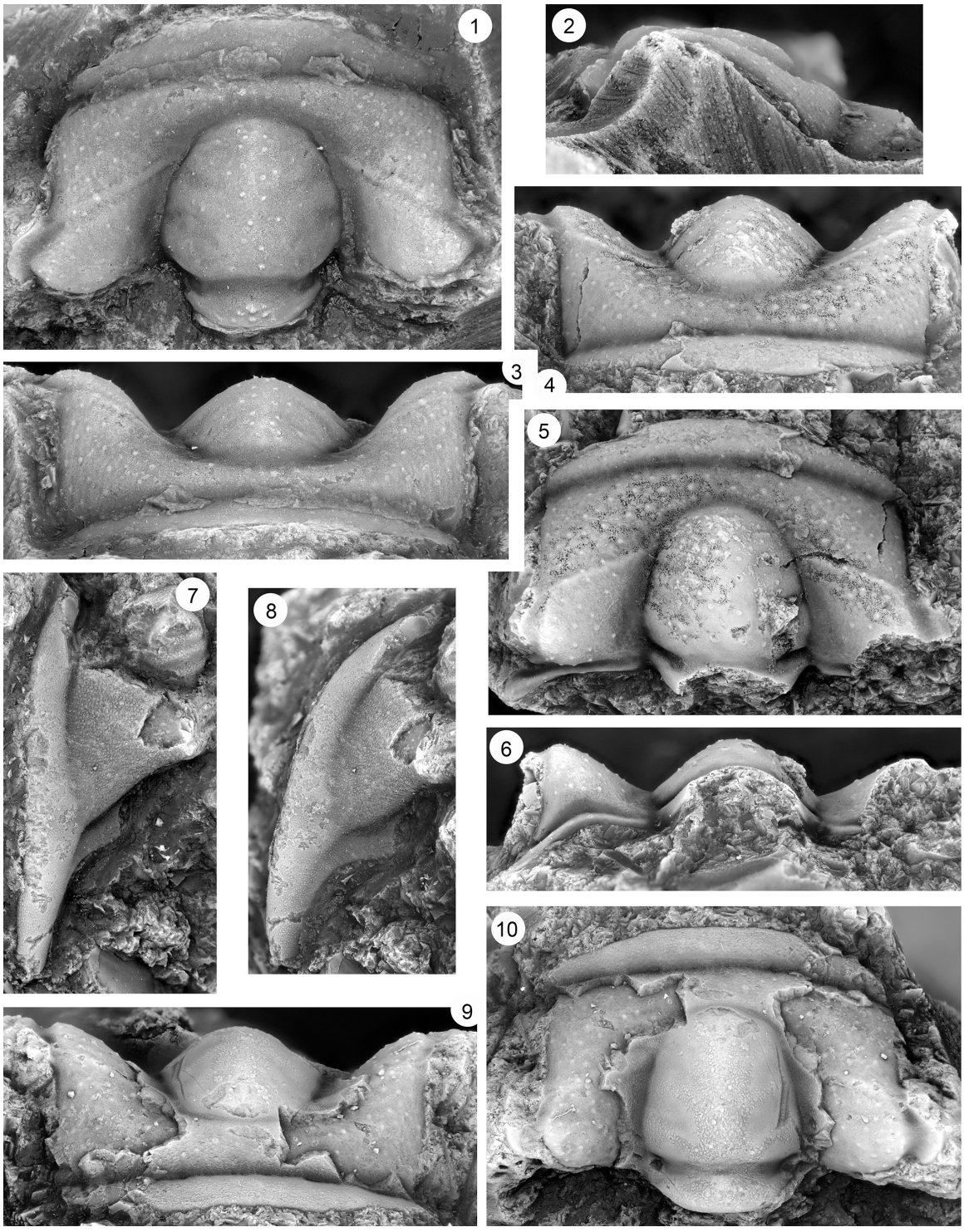
1
2
3
4
5
6
7
8
9
10

Plate 7

Fig. 1-3, 7-9. *Deckera* cf. *D. completa* Wilson 1951 from the Sneakover Member of the Orr Formation.

1, 2, 3. Cranidium, dorsal, left lateral, and anterior views, ORR 59.4 OU 238141, x9.

7, 8, 9. Pygidium, right lateral, posterior, and dorsal views, ORR 59.4 OU 238142, x6.5

Fig. 4-6. *Deckera completa* Wilson 1951 from the Gatesburg Formation.

4, 5, 6. Pygidium, dorsal, posterior, and right lateral views, YPM 18567, x12.

Fig. 10-15. *Deckera aldenesis* Frederickson 1949 from the Honey Creek Formation.

10, 11, 12. Pygidium, posterior, dorsal, and right lateral views, KR2 50.3 OU 238143, x20.

13, 14, 15. Cranidium, anterior, left lateral, and dorsal views, KR2 50.3 OU 238144, x15.

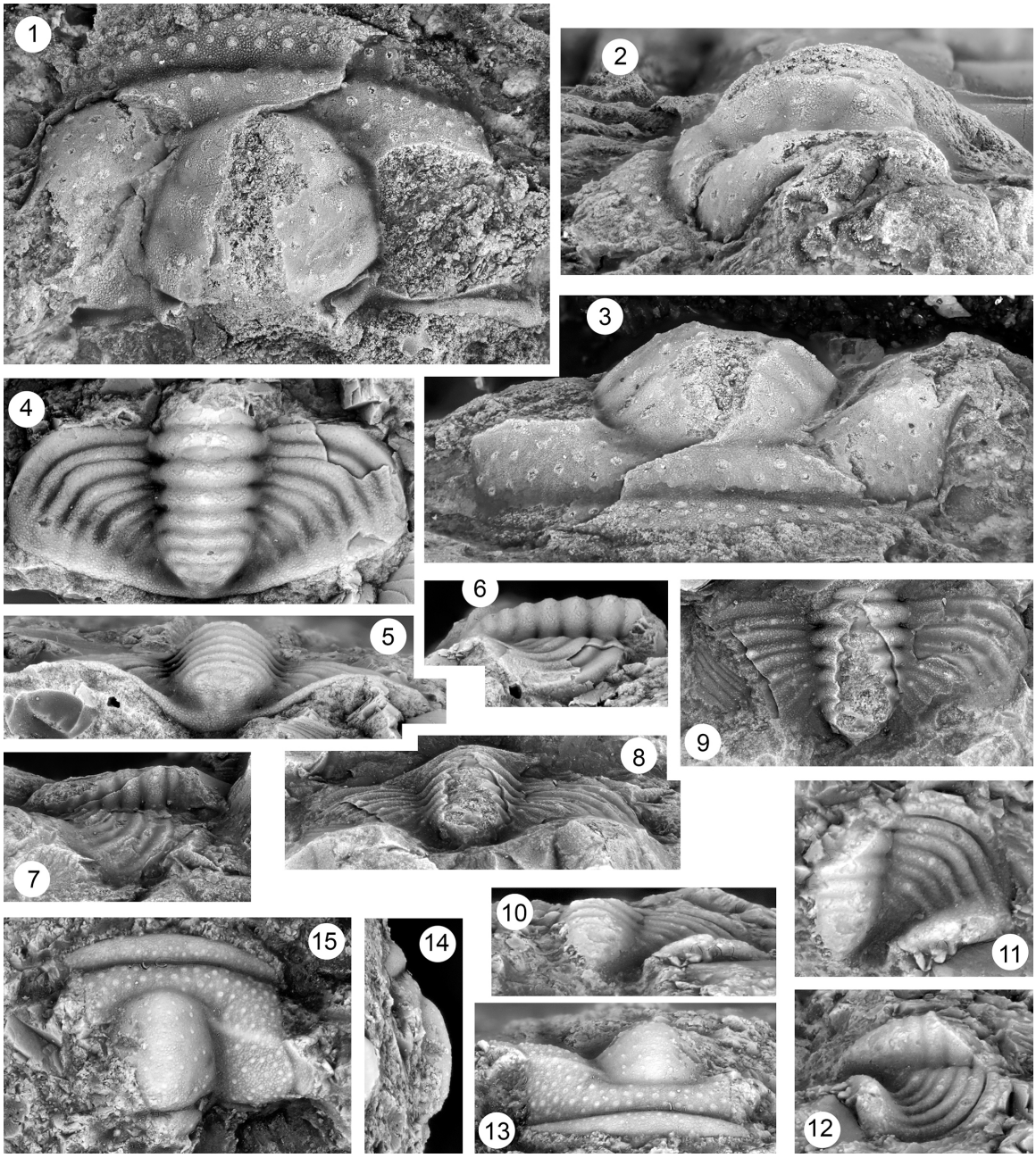
1
2
3
4
5
6
7
8
9
10
11
12
13
14
15

Plate 8

Fig. 1-15. *Labiocephalus cassia* sp. nov. from the Barton Canyon Member of the Windfall Formation and Sneakover Member of the Orr Formation.

1, 2, 3. Cranidium, dorsal, anterior, and left lateral views, CHC-2-216.9 5 OU 237974, x3.

4, 5, 6. Cranidium, anterior, dorsal, and left lateral views, CHC-2-216.9 5 OU 237975, x2.5.

7, 11, 12. Cranidium, dorsal, right lateral, and anterior views, CHC-2-216.9 5 OU 237976, x5.

8, 9, 10. Cranidium, left lateral, dorsal, and anterior views, CHC-2-216.9 5 OU 237977 (holotype), x5.

13, 14, 15. Pygidium, posterior, left lateral, and dorsal views, CHC-2-216.9 5 OU 237978, x7.

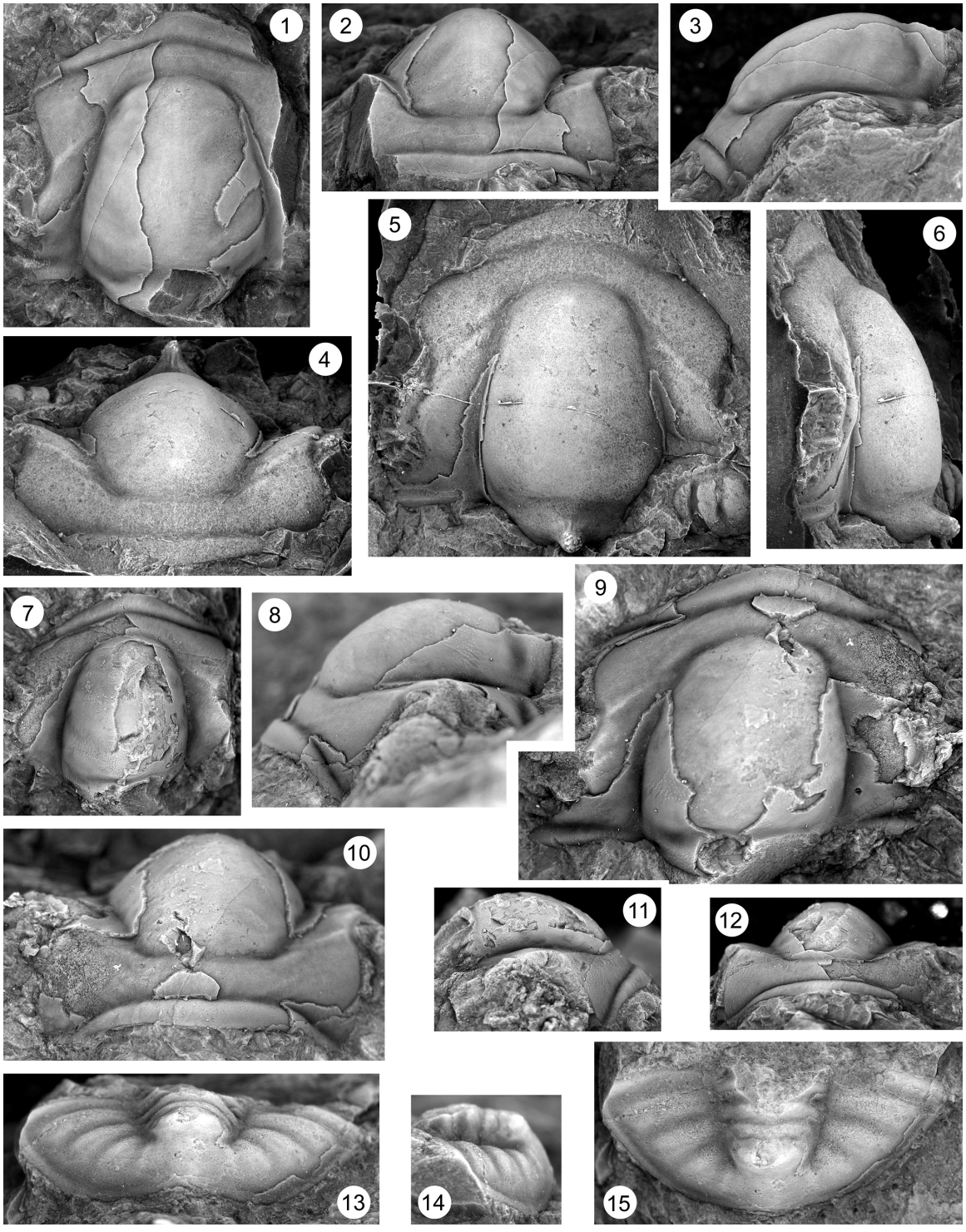
1
2
3
5
6
4
7
8
9
10
11
12
13
14
15

Plate 9

Fig. 1-3. *Elvinia* sp. 1 from the Barton Canyon Member of the Windfall formation.

1, 2, 3. Cranidium, dorsal, right lateral, and anterior views, CHC-2-216.95 OU 237979, x7.

Fig. 4-10. *Elvinia roemeri* (Shumard, 1861) from the Barton Canyon Member of the Windfall Formation and the Sneakover Member of the Orr Formation.

4, 5, 6. Cranidium, dorsal, anterior, and right lateral views, CHC-2-216.95 OU 237980, x15.

7, 8. Cranidium, dorsal and left lateral views, CHC-2-216.95 OU 237981, x5.

9. Cranidium, dorsal view, CHC-2-216.95 OU 237982, x9.

10. Cranidium, dorsal view, CHC-2-216.95 OU 237983, x11.

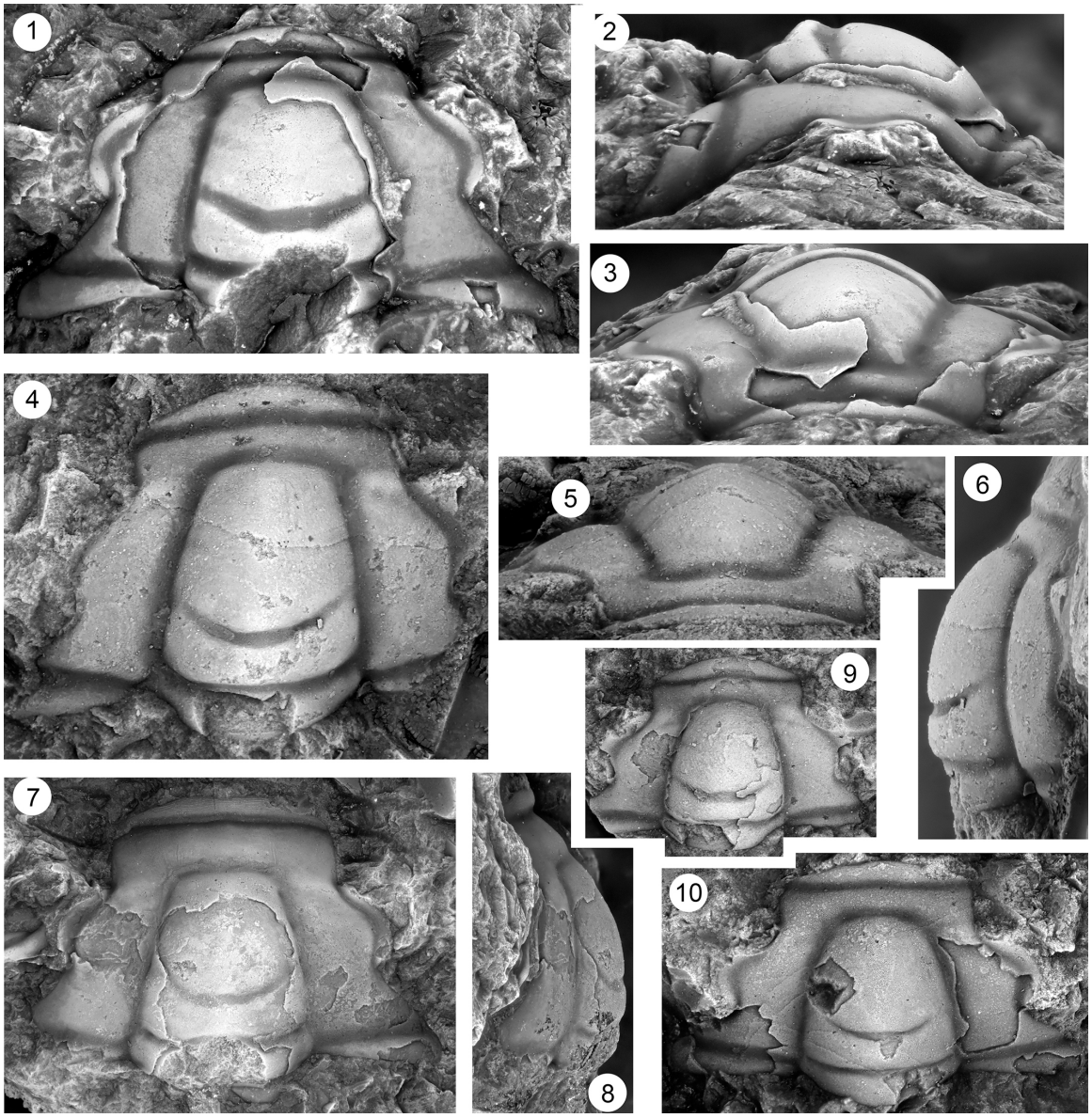
1
2
3
4
5
6
9
7
8
10

Plate 10

Fig. 1-3. *Elvinia* sp. 2 from the Barton Canyon Limestone Member of the Windfall Formation.

1, 2, 3. Cranidium, dorsal, left lateral, and anterior views, STR 9.5 OU 237984, x15.

Fig. 4-7. *Elvinia roemeri* (Shumard, 1861) from the Barton Canyon Member of the Windfall Formation and the Sneakover Member of the Orr Formation.

4. Cranidium, dorsal view, STR 10.9-11.1 OU 237985, x12.

5, 6, 7. Cranidium, right lateral, dorsal, and anterior views, ORR 59.4 OU 237986, x14.

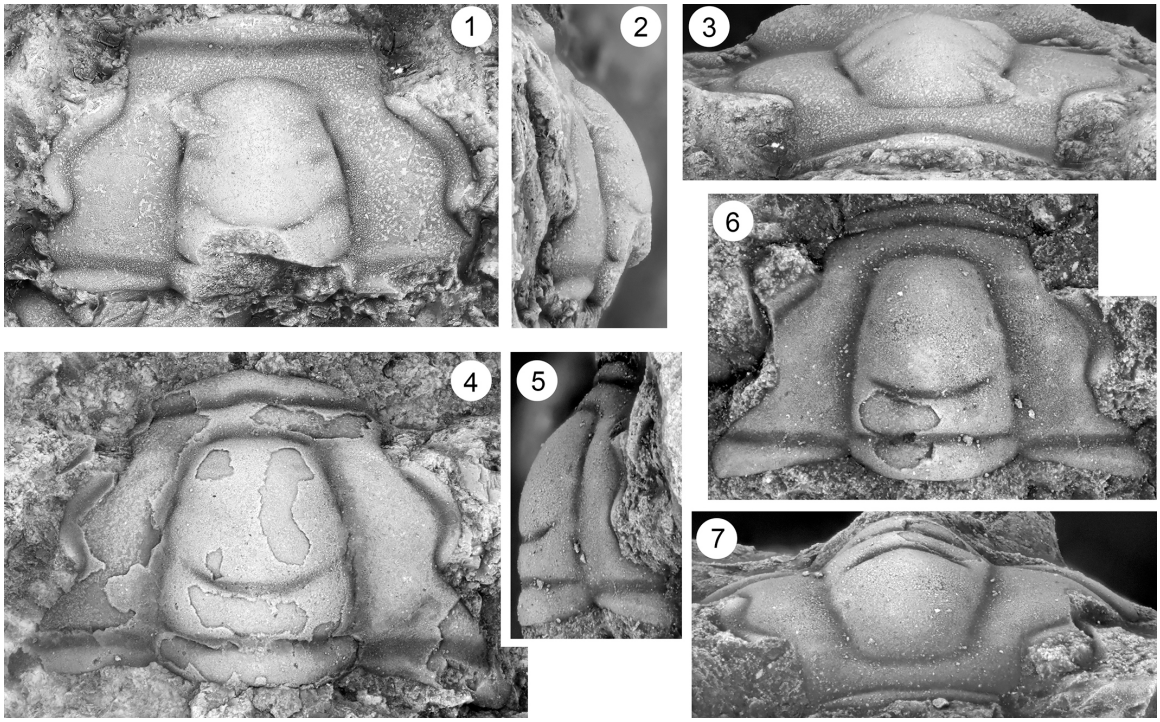
1
2
3
4
5
6
7

Plate 11

Fig. 1-11. *Anechocephalus ralphi* n. sp. from the Barton Canyon Member of the Windfall Formation and the Sneakover Member of the Orr Formation.

1, 2, 3. Pygidium, dorsal, left lateral, and posterior views, STR 10.9-11.1 OU 237987, x15.

4, 5, 6. Cranidium, dorsal, right lateral, and anterior views, CHC-2-216.95 OU 237988, x16.

7, 8, 9. Cranidium, anterior, right lateral, and dorsal views, STR 10.9-11.1 OU 237989, x15.

10, 11. Pygidium, posterior and dorsal views, CHC-2-216.95 OU 237990, x10.

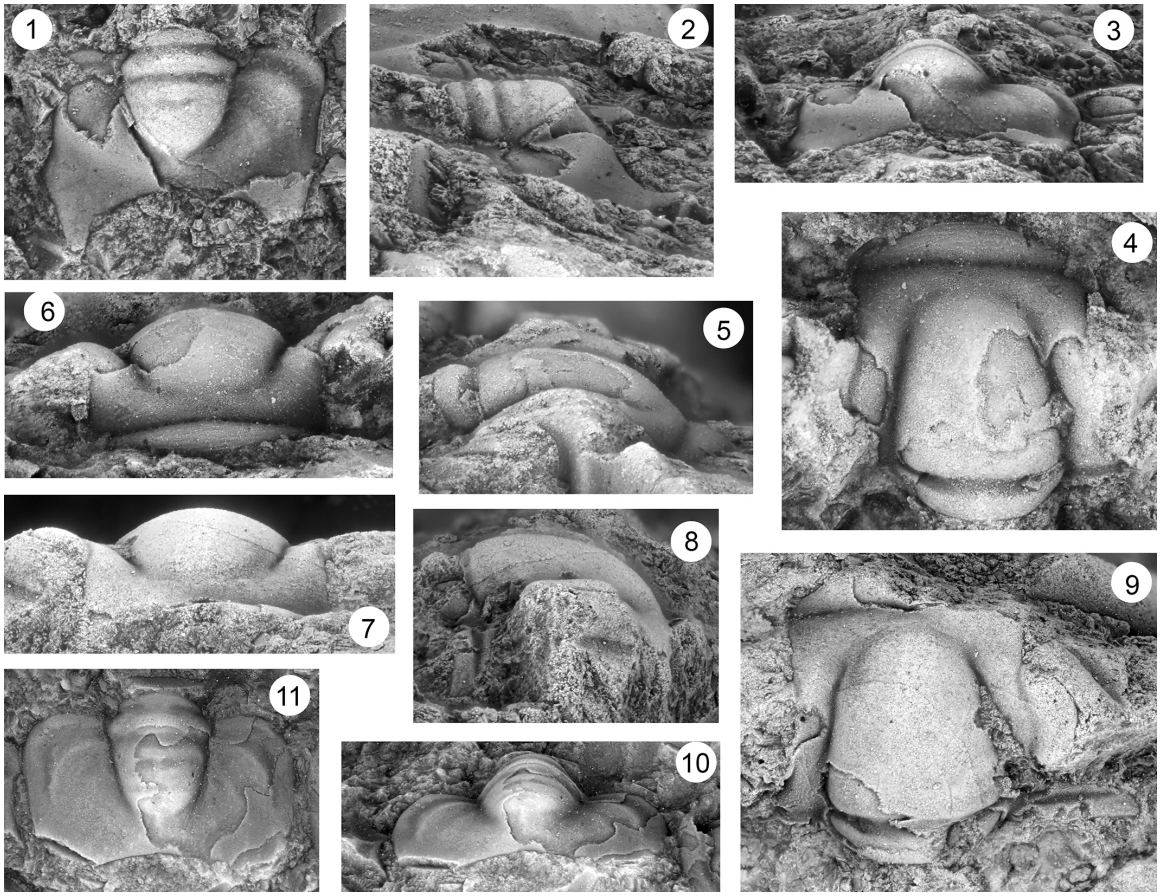
1
2
3
4
5
6
7
8
9
10
11

Plate 12

Fig. 1-15. *Anechocephalus ralphi* n. sp. from the Barton Canyon Member of the Windfall Formation the Sneakover Member of the Orr Formation.

1, 2, 3. Cranidium, dorsal, right lateral, and anterior views, CHC-2-216.95 OU 237991, x14.

4, 5, 6. Pygidium, dorsal, right lateral, and posterior views, CHC-2-216.95 OU 237992 (holotype), x6.

7, 8, 9. Cranidium, dorsal, left lateral, and anterior views, CHC-2-216.95 OU 237993, x14.

10, 11, 12. Cranidium, dorsal, right lateral, and anterior views, CHC-2-216.95 OU 237994, x16.

13, 14, 15. Cranidium, dorsal, right lateral, and anterior views, CHC-2-216.95 OU 237995, x9.

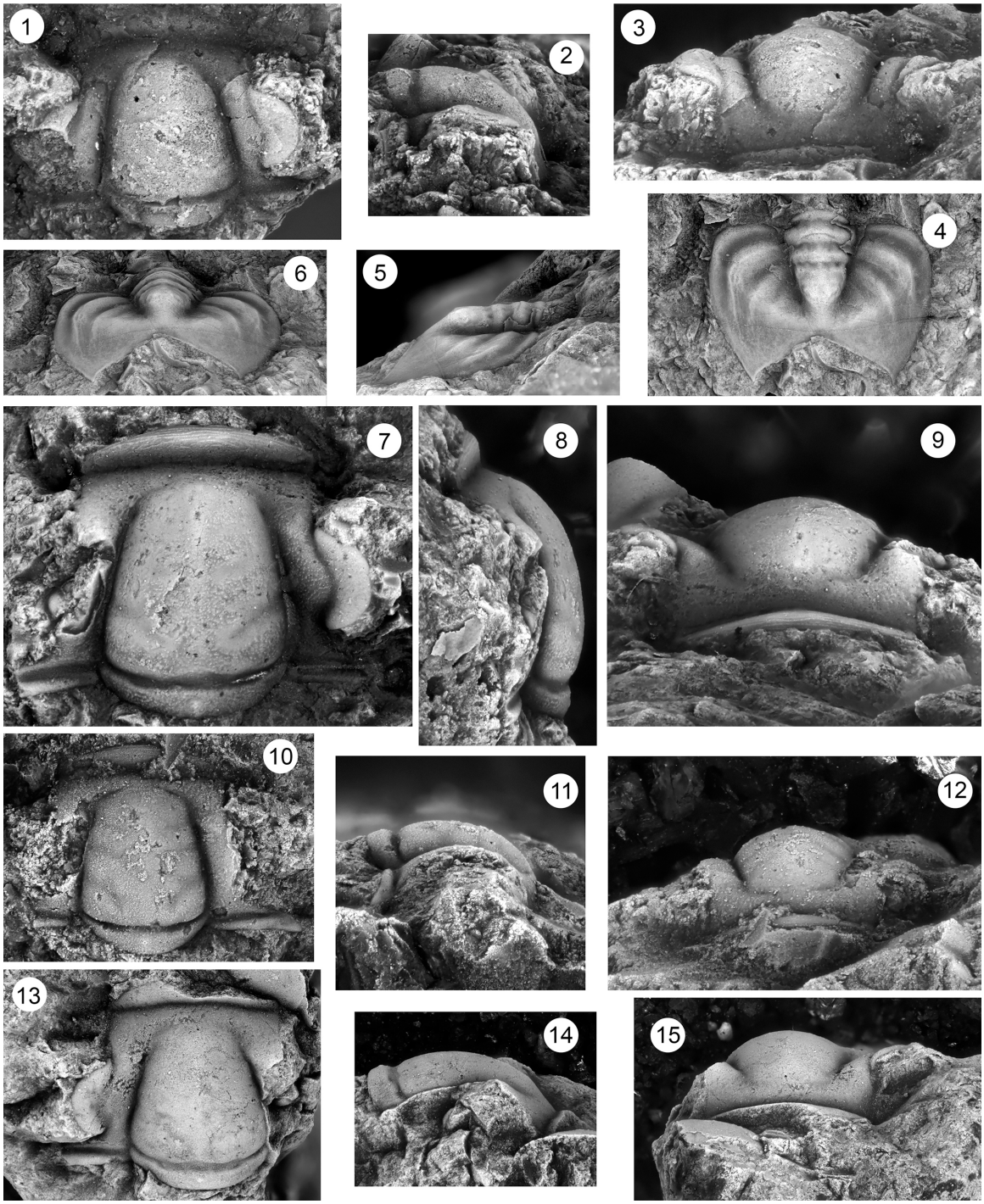
1
2
3
4
5
6
7
8
9
10
11
12
13
14
15

Plate 13

Fig. 1-10. *Anechocephalus ralphi* n. sp. from the Barton Canyon Member of the Windfall Formation the Sneakover Member of the Orr Formation.

1, 2, 3. Cranidium, dorsal, left lateral, and anterior views, CHC-2-216.95 OU 237996, x15.

4, 5. Cranidium, dorsal and anterior views, CHC-2-216.95 OU 237997, x16.

6, 7. Cranidium, dorsal and anterior views, CHC-2-216.95 OU 237998, x12.

8, 9, 10. Cranidium, dorsal, right lateral, and anterior views, CHC-2-216.95 OU 237999, x9.

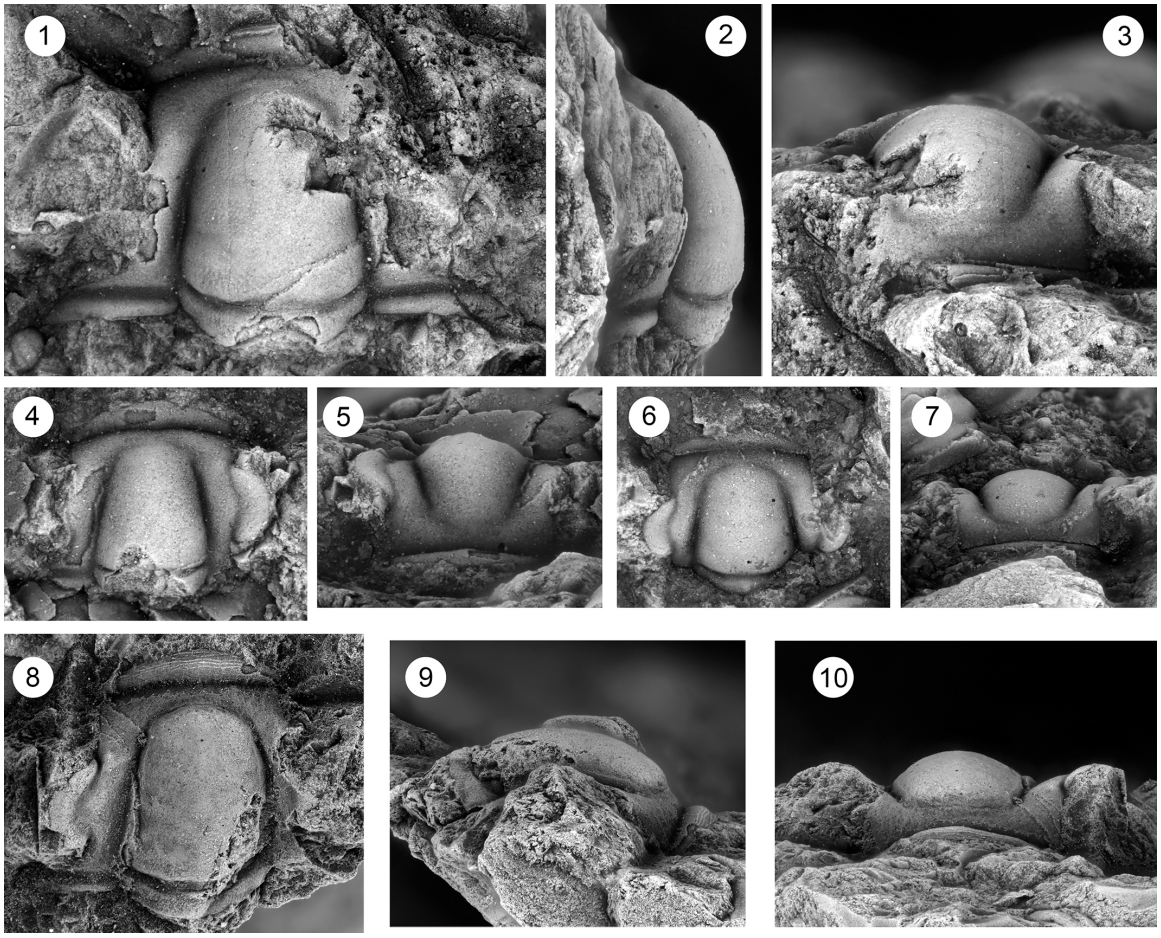
1
2
3
4
5
6
7
8
9
10

Plate 14

Fig. 1-9. *Pterocephalia* sp. indet. from the Sneakover Member of the Orr Formation.

1, 2. Cranidium, dorsal, and right lateral views, ORR 59.4 OU 238000.

3. Pygidium, dorsal view, ORR 59.4 OU 238001.

4, 5, 6. Cranidium, dorsal, anterior, and left oblique (?) views, ORR 59.4 OU 238002, x4.

7, 8, 9. Cranidium, dorsal, left lateral, and anterior views, ORR 59.4 OU 238003, x9.

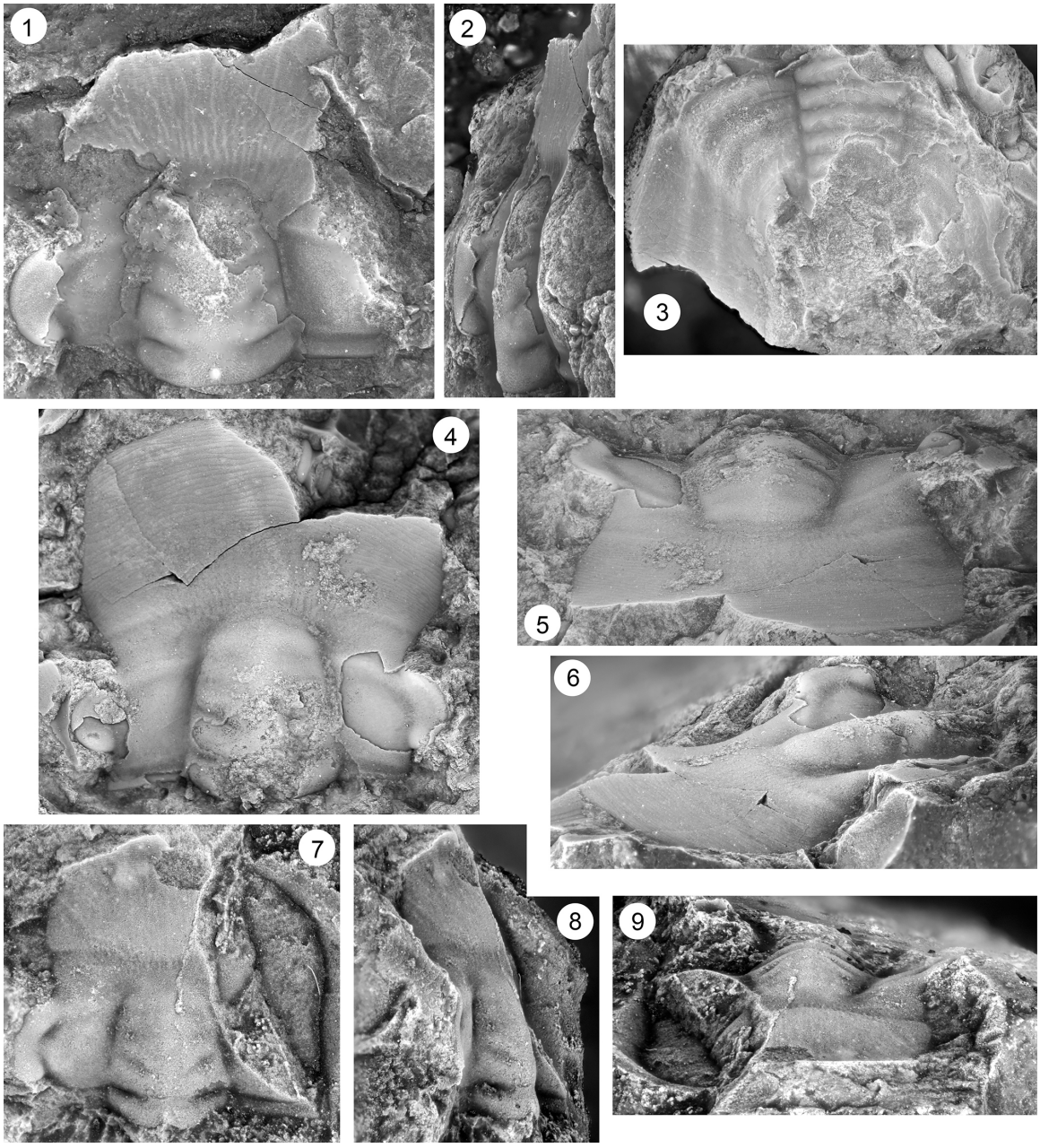
1
2
3
4
5
6
7
8
9

Plate 15

Fig. 1-8. *Labiostria conveximarginata* Palmer, 1954 from the Riley Formation.

1, 2, 3. Cranidium, dorsal, right lateral, and anterior view, USNM 185962 (holotype), x7.5

4, 5, 6. Cranidium, dorsal, right lateral, and anterior views, USNM 123322 (paratype), x7.

7, 8. Free cheek, dorsal and right lateral views, USNM 185964 (paratype), x6.

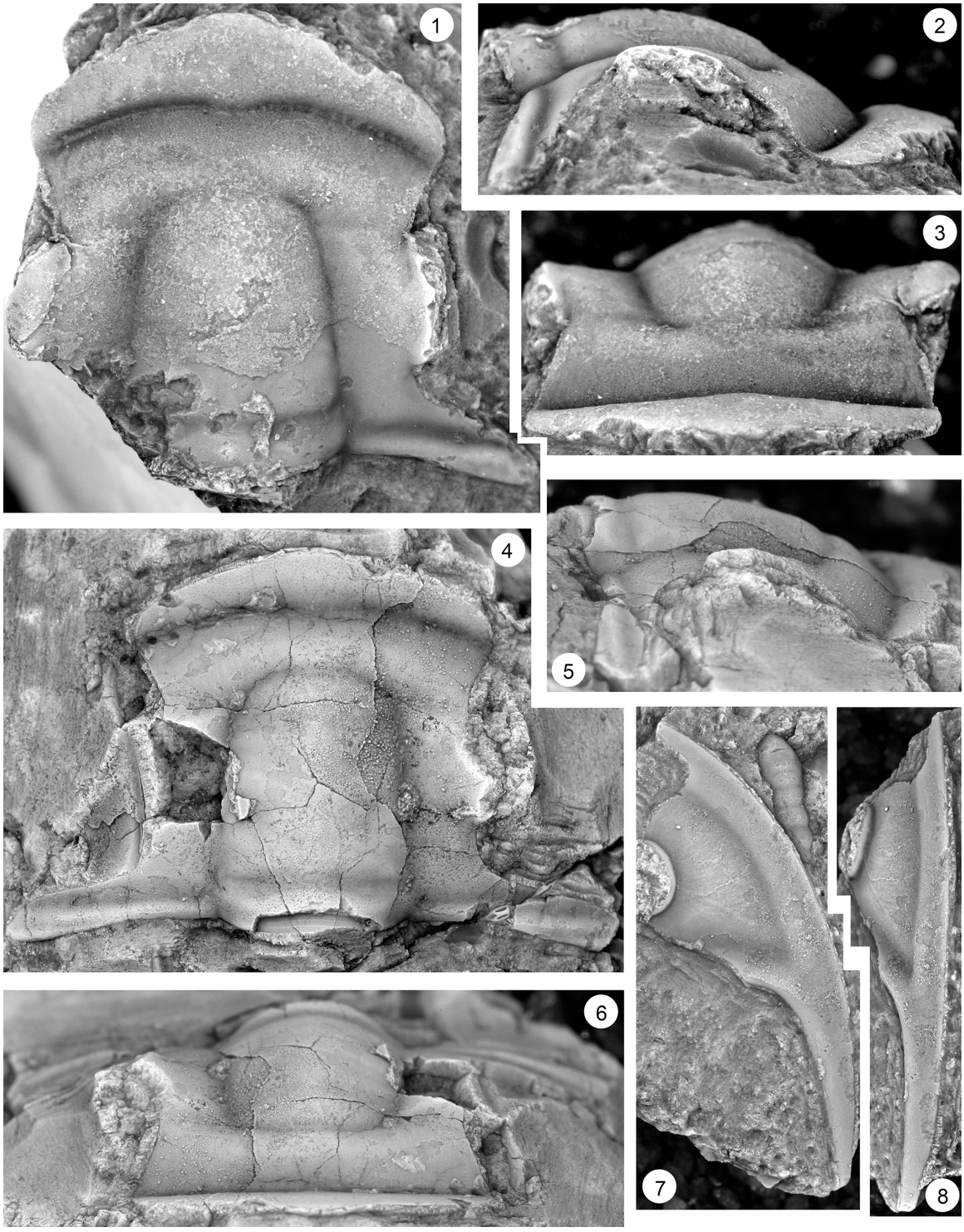
1
2
3
4
5
6
7
8

Plate 16

Fig. 1-3. *Labiostria sigmoidalis* from the Riley Formation, central Texas.

1, 2, 3. Cranidium, anterior, left lateral, and dorsal views, USNM 165968 (holotype), x8.

Fig. 4-9. *Labiostria. platifrons* Palmer, 1954 from the Riley Formation, central Texas.

4. Pygidium, dorsal view, USNM 185966 (paratype), x5.

5, 6. Free cheek, left lateral and dorsal views, USNM 185967 (paratype), x6.

7, 8, 9. Cranidium, dorsal, anterior and right lateral views, USNM 185965 (holotype), x8.

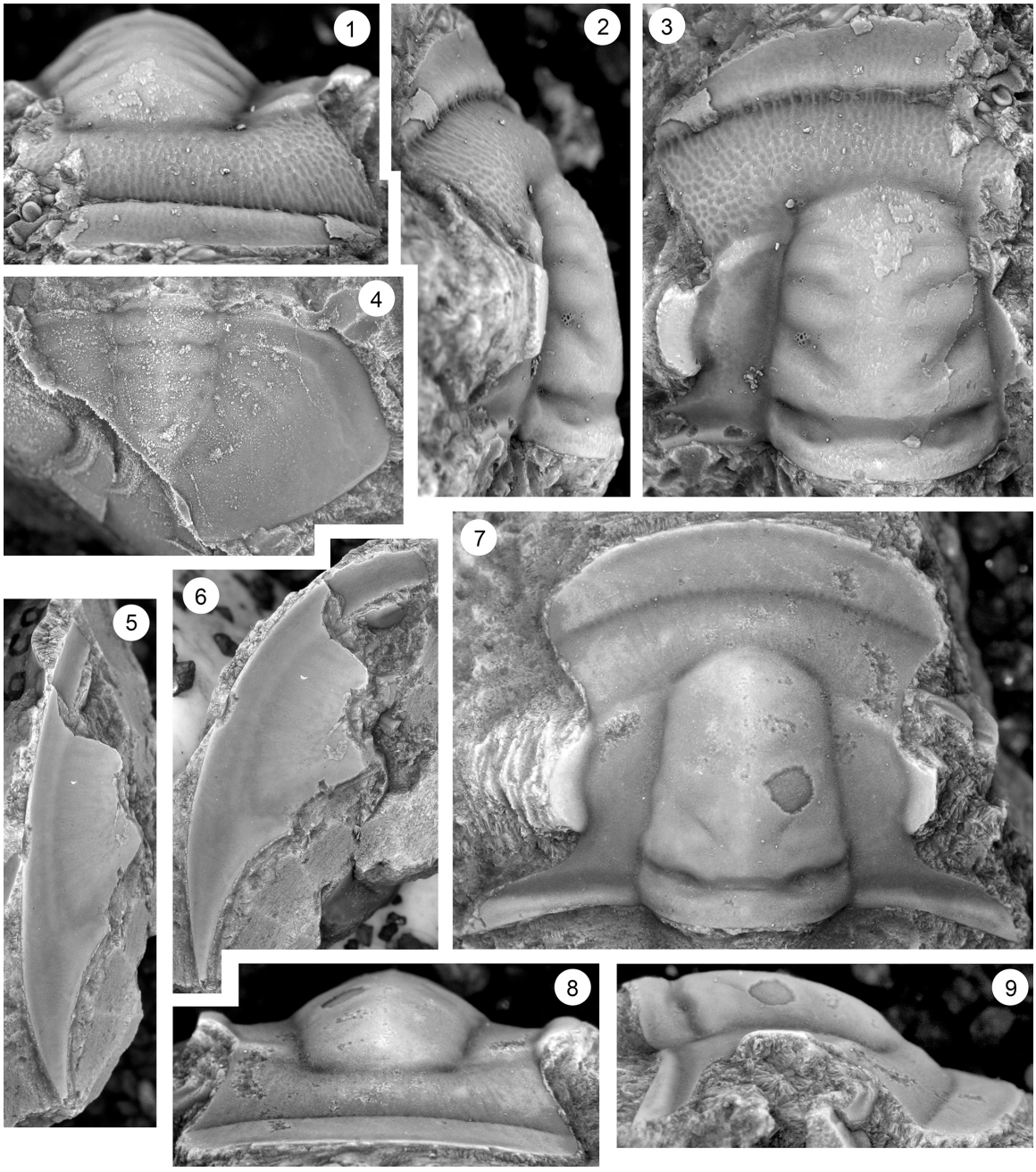
1
2
3
4
5
6
7
8
9

Plate 17

Fig. 1-13. *Labiostria westropi* Chatterton and Ludvigsen 1998 from the Barton Canyon Member of the Windfall Formation.

1, 2, 3. Cranidium, dorsal, anterior, and left lateral views, CHC-2-216.95 OU 238004, x5.

4. Free cheek, dorsal view, CHC-1-0 OU 238005, x3.5.

5, 6, 7. Pygidium, dorsal, right lateral, and posterior views, CHC-2-216.95 OU 238006, x5.

8, 9, 10. Cranidium, dorsal, left lateral, and anterior views, CHC-2-216.95 OU 238007, x5.

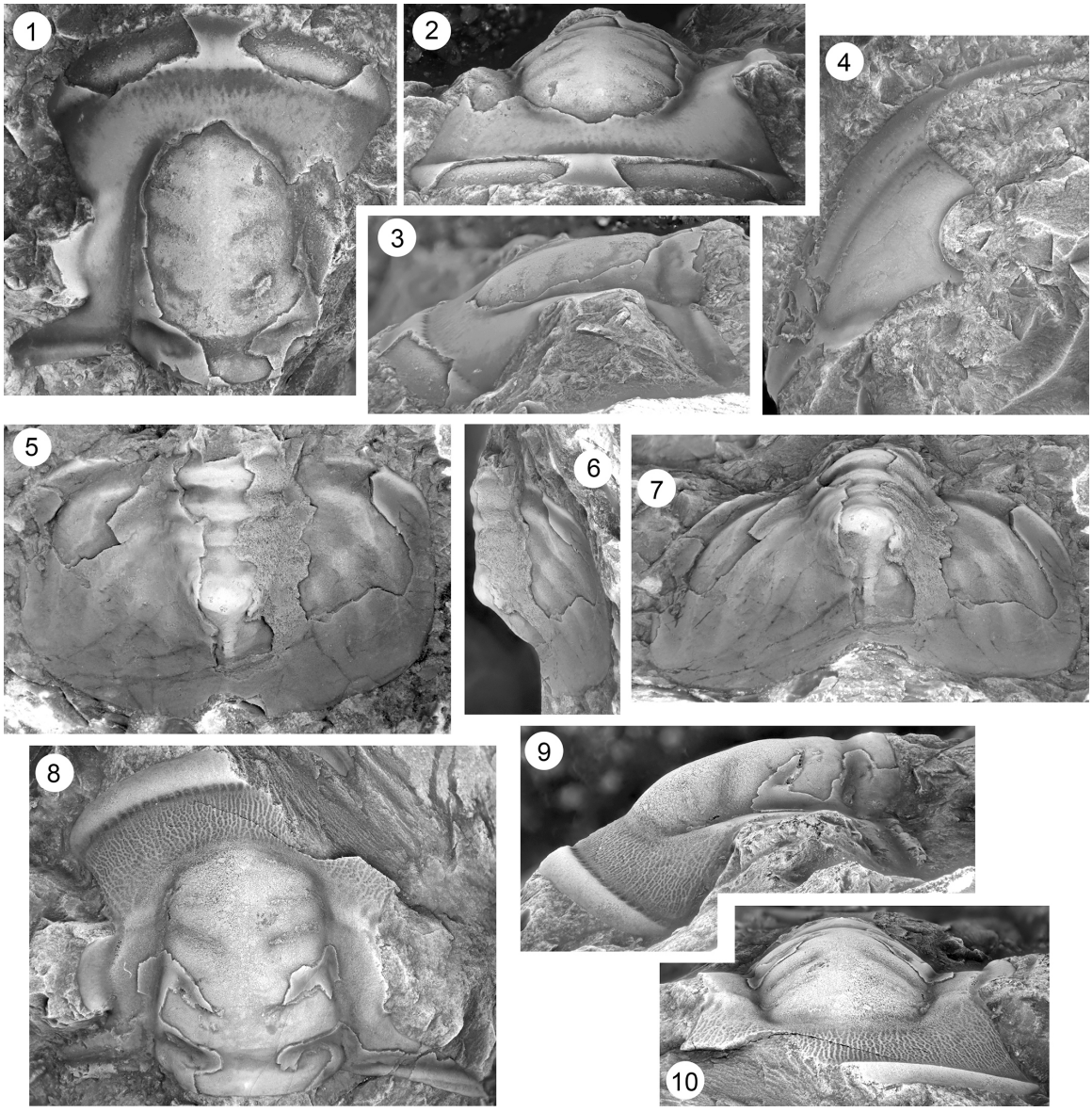
1
2
3
4
5
6
7
8
9
10

Plate 18

Fig. 1-15. *Labiostria westropi* Chatterton and Ludvigsen 1998 from the Barton Canyon Member of the Windfall Formation.

1, 2, 3. Cranidium, dorsal, right lateral, and anterior views, CHC-2-216.95 OU 238008, x6.

4, 5, 6. Cranidium, anterior, right lateral, and dorsal views, CHC-2-216.95 OU 238009, x5.5.

7, 8, 9. Cranidium, dorsal, left lateral, and anterior views, CHC-2-216.95 OU 238110, x5.5.

10, 11, 12. Pygidium, dorsal, right lateral, and posterior views, CHC-2-216.95 OU 238111, x5.

13, 14, 15. Cranidium, left lateral, dorsal, and anterior views, CHC-2-216.95 OU 238112, x4.5.

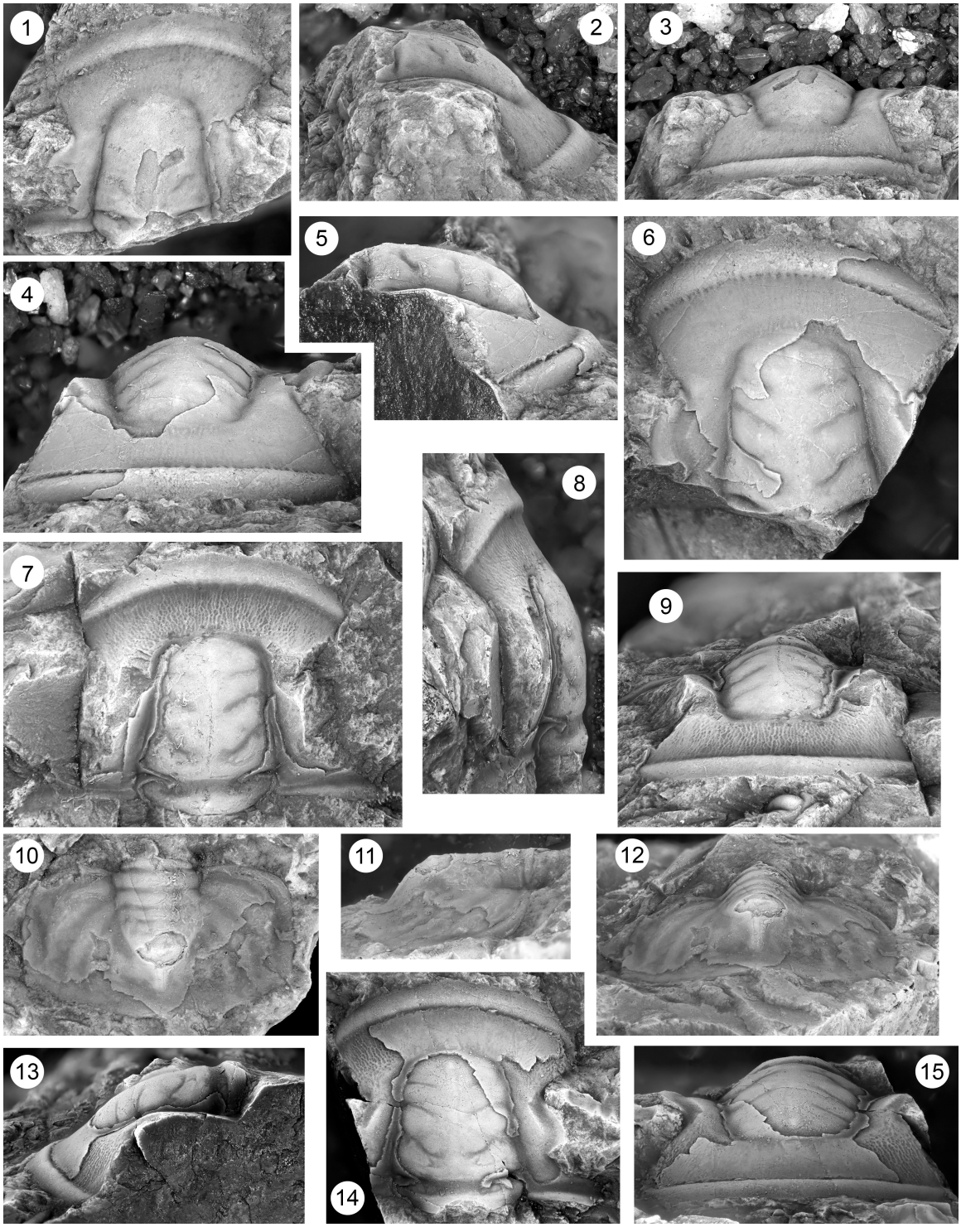
1
2
3
4
5
6
7
8
9
10
11
12
13
14
15

Plate 19

Fig. 1-15. *Labiostria westropi* Chatterton and Ludvigsen 1998 from the Barton Canyon Member of the Windfall Formation.

1, 2, 3. Cranidium, dorsal, right lateral, and anterior views, CHC-2-216.95 OU 238113, x5.

4, 5, 6. Cranidium, right lateral, anterior, and dorsal views, CHC-2-216.95 OU 238114, x4.

7, 8, 9. Cranidium, dorsal, right lateral, and anterior views, CHC-2-216.95 OU 238115, x3.

10, 11, 12. Cranidium, anterior, left lateral, and dorsal views, STR 9.5 OU 238116, x4.

13. Cranidium, dorsal view, CHC-2-216.95 OU 238117, x5.

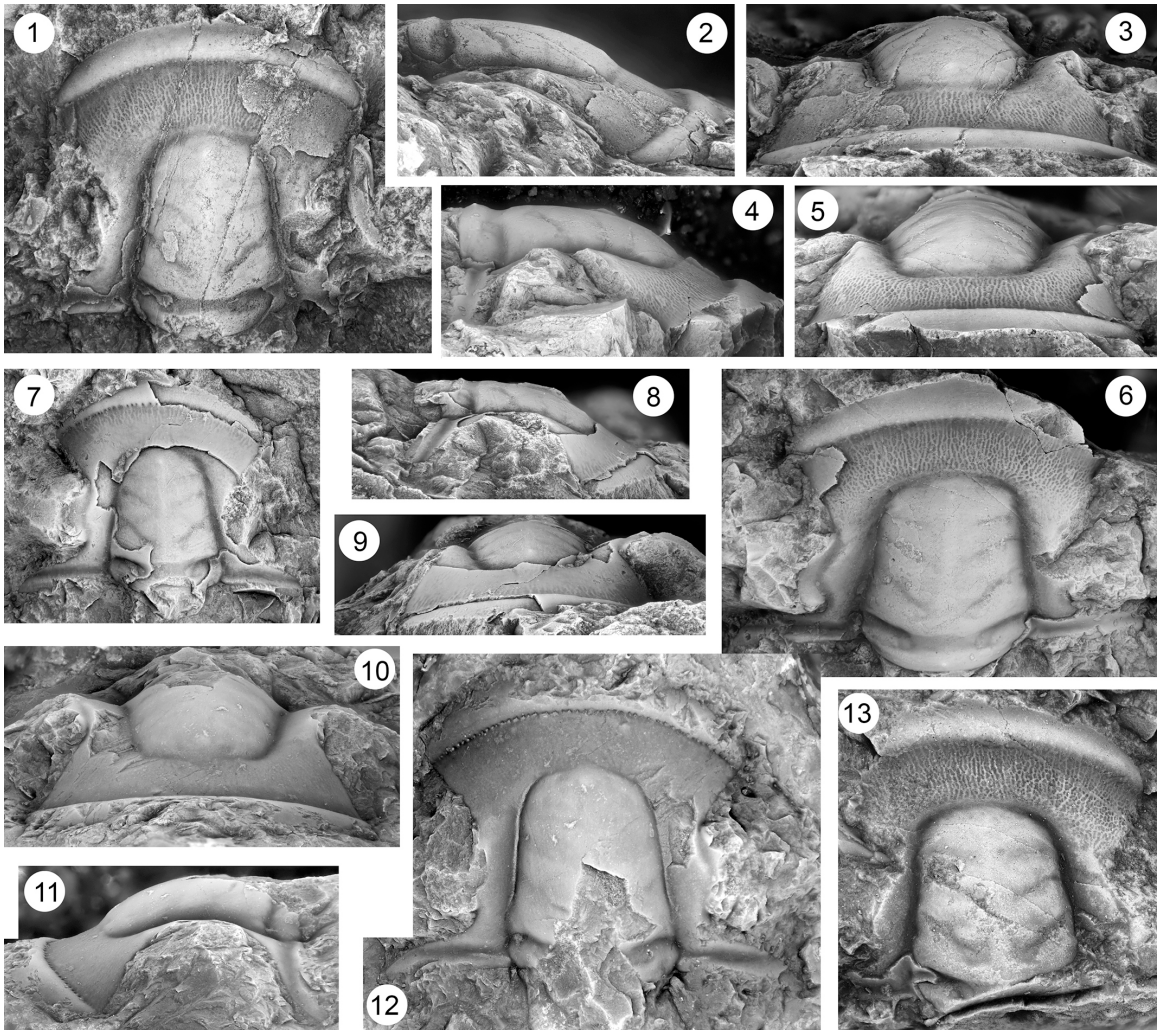
1
2
3
4
5
7
8
6
9
10
13
11
12

Plate 20

Fig. 1-18. *Labiostria westropi* Chatterton and Ludvigsen 1998 from the Barton Canyon Member of the Windfall Formation.

1, 2, 3. Cranidium, dorsal, left lateral, and anterior views, STR 9.5 OU 238118, x3.5.

4, 5, 6. Pygidium, dorsal, right lateral, and posterior views, STR 9.5 OU 238119, x3.5.

7, 8, 9. Cranidium, dorsal, right lateral, and anterior views, STR 9.5 OU 238120, x4.

10, 11, 12. Cranidium, dorsal, right lateral, and anterior views, STR 9.5 OU 238121, x3.5.

13, 14, 15. Cranidium, dorsal, right lateral, and anterior views, STR 9.5 OU 238122, x3.5.

16, 17, 18. Cranidium, dorsal, anterior, and left lateral views, CHC-1-0 OU 238123, x3.5.

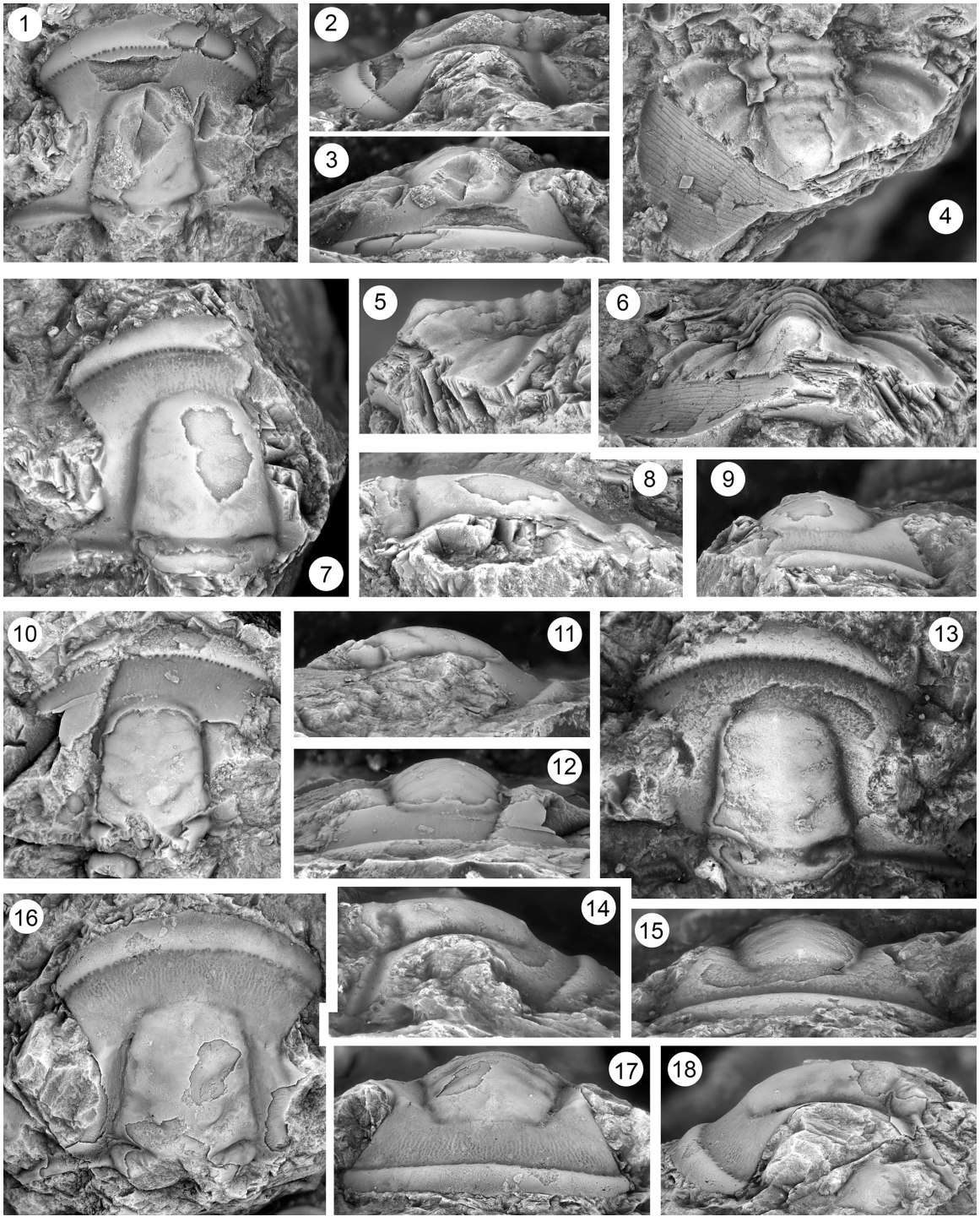
1
2
3
4
5
6
7
8
9
10
11
12
13
14
15
16
17
18

Plate 21

Fig. 1-6. *Labiostria westropi* Chatterton and Ludvigsen 1998 from the Barton Canyon Member of the Windfall Formation.

1, 2, 3. Pygidium, dorsal, posterior, and right lateral views, CHC-1-0 OU 238124, x7.

4, 5. Pygidium, dorsal and posterior views, CHC-1-0 OU 238125, x7.

6. Pygidium, dorsal view, CHC-2-216.95 OU 238126, x6.

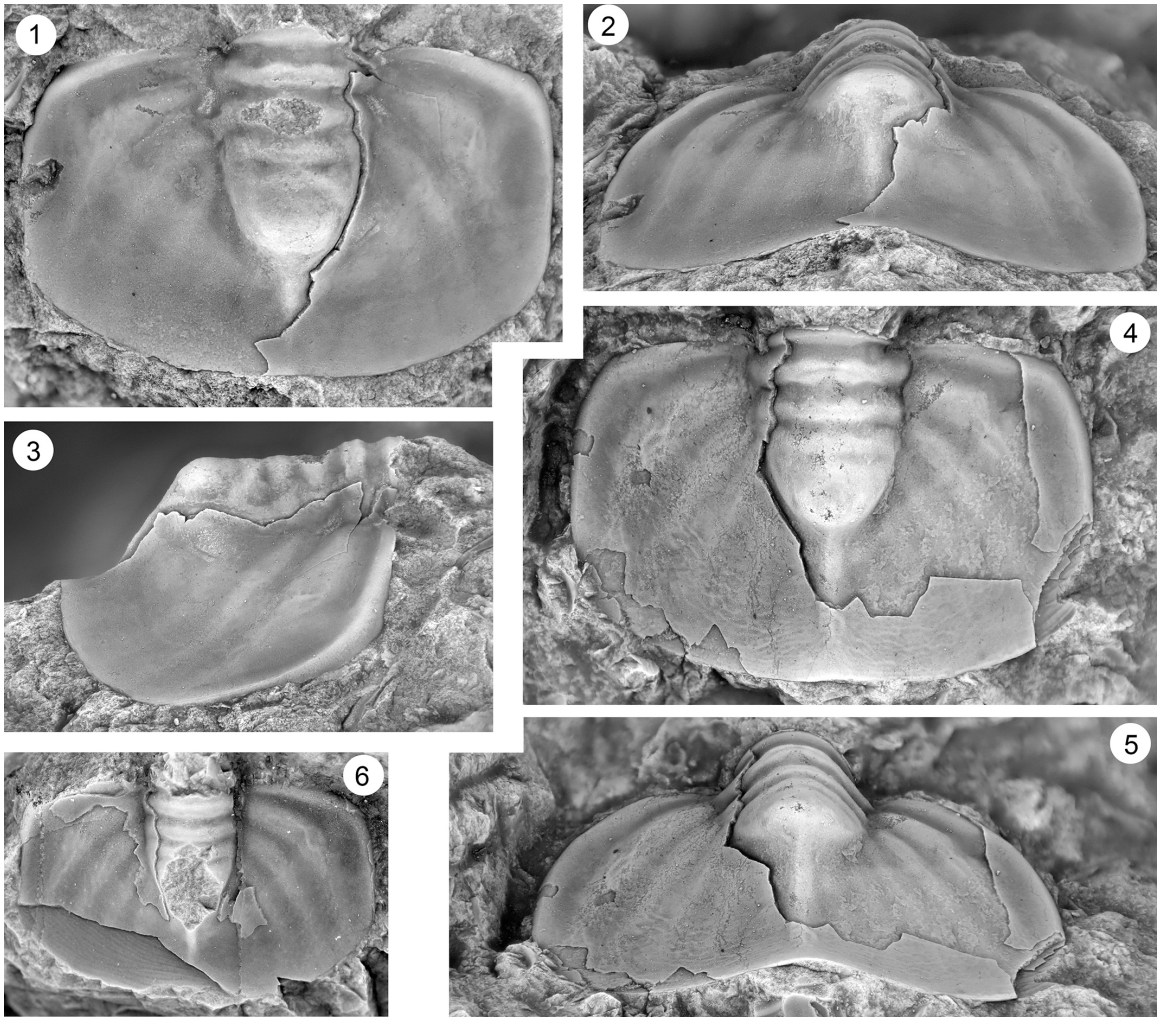
1
2
3
4
5
6

Plate 22

Fig. 1-15. *Stenambon paucigranulus* Palmer, 1965 from the *Irvingella major* Zone, Barton Canyon Member, Windfall Formation, Barton Canyon, Section CHC-1.

1, 2, 3. Cranidium, dorsal, right lateral, and anterior view, OU 238149, x8.

4, 5. Pygidium, dorsal and postrior view, CHC-1-0 upper bed OU 238150, x12.

6. Cranidium, dorsal view, CHC-1-0 upper bed OU 238151, x10.

7. Free cheek, dorsal view, CHC-1-0 upper bed OU 238152, x7.

8. Cranidium, dorsal view, CHC-1-0 upper bed OU 238153, x8.

9, 10. Cranidium, dorsal and anterior views, CHC-1-0 upper bed OU 238154, x8.

11, 12, 13. Cranidium, dorsal, anterior, and right lateral views, CHC-1-0 upper bed OU 238155, x8.

14. Pygidium, dorsal view, CHC-1-0 upper bed OU 237960.

15. Cranidium, dorsal view, CHC-1-0 upper bed OU 237961.

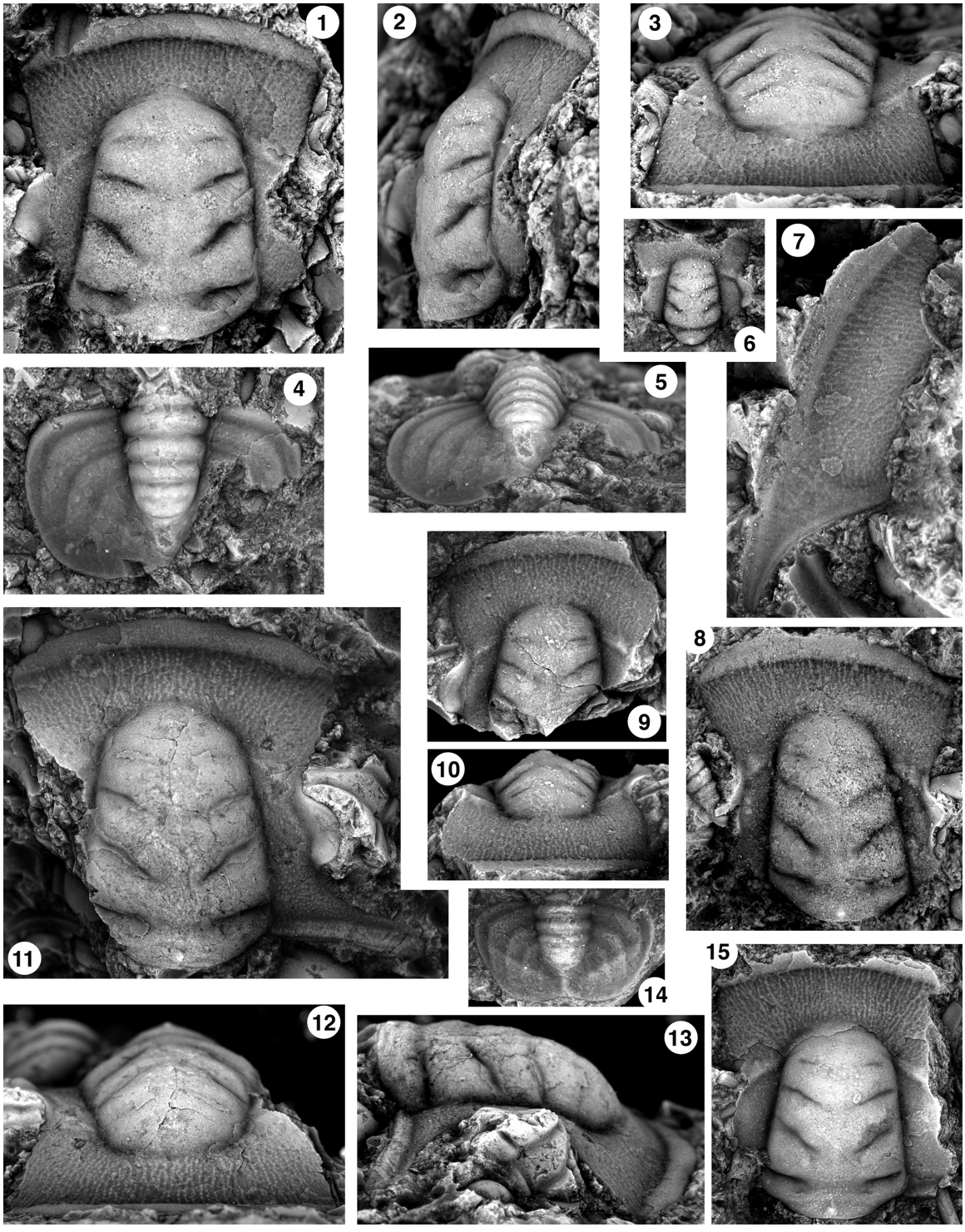
1
2
3
6
7
4
5
9
8
10
11
14
15
12
13

Plate 23

Fig. 1-7. *Stenambon paucigranulus* Palmer, 1965 from the Barton Canyon Limestone Member, Windfall Formation, *Irvingella major* Zone, Cherry Creek Range, Nevada and Sneakover Member, Orr Formation, Orr Ridge, northern House Range, Utah.

1. Cranidium, dorsal view, CHC-1-0 upper bed u4 OU 238127, x8.

2. Cranidium, dorsal view, CHC-1-0 upper bed u4 OU 238128, x8.

3, 4, 5. Pygidium, dorsal, posterior, and right lateral views, CHC-2-216.95 OU 238129, x8.

6. Cranidium, dorsal view, ORR 60.2 OU 238130, x8.

7. Cranidium, dorsal view, ORR 60.2 OU 238131, x6.65.

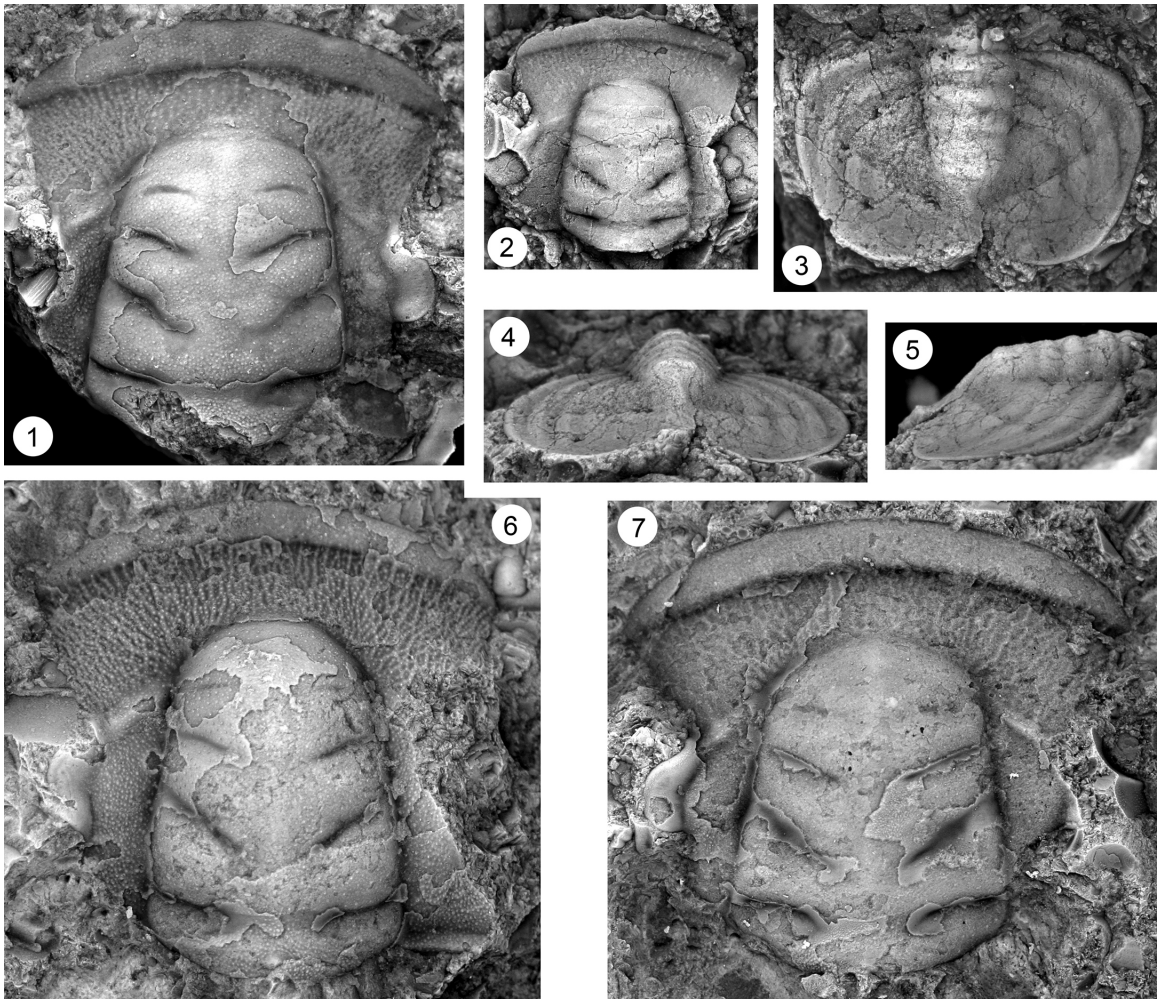
1
2
3
4
5
6
7

Plate 24

Fig, 1-6. *"Morosa"*? *bothra* Stitt, 1971 from the Honey Creek Formation, central Oklahoma.

1, 2, 3. Cranidium, dorsal, right lateral, and anterior views, OU 6506 (holotype), x18.

4, 5, 6. Cranidium, anterior, right lateral, and dorsal views, OU 6507, x20.

Fig. 7-9. "*Morosa*" *simplex* from the Honey Creek Formation.

7. Cranidium, dorsal, right lateral, OU 6509 (holotype), x15.

8, 9. Cranidium, right lateral and dorsal view, OU 6508, x16.

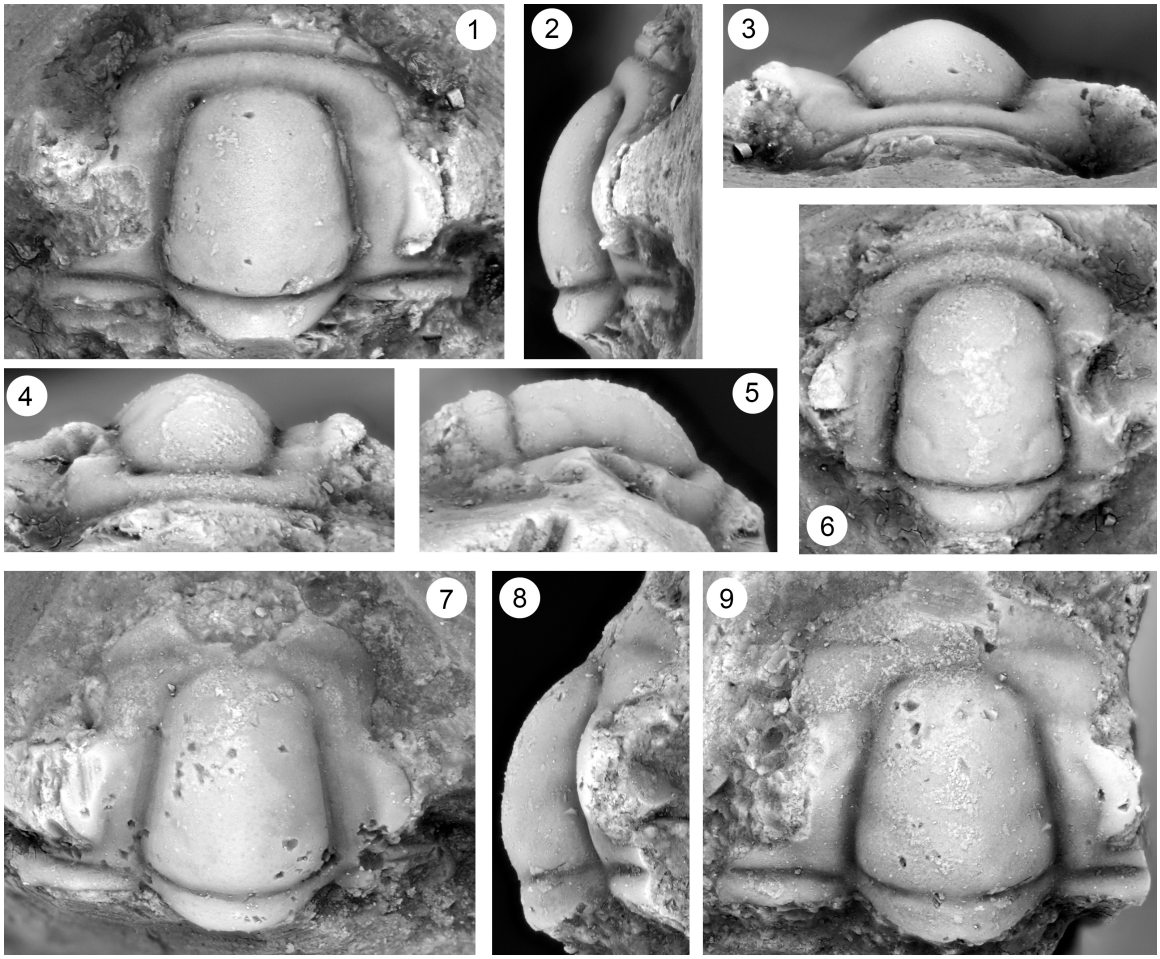
1
2
3
4
5
6
7
8
9

Plate 25

Fig. 1-14. "*M.*" cf. *bothra* from the Sneakover Member of the Orr Formation.

1, 2, 3. Pygidium, dorsal, left lateral, and posterior views, ORR 59.4 OU 238132.

4, 5, 6. Pygidium, dorsal, left lateral, and posterior views, ORR 59.4 OU 238133.

7, 8. Pygidium, dorsal and posterior views, ORR 59.4 OU 238134.

9, 10. Cranidium, left lateral and dorsal views, ORR 59.4 OU 238135.

11, 12, 13. Cranidium, right lateral, anterior, and dorsal views, ORR 59.4 OU 238136.

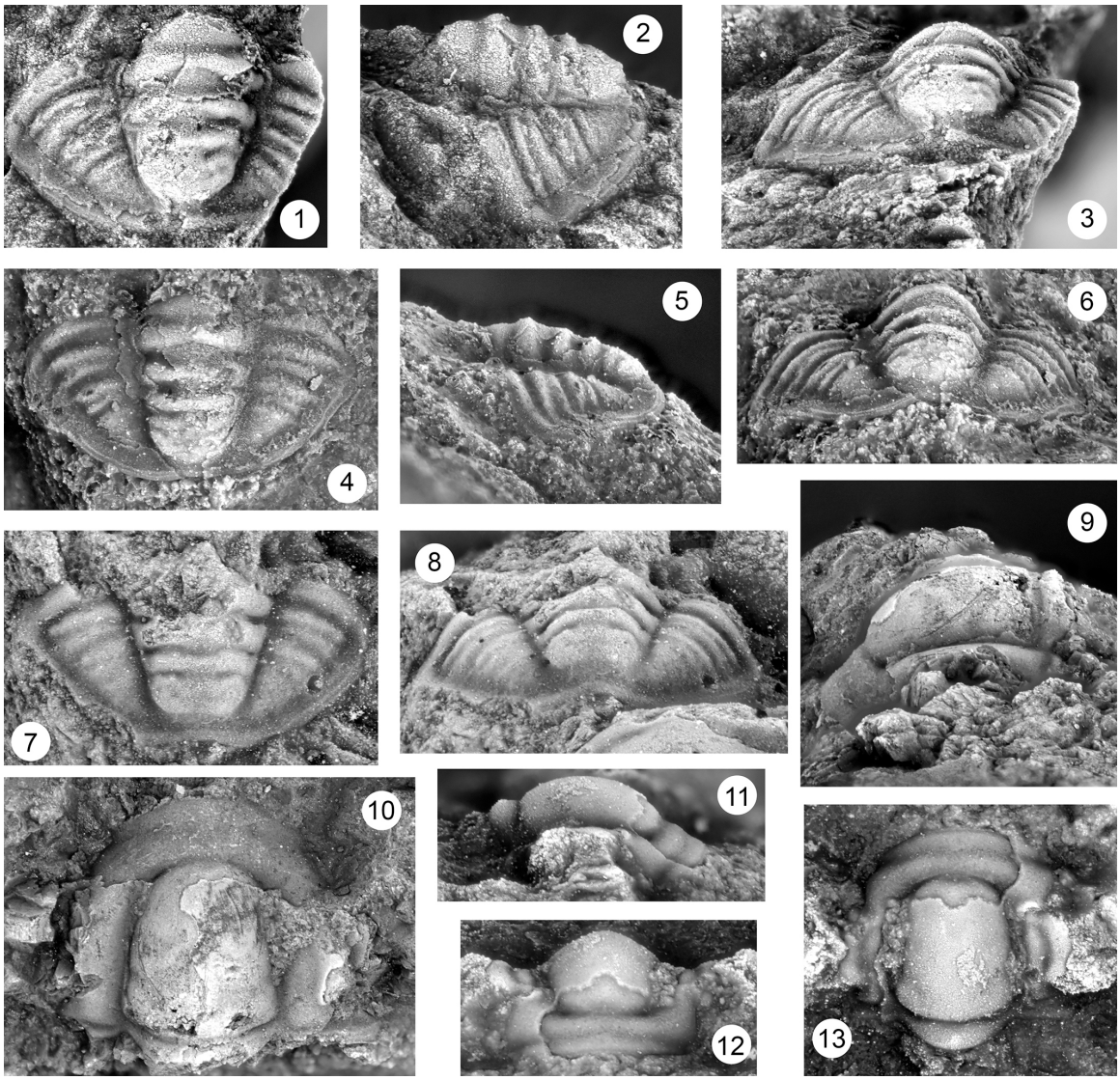
1
2
3
4
5
6
7
8
9
10
11
12
13

Plate 26

Fig. 1-3. *Deckera* n. sp. 1 from the Dunderberg Formation.

1, 2, 3. Cranidium, dorsal, left lateral, and anterior views, CCDu 138.5 OU 238145, x18

Fig. 4-6. *Labiocephalus* sp. 1 from the Honey Creek Formation.

4, 5, 6. Cranidium, anterior, left lateral, and dorsal views, RR 140 OU 238146, x7.

Fig. 7-9. *Labiocephalus cassia* sp. nov. from the Barton Canyon Member of the Windfall Formation and Sneakover Member of the Orr Formation.

7. Cranidium, dorsal view, ORR 59.4 OU 238147, x5.

8,9. Pygidium, dorsal and posterior views, ORR 59.4 OU 238148, x5.

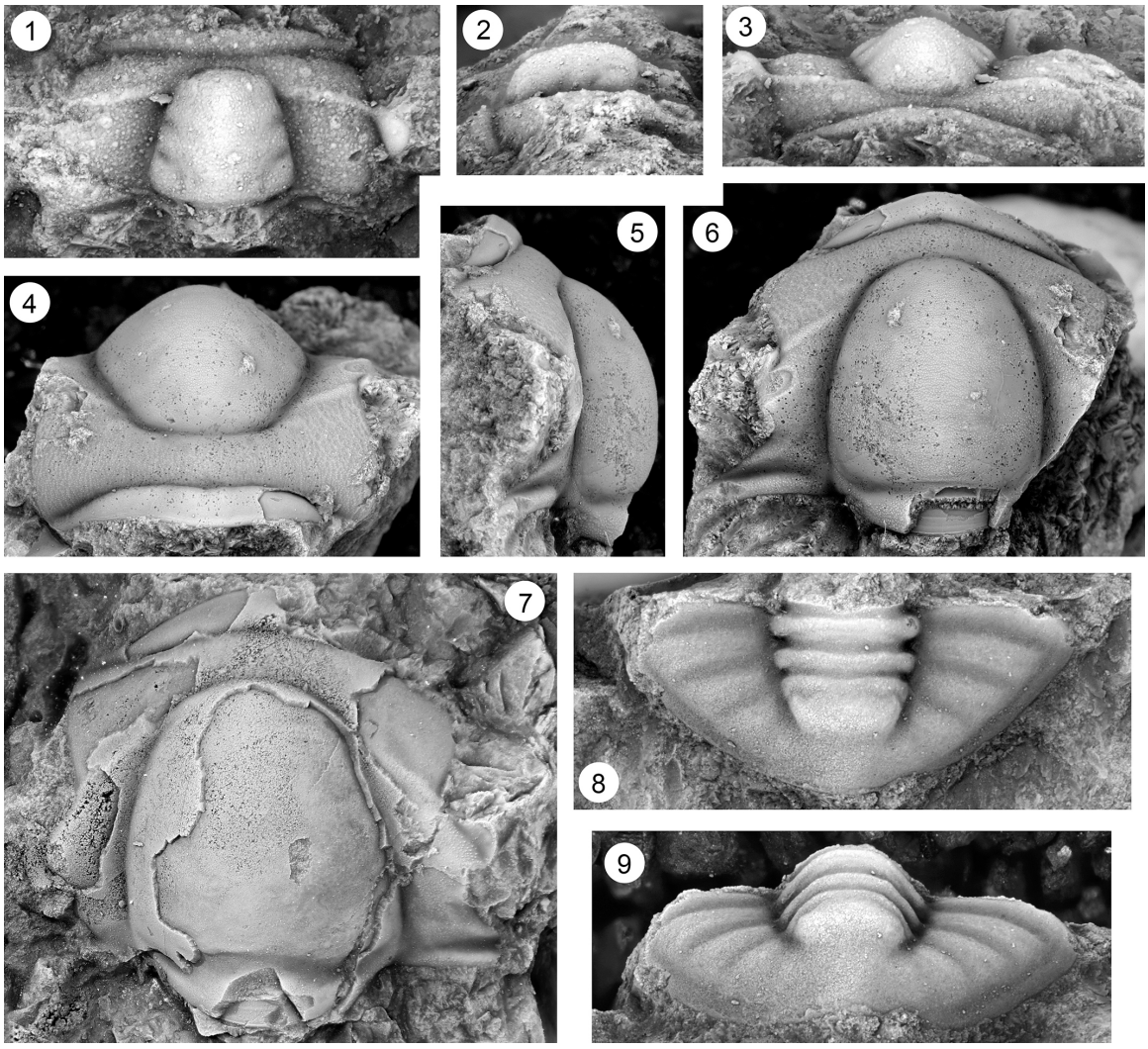
1
2
3
4
5
6
7
8
9